universität wien

DIPLOMARBEIT

Titel der Diplomarbeit

„Expression and function of multidrug resistance-related protein 1 in human lung epithelial cells"

verfasst von

Viktoria Elisabeth Muchitsch

angestrebter akademischer Grad

Magistra der Pharmazie (Mag.pharm.)

Wien, 2014

DANKSAGUNG

Besonders herzlich möchte ich mich bei Dr. Carsten Ehrhardt bedanken, der es mir ermöglicht hatte am Trinity College Dublin an meiner Diplomarbeit zu arbeiten. Er ist mir stets mit seiner kompetenten Betreuung, viel Geduld und neuen Ideen zur Seite gestanden und hat mich sowohl bei der praktischen Arbeit im Labor als auch beim Verfassen der Diplomarbeit unterstützt.

An diesem Punkt gilt mein Dank ebenso ao. Univ.-Prof. Mag. Dr. Franz Gabor, der mich ermutigt hat an meiner Diplomarbeit im Ausland zu arbeiten und mir anschließend bei der Organisation der Diplomarbeit am Trinity College behilflich war.

Des Weiteren bedanke ich mich beim gesamten Laborteam des Trinity College für das nette Arbeitsklima, insbesondere bei Camille Grousson, Svenja Sladek und Sergey Zaichik, die mir mit Rat und Tat zur Seite standen. Ein Dankeschön gebührt ebenfalls Sanghee Park, der mich auf seine ganz spezielle, unverwechselbare Art und Weise zum eigenständigen Arbeiten angeregt hat.

Ein großes Danke möchte ich hier auch an meinen Freund richten, der mich mit viel Verständnis, Gelassenheit und Motivation durch mein gesamtes Studium sowie meine Diplomarbeit begleitet hat.

Mein größter Dank gilt meinen Eltern für ihr ihren Zuspruch, ihr Verständnis und ihre emotionale und finanzielle Unterstützung im Studium.

Danke an alle, die mich auf meinen Weg durch mein Studium begleitet haben und mich in jeder erdenklichen Weise motiviert, unterstützt und aufgebaut haben.

TABLE OF CONTENTS

LIST OF ABBREVIATIONS

a-b	Apical to basolateral
ABC	ATP Binding Cassette
ATP	Adenosine triphosphate
b-a	Basolateral to apical
BCRP	Breast cancer-related protein
BSA	Bovine serum albumin
CF	5(6)-Carboxyfluorescein
CFDA	5(6)-Carboxyfluorescein-diacetate
CFTR	Cystic fibrosis transmembrane conductance regulator
COPD	Chronic obstructive pulmonary disease
CSE	Cigarette smoke extract
DMSO	Dimethyl sulfoxide
FBS	Foetal bovine serum
FEV_1	Forced expiratory volume in one second
FITC	Fluoresceinisothiocyanate
GSH	Glutathione
HRP	Horseradish peroxidase
IgG	Immunoglobulin G
KRB	Krebs-Ringer buffer
MRP	Multidrug resistance-related protein

NBD	Nucleotide binding domain
OAT	Organic anion transporter
OATP	Organic anion transporting polypeptide
OCT	Organic cation transporter
P-gp	P-glycoprotein
P_{app}	Apparent permeability coefficient
PBS	Phosphate buffered saline
PEPT1/PEPT2	Peptide transporter 1/2
Rh123	Rhodamine123
RNAi	RNA interference
RT-PCR	Reverse-transcription polymerase chain reaction
SD	Standard deviation
SDS-PAGE	Sodium dodecyl sulphate-polyacrylamide gel electrophoresis
SE	Standard error
SNP	Single nucleotide polymorphisms
SUR1/2	Sulfonylurea receptor
TEER	Transepithelial electrical resistance
TMD	Transmembrane domain
TRITC	Tetramethylrhodamine isothiocyanate

ABSTRACT - ENGLISH

The multidrug resistance-related proteins (MRP1-9, *ABCC1-6*, *10-12*) belong to the *ABCC* subfamily of ATP binding cassette (ABC) proteins and represent an important group of transporters in the human lung. Physiologically, they facilitate the transmembraneous transport of endogenous substrates ranging from chloride ions to phase II metabolites. In addition, MRP transporters are known to efflux exogenous substances, which can have a major impact on their bioavailability.

MRP1 (ABCC1) is present in the human bronchiolar and alveolar epithelial cells *in vitro* and shows the highest expression levels in the distal region of the lung.

The human distal lung epithelium cell line NCI-H441 was derived from a papillary adenocarcinoma of the lung. This cell line requires further characterisation for its establishment in biopharmaceutical research. Therefore, the abundance of multidrug resistance-related protein 1 in NCI-H441 cells was studied using Western blot. Confocal laser scanning microscopy was employed to determine its membrane localisation, which was confirmed by transport studies. Release studies, uptake studies and transport studies with the fluorescent MRP1 substrate, 5(6)-carboxyfluorescein-diacetate, which could be specifically inhibited by MK-571, confirmed the function of MRP1 in NCI-H441 cells. Potentially inhibiting or stimulating effects of verapamil, a calcium channel blocker, quinidine, an anti-arrhythmic drug and indomethacin, a non-steroidal anti-inflammatory drug, on MRP1 were also investigated.

Furthermore, the β_2-mimetics, formoterol, terbutaline, salbutamol and GW597901, inhaled glucocoticoids, budesonide and beclomethasone as well as the mast cell stabiliser, chromolyn sodium were tested regarding their influence on MRP1-mediated transport in release studies.

In a side project efflux studies using the fluorescent probe rhodamine123 revealed the functional expression of P-gp. Transport studies with paracellular marker compounds confirmed the tightness of the cell monolayers.

ABSTRACT - DEUTSCH

Die Multidrug Resistance-assoziierten Proteine (MRP1-9, *ABCC1-6*, *ABCC10-12*) stellen eine wichtige Gruppe von Transportern in der Lunge dar und gehören der *ABCC* Unterfamilie der ATP Binding Cassette (ABC) Proteinen an. Sie spielen eine wichtige physiologische Rolle im Transport von endogenen Substanzen, angefangen bei Chloridionen bis zu Phase II Metaboliten. Zusätzlich sind MRP-Transporter am Efflux exogener Substanzen beteiligt und können einen großen Einfluss auf ihre Bioverfügbarkeit ausüben.

MRP1 (*ABCC1*) wurde in humanen bronchiolaren und alveolaren Zellkulturen nachgewiesen und ist am stärksten in der distalen Region der menschlichen Lunge ausgebildet.

Die humane Bronchiolarepithelialzelllinie NCI-H441 wurde aus einem papillaren Adenokarzinom der Lunge isoliert. Für die Verwendung der Zelllinie in der biopharmazeutischen Forschung werden weitere Daten, wie zum Beispiel die Ausbildung von Transporterproteinen, benötigt. In der vorliegenden Arbeit wurde die Expression von MRP1 in NCI-H441 Zellen mittels Western Blot untersucht. Konfokale Laser-Scanning-Mikroskopie wurde eingesetzt, um die Membranlokalisation von MRP1 zu ermitteln, welche dann durch Transportstudien bestätigt wurde. Um die Funktionalität von MRP1 in NCI-H441 Zellen nachzuweisen, wurden Effluxstudien, Aufnahmestudien und Transportstudien mit dem fluoreszierenden MRP1-Substrat 5(6)-Carboxyfluorescein-diacetat durchgeführt und mittels MK-571, einem MRP-Inhibitor, gehemmt. Des Weiteren wurden Verapamil, ein Kalziumkanalblocker und Chinidin, ein Antiarrythmikum, sowie Indomethacin, ein nicht steriodales Antiphlogistikum, auf einen möglichen inhibitorischen oder stimulierenden Effekt auf MRP1 mittels Effluxstudien untersucht. Danach wurden die β_2-Mimetika Formoterol, Terbutalin, Salbutamol und GW597901, die inhalativen Glukokortikoide Budesonid und Beclomethason sowie der Mastzellstabilisator Cromoglicinsäure auf ihren Einfluss auf den MRP1-vermittelten Transport mittels Effluxstudien untersucht.

Ein Nebenprojekt bestätigte die Funktion von P-Glykoprotein mittels Rhodamin123 Effluxstudien. Die Dichtheit der Zellmonolayer wurde mittels Transport von parazellulären Markern nachgewiesen.

x

1 INTRODUCTION AND BACKGROUND

1.1 TRANSPORTERS IN THE LUNG

Inhalation therapy is used for the treatment of respiratory diseases such as chronic obstructive pulmonary disease, bronchial asthma and cystic fibrosis. Commonly prescribed drugs include bronchodilators, for example β_2 agonists (e.g. formoterol, salbutamol, terbutaline) anticholinergics (e.g. ipratropium bromide), glucocorticoids (e.g. budesonide, beclomethasone) and cromolyn sodium but also antibiotics (aztreonam, tobramycin) (Döring et al., 2012; Ejiofor and Turner, 2013). Moreover, the pulmonary application of drugs offers an alternative to the oral administration due to the high surface area available, the fast absorption, and avoidance of the liver first pass metabolism. In addition to low molecular weight drugs, the inhalation of peptides can result in significant bioavailability as shown, e.g. in the case of insulin (Patton et al., 2010).

Until the 1970s, the general opinion was that pulmonary administered drugs were absorbed by diffusion only. Nowadays, it is believed that small hydrophobic substances are absorbed by diffusion, whereas small hydrophilic substances are absorbed by diffusion via tight junctional pores or are transported by carrier proteins, for example transporters (Patton and Byron, 2007). Different mechanisms of drug absorption are shown in Figure 1.
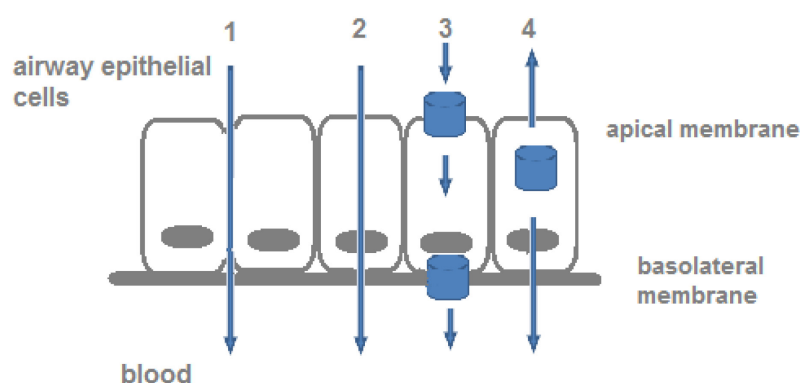

FIGURE 1

Different mechanisms of drug absorption in the lung epithelium; 1. paracellular diffusion (small hydrophilic substances), 2. transcellular diffusion (small hydrophobic substances), 3. carrier mediated transport (e.g. SLC transporter), 4. efflux transporters (e.g. multidrug resistance-related proteins, P-glycoprotein)

1

There is increasing evidence that drugs used in the treatment of respiratory diseases interact with transporter proteins. It was shown that salbutamol is transported actively in human bronchial epithelial cell lines and primary cell cultures (Ehrhardt et al., 2005; Horvath et al., 2007). In addition, the transport of ipratropium, another cationic and hydrophilic substance, in a human bronchial epithelial cell line was also mediated by the organic cation/carnitine transporter (Nakamura et al., 2010).

Therefore, the role of transporters in the pulmonary drug disposition is increasingly recognised, but requires further investigations.

Generally, transporters are encoded by three gene superfamilies', the solute carrier transporter (SLC) family, the organic anion transporting polypeptides (OATP, SLCO) and the ATP Binding Cassette (ABC) transporters (Bosquillon, 2010; Gumbleton et al., 2011). In the human lung several transporters are expressed, belonging to one of these three families. Sakamoto *et al.* examined the expression levels of different transporter proteins in human lung tissues. The organic cation/carnitine transporter 1 (OCTN), a member of the solute carrier transporter family, was detected in the highest abundance of all tested transporters, followed by multidrug resistance-related protein 1 (MRP1) and breast cancer-resistance protein (BCRP), both members of the ABC transporter family. Interestingly, P-glycoprotein, which is highly expressed at other biological barriers, was detected in lower amounts (Sakamoto et al., 2013).

1.2 SOLUTE CARRIER TRANSPORTER (SLC)

The SLC superfamily of transporter is composed of 55 families including the organic cation transporters (OCT), the organic anion transporters (OAT) and the proton-coupled oligopeptide transporters (PEPT1, PEPT2). In addition, the organic anion transporting polypeptides (OATP) were classically allocated to the SLC family, however, OATP are reclassified to a separate transporter gene family, SLCO (He et al., 2009). Generally, SLC transporters are known as uptake transporter mediating the transport of substances from the outside into the cells (König et al., 2013).

OCT have been detected in human lungs and comprise of five main subtypes, the electrogenic OCT1, OCT2 and OCT3 and the electroneutral organic cation/ carnitine transporters OCTN1 and OCTN2 (Bleasby et al., 2006; Sakamoto et al., 2013). OCT mainly transport substrates, which are positively charged at physiological pH, but also some neutral molecules (Koepsell, 2013).

OAT are composed of seven members, which are expressed in humans, OAT1-4, OAT7, OAT10 and URAT1, as well as Oat1–3, Oat5, Oat6, Oat8, Oat9, and Urat1/Rst, which are only detected in rodents. OAT play a role in renal excretion of water-soluble, negatively charged organic compounds including endogenous waste products, drugs and drug metabolites. OAT are highly expressed in the human kidneys but they are also present in placenta, nasal epithelium, and blood-brain barrier (Burckhardt, 2012). OAT are generally known as uptake transporters, however, OAT4 also mediates the efflux of substances from cells (König et al., 2013).

Sakamoto *et al.* discovered the expression of OAT2, OAT3 and OAT4 in human lung tissues. OAT3 was also detected in human bronchial epithelial cells (Sakamoto et al., 2013). Bleasby *et al.* stated the expression of OAT2 in human lung samples using microarray analysis (Bleasby et al., 2006). In addition, the OAT4 gene expression was detected in different human lung epithelial cell lines by RT-PCR (Endter et al., 2009). Up to the present, the membrane expression and the function of the OAT in the lung or in lung cell lines is unknown.

1.3 ABC TRANSPORTERS (ATP-BINDING CASSETTE TRANSPORTERS)

ABC transporters are divided into seven distinct subfamilies (i.e. A-G) of proteins, based on organisation of domains and amino acid homology. Up to now, 49 ABC transporter genes have been discovered in humans (Cole, 2013).

On characteristic of this family is the binding and hydrolysis of ATP. This causes a conformational change in the protein and provides the necessary energy to transport their substrates actively across cell membranes (Sharom, 2008). These transporters are transmembrane proteins and generally known as efflux pumps, while other transporters, e.g. many SLC transporters, mediate the uptake of substances in the cells (König et al., 2013).

ABC transporters are essential for many processes in the cells. Therefore, genetic variations can cause diseases, e.g. mutations in the cystic fibrosis transmembrane conductance regulator CFTR (*ABCC7*) are associated to cystic fibrosis (Bosquillon, 2010). Moreover, ABC transporters play important roles in the transport of endogenous substances and in the transport of xenobiotics alike. Some members, for example P-glycoprotein, are also related to relevant drug-drug interactions and associated side effects (König et al., 2013). An over-expression of ABC transporters (P-glycoprotein, BCRP, some members of the MRP family) in tumour cells can induce multidrug-resistance, a phenomenon, which is often the ultimate cause of cancer therapy failure. The chemotherapeutic drugs are rapidly exported by the over-expressed transporters in the tumour (Boumendjel et al., 2009; Cole, 2013).

Tissues, that function as a biological barrier, e.g. the intestine, the placenta or the blood-brain barrier, express ABC transporters at high levels. Several ABC transporters were also detected in the human lung, including P-glycoprotein (P-gp, *ABCB1*), the multidrug resistance-related proteins (MRP 1-9, *ABCC1-6, 10-12*) and the breast cancer resistance protein (BCRP, *ABCG2*) (Bleasby et al., 2006; Sakamoto et al., 2013).

1.4 Multidrug resistance-related proteins 1-9 (MRP1-9, *ABCC1-6, ABCC10-13*)

Multidrug resistance-related proteins are encoded by the C subfamily of the ABC transporter genes. The C subfamily also includes CFTR and two sulfonylurea receptors (SUR1, SUR2, *ABCC8, ABCC9*), which are targets of the sulfonylurea class of anti-diabetic drugs used in the therapy of diabetes mellitus (Bakos and Homolya, 2007).

Mutations can cause diseases, for example inherited or acquired mutations in the MRP2 protein lead to the Dubin-Johnson syndrome, causing hyperbilirubinaemia. Patients suffer from increased concentrations of bilirubin glucuronides in the blood. Furthermore, mutations in the *ABCC6* gene have been identified to cause the heritable recessive disorder *pseudoxanthoma elasticum* characterised by the loss of tissue elasticity affecting the skin, retina and blood vessels (Boumendjel et al., 2009; Keppler, 2011).

1.4.1 MULTIDRUG RESISTANCE-RELATED PROTEIN 1 (MRP1)

MRP1 was detected by Cole in 1992 and cloned from a multidrug resistant human lung cancer cell line (H69AR) (Cole et al., 1992).

1.4.1.1 MEMBRANE TOPOLOGY

The membrane topology of MRP1 is shown in Figure 2. Other members of the ABCC family (MRP1-3, 6, 7; SUR1, 2) have similar membrane topologies. MRP1 is composed of three transmembrane domains, which consist of five, six and another six transmembrane alpha helices. The amino-terminus is located extracellularly. The first transmembrane region (TMD_0) is important for the maintenance of the correct structure of the protein. It is connected to the linker region, which is essential for its functionality, the substrate recognition and proper transport activity (Bakos et al., 2000).

Transmembrane domain 1 (TMD_1) and transmembrane domain 2 (TMD_2) are separated by the first nucleotide binding domain (NBD) while the second nucleotide binding domain is located near the intracellular carboxy-terminus. The nucleotide binding regions are composed of different amino acid sequences. The binding of ATP at the NBD leads to conformation changes. The substrate, which binds to TMD_1 or TMD_2 is transported across the membrane to the extracellular side due to ATP binding and hydrolysis at the two nucleotide binding domains. The "pore" in the membrane is formed by TMD_1 and TMD_2. Mutations of NBD lead to an inactivated protein (Bakos and Homolya, 2007).
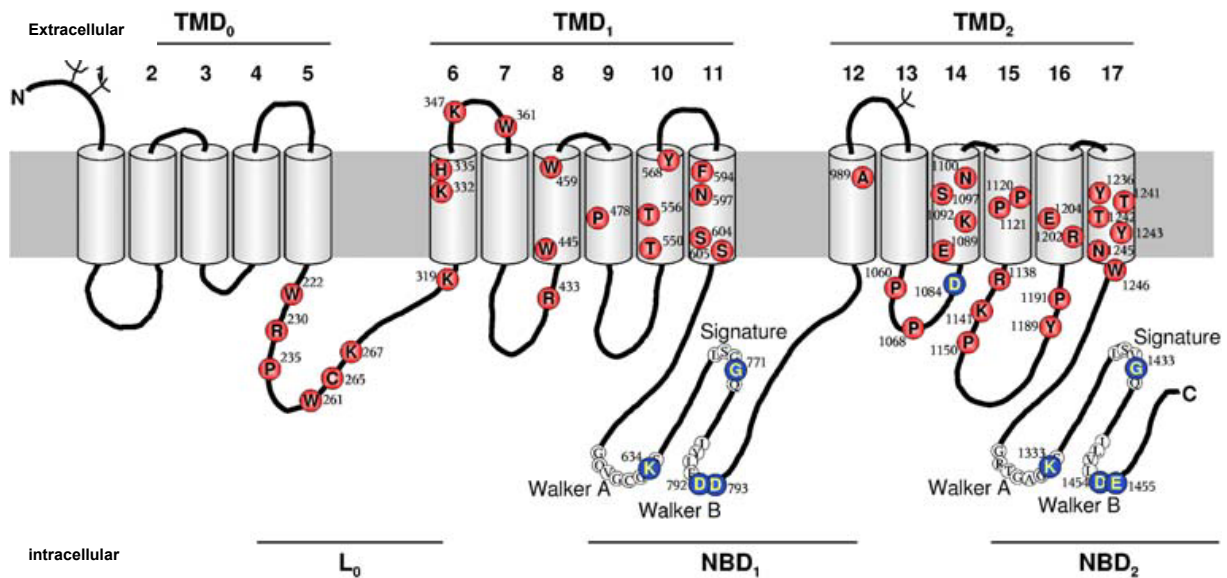
FIGURE 2

Multidrug resistance-related protein 1 membrane topology model. MRP2, 3, 6 and 7 show a similar topology. MPR1 is composed of three transmembrane domains (TMD), consisting of five, six and another six transmembrane helixes. It exhibits two nucleotide-binding domains (NBD) with a different amino acid sequence. The amino-terminus is located extracellularly and the carboxy-terminus intracellularly. The characteristic intracellular linker region (L_0) is connecting TMD_0 with TMD_1 (Bakos and Homolya, 2007).

1.4.1.2 LOCALISATION AND EXPRESSION IN CELLS

MRP1 is a 190 kDa transmembrane glycoprotein that is located mainly to the basolateral membrane of endothelial cells. In the placenta and in brain capillary endothelial cells, however, it was detected apically. It is ubiquitously expressed in the body with the highest levels detected in the lung, testis, kidney, skeletal and cardiac muscles, macrophages and placenta. A moderate level was found in the small intestine, colon, erythrocytes, T-cells, mast cells and brain (Boumendjel et al., 2009; Keppler, 2011).

1.4.1.3 EXPRESSION IN THE LUNG

The MRP1 expression in normal human bronchiolar epithelial cells was demonstrated by immunoblot (Lehmann et al., 2001). Membrane localisation studies by immunofluorescence microscopy confirmed its presence on the basolateral membrane of human lung epithelial cells (Scheffer et al., 2002). Furthermore, the protein function was shown by means carboxydichlorofluorescein efflux studies (Lehmann et al., 2001). MPR1 is expressed in the bronchial and bronchiolar epithelia, alveolar epithelia (Sakamoto et al., 2013), alveolar

macrophages (Flens et al., 1996), goblet cells and seromucinous glands (Bréchot et al., 1998).

Endter *et al.* investigated the presence of MRP1 in different human lung epithelial cell lines using RT-PCR and discovered high expression in hBEpC, Calu-3, 16HBE14o, BEAS-2B, ATII, ATI-like and A549 cells (Endter et al., 2009).

Multiple reaction monitoring-based analysis using liquid chromatography–tandem mass spectrometry (LC–MS/MS) was employed by Sakamoto *et al.* to quantify the expression levels of membrane transporters in human lung tissues. MRP1 showed the highest protein abundance of all ABC transporters investigated, especially in the bronchiolar and the alveolar region, whereas P-gp levels were significantly lower. This implies a higher significance of MRP1 in the human lung compared to P-gp. However, individual differences in the expression levels of MRP1 were also detected (Sakamoto et al., 2013).

The basolateral localisation suggests that MRP1 pumps substrates out of the epithelial cells towards the circulating blood. Thus, on the one hand, MRP1 could influence the transport of various pulmonary administered substances from airways towards blood circulation. On the other hand, MRP1 could also affect the transport of substances from the blood towards the lung epithelial cells, possibly as a protective mechanism.

1.4.1.4 FUNCTION AND ASSOCIATED DISEASES

MRP1 is an ATP dependent efflux pump that transports glutathione S-conjugates, glucuronates, sulphates and phosphates. It plays a physiologically important role as a member of the 'phase II' system in xenobiotic metabolism and is responsible for the efflux of phase II conjugates as well as in the release of biologically active endogenous substances from cells.

Furthermore, MRP1 protects cells from oxidative stress by exporting substances in the presence of glutathione or in form of glutathione conjugates. Reduced glutathione (GSH) is important for maintaining and regulating the redox status of the cells and one of the most effective antioxidants especially in the lung (Cole, 2013).

7

However, smoking is generating oxidative stress by the production of free radicals and can cause chronic obstructive pulmonary disease (COPD). Patients suffering from COPD show a reduced expression of MRP1 in bronchial epithelial cells compared to healthy persons (van der Deen et al., 2006). In addition, the level of the MRP1 expression in the lung correlates with the decline of lung function in COPD patients (Budulac et al., 2012).

Interestingly, cigarette smoke extract (CSE) competitively inhibits MRP1 in human bronchial epithelial cells in vitro and the inhibition of MRP1 by MK-571 caused increased toxicity of the CSE (van der Deen et al., 2007). On the other hand, Leslie *et al.* reported mediated-MRP1 transport of NNAL-O-glucuronide, a tobacco specific carcinogen (Leslie et al., 2001). Both can be associated with a protective function of MRP1 against tobacco smoke in the lung.

Van der Deen *et al.* examined the influence of drugs used in the therapy of COPD and bronchial asthma on MRP1 in the human bronchial epithelial cell line, 16HBE14o-. The glucocorticoid, budesonide, the β_2-agonist, formoterol, N-acetylcysteine and the anti-cholinergic drug, ipratropium bromide altered MRP1-mediated transport (van der Deen et al., 2008).

Single nucleotide polymorphisms (SNP) in MRP1 have been identified and were significantly associated with an altered the FEV_1 level (forced expiratory volume in one second) and inflammatory markers in COPD patients (Budulac et al., 2010). However, these findings were not confirmed in subsequent studies (Budulac et al., 2012).

The present knowledge suggests an important role of MRP1 as a defence mechanism in the lung and in the prevention of COPD.

Moreover, SNP in MRP1 alter the response to the leucotriene antagonist, montelukast in the therapy of bronchial asthma (Lima et al., 2006).

MRP1 is over-expressed in many tumour cells and can lead to multidrug resistance in cancer cells. Over-expression was reported for solid tumours, e.g. non-small-cell lung cancer, prostate cancer and some types of breast cancer, but also for acute myeloblastic/lymphoblastic leukaemia and neuroblastoma (Cole, 2013). The expression of MRP1 in normal human cells is controlled by the p53 tumour suppressor protein. Mutations of this protein can cause up-regulation of the

MRP1 gene resulting in over-expression of MRP1 and multidrug resistance (Wang and Beck, 1998).

SNP in MRP1 influence the efficacy and the toxicity in several chemotherapeutic treatments, e.g. the cardiotoxicity of doxorubicin is increased (Cole, 2013).

1.4.1.5 MRP1 SUBSTRATES

MRP1 mainly transports organic anions, however, some organic cations also become substrates in the presence of glutathione (GSH), which is present in most living cells. Many of these organic anions are transported as GSH (e.g. leucotienes), sulphate (e.g. oestrone) or glucuronide (e.g. bilirubin) conjugates. MRP1 is the major transporter of leucotriene C_4 (LTC_4), leucotriene D_4 (LTD_4) and leucotriene E_4 (LTE_4), potent pro-inflammatory mediators, which play a role, for example in the primary and late response in the asthmatic reaction. MRP1 is involved in the transport of several therapeutic drugs, e.g. chemotherapeutic drugs or HIV-protease inhibitors, but also in the transport of tobacco specific carcinogens. Table 1 gives a detailed overview on the substrates of MRP1.

5(6)-Carboxyfluorescein is a fluorescent substrate of MRP1, which is used experimentally for the detection of the functionality of MRP1 as well as to discover substances, which interfere with the MRP1 mediated transport (de Groot et al., 2007; van der Deen et al., 2008). 5(6)-Carboxyfluorescein-diacetate permeates the cell membrane. For the activation of its fluorescence intracellular esterase activity is required. The enzymes cleave the acetate groups. As compared to fluorescein it contains extra negative charges and therefore, 5(6)-carboxyfluorescein is retained in the cell. It needs an active transport mechanism to cross the plasmalemma.

Substrates of MRP1	References
Endobiotic conjugates	
GSH conjugates	
Leucotrienes C_4, D_4, E_4	(Leier et al., 1994)
5-Glutathionyl prostaglandin A_2	(Evers et al., 1997)
Glucuroninde conjugates	
Estradiol-17-β-D-glucuronide	(Jedlitschky et al., 1996)
Glucuronosylbilirubin	(Jedlitschky et al., 1996)
Sulphate conjugates	
Oestrone 3-sulphate	(Qian et al., 2001)

Folic acid, bilirubin, glutathione	(Cole, 2013)
Therapeutic substrates	
Chemotherapeutic drugs	
Anthracyclines (i.e. daunorubicin, doxorubicin, epirubicin)	(Renes et al., 1999), (Grant et al., 1994)
Plant alkaloids: Vinca alkaloids (i.e. vinblastine, vincristine) Epipodophyllotoxins (i.e. etoposide, teniposide) Camptothecines (i.e. topotecan. irinotecan)	(Grant et al., 1994), (Renes et al., 1999), (Loe et al., 1998) (Boumendjel et al., 2009)
Tyrosine kinase inhibitors (imantinib, gefitinib)	(Boumendjel et al., 2009)
Mitoxanthrone	(Cole, 2013)
Methotrexate	(Hooijberg et al., 1999)
Flutamide	(Cole, 2013)
Antibiotics	
Ciprofloxacin	(Cole, 2013)
HIV protease inhibitors	
Ritonavir, indinavir, saquinavir	(Olson et al., 2002), (Cole, 2013)
Statins (atorvastatin,rosuvastatin)	(Cole, 2013)
Tobacco specific carcinogens	
NNAL-O-glucuronide (GSH dependent) 4(Methylnitrosamino)-1-(3-pyridyl)-1butanol	(Leslie et al., 2001)
Fluorescent substrate	
5(6)-Carboxyfluorescein	(van der Deen et al., 2008)

TABLE 1

Substrates of MRP1

1.4.1.6 INHIBITOR MK-571

MK-571 is a leucotriene D_4 receptor antagonist and inhibits MRP1 (Jedlitschky et al., 1996), but also other multidrug resistance-related proteins. Unfortunately, a more specific MRP1 inhibitor is currently not commercially available (Cole, 2013).

1.4.2 MULTIDRUG RESISTANCE-RELATED PROTEINS 2-9 (*ABCC2-6, ABCC10-12*), EXPRESSION, CELLULAR DISTRIBUTION AND LOCALISATION IN THE LUNG

The Table 2 provides an overview on the expression, cellular distribution and localisation of the multidrug resistance-related proteins in the human lung. In addition, it states the expression in human bronchial and alveolar epithelial cell lines.

There is some controversy in the literature about the expression of MRP2 and MRP3 in the human lung, however, the majority of the studies confirmed the expression. Information concerning the expression of MRP6-9 in the lung is mostly lacking.

Protein Name	Expression in Human Lungs	Cellular Distribution in the Lung	Cellular Localisation	Expression in Human Cell Lines (RT-PCR)	Ref.
MRP2 (*ABCC2*)	Low expression	Bronchial, bronchiolar and peripheral epithelial cells	Apical	ATI-like: low hBEpC, Calu-3, 16HBE14o, BEAS-2B, ATII: moderate A549: high	(Bleasby et al., 2006; Sakamoto et al., 2013; Sandusky et al., 2002; Scheffer et al., 2002; Torky et al., 2005)
MRP3 (*ABCC3*)	Low or high, variable levels	Primary bronchial and peripheral epithelial cells	Basolateral	hBEpC, 16HBE14o, BEAS-2B: moderate ATII, ATI-like, A549, Calu-3: high	(Bleasby et al., 2006; Sakamoto et al., 2013; Torky et al., 2005)
MRP4 (*ABCC4*)	Low to moderate	Human tracheal, bronchial, alveolar epithelial cells	Intracellular	BEAS-2B: not expressed Calu-3, A549, 16HBE14o :low hBEpC, ATII, ATI-like: moderate	(Bleasby et al., 2006; Sakamoto et al., 2013; Torky et al., 2005)
MRP5 (*ABCC5*)	Moderate to high	Human tracheal, bronchial, alveolar epithelial cells	Intracellular	16HBE14o, ATII, ATI-like, A549 : moderate BEAS-2B, hBEpC, Calu-3: high	(Bleasby et al., 2006; Sakamoto et al., 2013; Torky et al., 2005)
MRP6 (*ABCC6*)	Moderate	Human tracheal, bronchial, alveolar epithelial cells, alveolar macrophages	Unknown	hBEpC, A549: low Calu-3, 16HBE14o, BEAS-2B: moderate ATII, ATI-like: high	(Beck et al., 2005; Bleasby et al., 2006; Sakamoto et al., 2013)
MRP7 (*ABCC10*)	High expression/ not expressed	Unknown	Unknown	hBEpC, A549, ATII: moderate Calu-3, 16HBE14o, BEAS-2B, ATI-like: high	(Bleasby et al., 2006; Sakamoto et al., 2013)
MRP8 (*ABCC11*)	Low or high	Unknown	Unknown	16HBE14o, BEAS-2B, A549 :no expression, hBEpC, Calu-3: low expression ATII, ATI-like: high expression	(Bleasby et al., 2006; Sakamoto et al., 2013)
MRP9 (*ABCC12*)	Moderate expression/ not expressed	Unknown	Unknown	Unknown	(Bleasby et al., 2006; Sakamoto et al., 2013)

TABLE 2

Expression, cellular distribution and cellular localisation of MRP2- MRP9 in the human lung and the expression profile in human bronchial and alveolar epithelial cell lines (Bosquillon, 2010; Endter et al., 2009)

1.5 P-GLYCOPROTEIN (P-GP, *ABCB1*)

P-gp is a 170 kDa efflux transporter that is widely expressed throughout the human body. In contrast to MRP1, P-gp is mainly localised to the apical membrane of human lung epithelial cells. It was detected in human lung and is functional expressed in several human lung epithelial cell lines (Ehrhardt et al., 2003; Endter et al., 2007).

1.6 THE NCI-H441 CELL LINE

The bronchiolar NCI-H441 cell line is a human cancer cell line, which has characteristics of both alveolar ATII cells (Rehan et al., 2002) as well as bronchiolar (Clara) epithelial cells (Newton et al., 2006). NCI-H441 cells were isolated from the pericardial fluid of a patient with papillary adenocarcinoma of the lung. The cell line is able to form polarised monolayers, tight junctions and can exhibit significant transepithelial electrical resistance reaching TEER values of $1010 \pm 105 \ \Omega \cdot cm^2$ (Neuhaus et al., 2012; Salomon et al., 2014).

These features make the cell line an interesting candidate for pulmonary drug disposition studies. The only other commonly used human alveolar cell line, A549, does not form functional tight junctions and therefore, A549 cells show a limited suitability particularly for transport studies.
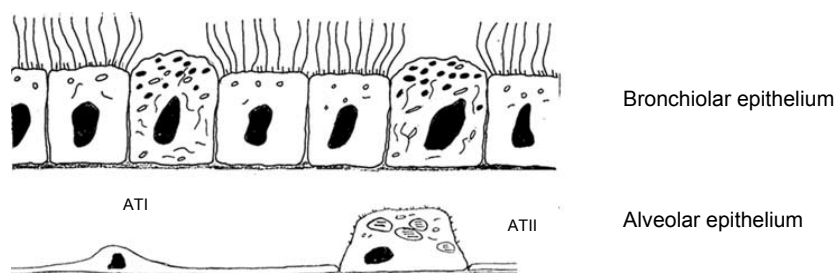
FIGURE 3

Bronchiolar and alveolar epithelium, NCI-H441 cells are developing characteristics of alveolar and bronchiolar cells (Forbes and Ehrhardt, 2005).

1.7 AIMS AND OBJECTIVES

The NCI-H441 cell line needs further characterisation for its establishment in the biopharmaceutical research. In this context, knowledge on the expression of drug transporters is essential. The objective of this thesis was to investigate the

expression, cellular localisation and function of multidrug resistant-related protein 1 in the NCI-H441 cells. Furthermore, drugs used in the inhalation therapy of chronic obstructive pulmonary disease and bronchial asthma, as well as several potential inhibitors or stimulating substances were investigated regarding their influence on MRP1-mediated transport. The side project of this thesis was aiming to test the function of P-glycoprotein in NCI-H441 cells. Additionally, the paracellular transport was assessed by fluorescein sodium and fluorescein isothiocyanate (FITC)-labelled dextrans transport studies.

2 MATERIALS AND METHODS

2.1 MATERIALS

5(6)-Carboxyfluorescsein-diacetate, MK-571, quinidine and formoterol fumarate were purchased from Santa Cruz Biotechnology (sc-210423, sc-201340, sc-212614, sc-203050, Heidelberg, Germany). LY335979 was obtained from Axon (Axon 1839, Groningen, The Netherlands). Mouse anti-MRP1 monoclonal antibody was purchased from Merck-Millipore (anti-MRP1 monoclonal antibody, clone QCRL-1, MAB4100, Carrigtwohill, Ireland). Anti-mouse IgG horseradish peroxidase (HRP) conjugate (Promega, Medical Supply Company, Dublin, Ireland) was used as secondary antibody for Western blot. Secondary Anti-mouse IgG Alexa Fluor 488 conjugates and the RPMI1640 cell culture media (Gibco) were purchased from Bio-Sciences (Dun Laoghaire, Ireland). All other substances were obtained from Sigma Aldrich.

2.2 CELL CULTURE

2.2.1 NCI-H441 CELL LINE

The bronchiolar epithelial NCI-H441 cell line (American Type Culture Collection, HTB-174) was isolated from the pericardial fluid of a patient with papillary adenocarcinoma of the lung. The cells were obtained from LGC Standards (Teddington, UK) and cultured at 37°C in 5% CO_2 atmosphere in Gibco RPMI1640 medium supplemented with 5% foetal bovine serum (FBS), 1% sodium pyruvate, 100 U/ml penicillin and 100 µg/ml streptomycin. NCI-H441 cells were routinely cultured in 75 cm^2 growth area tissue culture flasks (Greiner BioOne, Frickenhausen, Germany) and passaged weekly when approximately 90% confluence was reached. The media was exchanged every other day.

On Transwell Clear substrates a seeding density of 250,000 cells/cm^2 was used, otherwise 100,000 cells/cm^2.

For uptake and efflux studies cells were grown on 24-well plates (Greiner CELLSTAR, Frickenhausen, Germany) until confluence for 7 to 12 days.

Cells were seeded on Lab-Tek chamber slides (Nunc, Roskilde, Denmark) for confocal laser scanning microscopy (CLSM) and grown for 7 days.

For transport studies cells were grown on Transwell Clear inserts (Corning, Amsterdam, The Netherlands) and cultured under liquid-covered culture conditions. Twenty-four hours post-seeding, the medium was replaced with RPMI1640 medium, which in addition contained 200 nM dexamethasone and ITS supplement (10 µg/ml insulin, 5 µg/ml human transferrin, 5 ng/ml sodium selenite). The transepithelial electrical resistance (TEER) of insert-grown cell monolayers was measured using a Millicell ERS Volt-Ohm Meter with STX-2 chopstick electrodes (Millipore) and corrected for the background value contributed by the inserts and medium. Measurements were carried out every other day and the media was changed daily.

Cells were used from passage 55 to passage 78.

2.3 EFFLUX STUDIES

5(6)-carboxyfluorescein-diacetate (CFDA) and rhodamine123 (rh123) release studies were performed on NCI-H441 cell monolayers cultured for 7-12 days in 24-well plates. Cell layers were washed with warm bicarbonated Krebs-Ringer buffer (KRB) containing 15 mM HEPES, 116.4 mM NaCl, 5.4 mM KCl, 0.78 mM NaH_2PO_4, 25 mM $NaHCO_2$, 1.8 mM $CaCl_2$, 0.81 mM $MgSO_4$ and 5.55 mM glucose; pH 7.4. Next, cells were incubated with 500 µl KRB for 30 min at 37°C and 5% CO_2 for equilibration, before cells were loaded with 1 ml of CFDA solution (100 µM in KRB) or 1ml Rh123 solution (50 µM in KRB) for 60 min at 37°C and 5% CO_2. The 5(6)-carboxyfluorescein-diacetate solution was prepared from a 50 mM stock solution in dimethyl sulfoxide (DMSO). After washing the monolayers with warm KRB, the fluorescent solution was replaced with 1 ml KRB or KRB containing one of the following tested substances:

- 10 µM, 20 µM, 50 µM MK571 (prepared from a 20 mM stock solution in distilled water) ,
- 50 µM verapamil,
- 10 µM LY335979 (prepared from a stock solution in DMSO)
- 10 µM indomethacin (prepared from a 10 mM stock solution in ethanol),

16

- 100 µM quinidine (prepared from a 50 mM stock solution in methanol),

- 10 µM telmisartan (prepared from a 5 mM stock solution in DMSO)

- 20 µM, 50 µM budesonide (prepared from a 20 mM stock solution in ethanol),

- 50 µM beclomethasone (prepared from a 20 mM stock solution in ethanol),

- 100 µM cromolyn sodium,

- 100 µM formoterol fumarate (prepared from a stock solution in DMSO),

- 100 µM, 200 µM salbutamol,

- 100 µM, 200 µM terbutaline hemisulphate salt

- 100 µM GW597901, a developmental β_2-agonist, kindly provided by GlaxoSmithKline.

The solutions in KRB were prepared freshly. Stock solutions of MK-571 were stored at -20°C.

One hundred microliter samples were drawn at 0, 15, 30, 45 and 60 min and analysed in a black 96-well plate (Greiner Bio One, Frickenhausen, Germany). After each sample was taken, cell layers were washed twice with ice-cold KRB and lysed with a 1% solution of Triton X-100 in KRB to determine the intracellular activity of 5(6)-carboxyfluorescein.

Fluorescence was analysed using a fluorescence plate reader (FLUOstar Optima, BMG Labtech, Offenburg, Germany) at excitation and emission wavelengths of 485 and 520 nm, respectively. 5(6)-Carboxyfluorescein or Rh123 release from untreated NCI-H441 cell layers was used as control.

For standardisation, the total protein amount of the cell layers was determined by a Bradford protein assay according to the manufacturer's instruction (Bio Rad protein assay, Hemel Hempstead, UK).

Only cell layers which were not treated with CFDA/Rh123 were used for the determination of the protein concentration.

2.4 UPTAKE STUDIES

NCI-H441 cells were cultured in 24-well plates for 7 to 10 days until confluence. The cell monolayers were washed with warm KRB and were incubated in KRB at 37°C for 30 min to equilibrate. A 100 µM CFDA solution in KRB or a 100 µM CFDA solution in KRB containing 20 µM MK571 was added. After 0, 15, 30, 45 and 60 min the CFDA solution was removed. The monolayers were washed with ice-cold KRB and lysed with 1% Triton X-100 in KRB. The plates were analysed as described above.

2.5 TRANSPORT STUDIES

2.5.1 CFDA TRANSPORT STUDIES

NCI-H441 cells were grown in Transwell Clear inserts (3470) for 10 days. The transepithelial electrical resistance (TEER) was measured daily. Cells were washed with a pre-warmed KRB solution, followed by a 60 min equilibration in KRB or in case of inhibitor studies with a solution of 50 µM MK-571 in KRB at 37°C. Bidirectional transport was examined after the equilibration buffer was replaced by the relevant fluorescent solution (i.e. 100 µM CFDA solution, 100 µM CFDA solution plus 50 µM MK571, 100 µM CFDA solution plus 10 µM telmisartan (prepared from a stock solution in DMSO), or 100 µM CFDA solution plus 50 µM MK571 and 10 µM telmisartan) were added to the donor compartment. For apical to basolateral transport (a-b), 200 µl donor solution was added; for basolateral to apical (b-a) transport 800 µl. The acceptor compartment contained KRB. In inhibition experiments, all solution contained the relevant inhibitors at the concentrations indicated above. After 15, 30, 45, 60, 75 and 90 min a 100 µl sample was drawn from the acceptor compartment and replaced by 100 µl of the relevant acceptor solution. The fluorescence intensity was analysed in a black 96-well plate using fluorescence plate reader (FLUOstar Optima, BMG Labtech, Offenburg, Germany) at excitation and emission wavelength of 485 nm and 520 nm, respectively.

TEER values were measured before and after the experiment in KRB solution in order to verify the cell layer integrity.

After cell monolayers were rinsed with ice-cold KRB, the monolayers were lysed with a solution of 1% Triton X-100 in KRB in order to determine the intracellular concentration of 5(6)-carboxyfluorescein. The resulting solutions were analysed on a 24 well plate using fluorescence plate reader (FLUOstar Optima, BMG Labtech, Offenburg, Germany) at excitation and emission wavelength of 485 nm and 520 nm, respectively.

The apparent permeability coefficient (P_{app}) was calculated using the following equation:

$$P_{app}= (\Delta Q/\Delta t)/(A*C_0)$$

($\Delta Q/\Delta t$) = change in concentration of the transported substance over a designated time period

A = surface area of the inserts (0.33 cm^2 or in case of 3460 plates 1.13 cm^2)

C_0 = initial concentration of the drug in the donor compartment

2.5.2 FLUORESCEIN SODIUM SALT AND FLUORESCEINISOTHIOCYANATE (FITC)-DEXTRAN TRANSPORT STUDIES

NCI-H441 cells were grown under LCC conditions on Transwell Clear membranes (3460) for 12 days. TEER was measured daily. Prior to the experiment, both sides of the cell monolayers were washed twice with pre-warmed KRB solution, followed by 60 min equilibration in KRB at 37°C. To initiate transport studies, the incubation buffer was replaced with a solution of the relevant compound in KRB (i.e. fluorescein sodium (FNa, 50 µM), fluorescein isothiocyanate (FITC)-dextran 4,000 (FD4k, 1 mg/ml), FITC-dextran 10,000 (FD10k, 1 mg/ml), FITC-dextran 20,000 (FD20k, 1 mg/ml), FITC-dextran 70,000 (FD70k, 1 mg.ml) in the respective donor chamber. For apical-to-basolateral transport, 0.52 ml donor solution was added; for basolateral-to-apical transport, 1.52 ml. The initial donor concentration was determined by taking a 20-µl sample directly after addition of the donor fluids. The respective acceptor volumes were 1.5 ml in a-to-b and 0.5 ml in b-to-a transport studies. Cell monolayers were kept at 37°C during the experiment and 200-µl samples were drawn serially from the receiver compartments at 15, 30, 45, 60, 75 and 90 min. After each sampling, fresh transport buffer of an equal volume was

returned to the receiver side to maintain a constant volume. At the end of transport studies, another 20-µl sample was collected from the donor side for determination of mass balance. Each experiment was run at least in triplicates. TEER values were recorded before and after the transport studies, in order to verify the cell layer integrity. The plates were analysed as described above.

2.6 WESTERN BLOT ANALYSIS

Total cellular protein was isolated from confluent NCI-H441 cell monolayers. All following steps were performed on ice. Cells were lysed in cell extraction buffer (Invitrogen, Karlsruhe, Germany) supplemented with protease inhibitor cocktail (Sigma Aldrich) and sonicated twice for 10 s using a Microson-Ultrasonic-Cell Disruptor (Misonix, Farmingdale, NY). Next, cell lysates were centrifuged at 10,000 rpm for 20 min at 4°C in order to remove the cell debris. Supernatants were used for further analysis. Protein sample concentrations were determined using a standard protein assay (Bio-Rad) according to the manufacturer's instructions. Samples were stored at -80°C.

Samples were standardised to equal protein concentrations. Laemmli loading buffer composed of 2% SDS, 10% glycerol, 62.5 mM Tris-HCl, 0.0025% bromophenol blue, 5% β-mercaptoethanol, pH 6.8 was added and samples were heated to 95°C for 5 min. In total, 25 µg of protein were loaded for each sample. Samples were separated by a sodium dodecyl sulphate-polyacrylamide gel electrophoresis (SDS-PAGE, 7% acrylamide) at 120 V for 200 min and transferred to immunoblot polyvinylidene fluoride membranes (Bio-Rad) at 25 V for 30 min. Membranes were blocked with 5% bovine serum albumin (BSA) in Tris-buffered saline (0.1% Tween 20, pH 7.4) for 60 min at room temperature to avoid unspecific binding. Incubation with the MRP1 primary antibody was carried out overnight at 4°C, using a dilution of 1:5,000 in blocking buffer. After three washing steps with Tris-buffered saline (0.1% Tween 20, pH 7.4), the membrane was incubated with a solution of HRP-conjugated anti-mouse secondary antibody (1:12,500) in blocking buffer for 2 h at room temperature. Peroxidase activity was detected with Immobilon Western Chemiluminescent HRP substrate (Millipore). Analysis of the immunoblot was carried out using a ChemiDoc documentation system (Bio-Rad).

2.7 CONFOCAL LASER SCANNING MICROSCOPY

NCI-H441 cells were grown in chamber slides for 8 days. The monolayers were washed twice with 1% BSA in PBS and subsequently fixed with 500 µl of a 4% paraformaldehyde solution for 15 min. Next, cells were incubated in a 50 mM NH_4Cl solution in PBS for 15 min and afterwards permeabilised with 0.1% Triton X-100 in PBS for 8 min. The monolayers were washed 3 times with 1% BSA in PBS, followed by an incubation with 150 µl of the primary antibody (1:50 - 1:200) for 1 h at room temperature or overnight at 4°C. The cell monolayers were rinsed three times with PBS containing 1% BSA and incubated with 200 µl of a 1:200 dilution of the secondary antibody, an Alexa Fluor 488-labelled $F(ab')_2$ fragment for 30 min. Life Technology NucBlue (Bio-Sciences; 3 drops/ml) were used to counterstain cell nuclei. TRITC phalloidin (0.5 µg) was added to stabilise and stain the actin filaments. Following the 30 min incubation, cells were again washed three times with PBS containing 1% BSA and embedded in FluorSave anti-fade medium (Merck, Nottingham, UK). Images were obtained using a confocal laser scanning microscope (Zeiss LSM 510, Göttingen, Germany). The instrument's settings were adjusted so that no positive signal was observed in the channel corresponding to the fluorescence of the relevant controls.

For comparison, a fixation with ice-cold methanol at -20°C was tested. Cells were incubated in ice-cold methanol at -20°C for 12 min. After a permeabilisation with 0.1% Triton X-100 for 3 min and after three washing steps, cells were treated as described above.

2.8 STATISTICAL ANALYSIS

Each experiment was carried out at least in triplicate and was repeated three times using cells from different passages unless stated otherwise. Results were expressed as means ± SD unless mentioned otherwise. Outliers were detected by Grubb's test analysis. Two groups were compared using unpaired, two-tailed Student's t-test and f-test. $P < 0.05$ was considered significant.

3 RESULTS

Parts of this thesis contributed to the article:

The cell line NCI-H441 is a useful in vitro model for transport studies of human distal lung epithelial barrier.

Johanna J. Salomon, Viktoria E. Muchitsch, Julia C. Gausterer, Elena Schwagerus, Hanno Huwer, Nicole Daum, Claus-Michael Lehr, Carsten Ehrhardt

The article was published in Molecular Pharmaceutics (Salomon et al., 2014).

3.1 EXPRESSION AND MEMBRANE LOCALISATION OF MRP1 IN NCI-H441 CELLS

In order to determine the expression of MRP1 in NCI-H441 cells, Western blot and confocal laser scanning microscopy were employed.

3.1.1 WESTERN BLOT ANALYSIS - EXPRESSION OF MRP1 ON PROTEIN LEVELS IN NCI-H441 CELLS

When incubated with the monoclonal MRP1 antibody, NCI-H441 immunoblots revealed a prominent band corresponding to the MRP1 protein with a molar mass of 190 kDa. The analysis was performed using protein isolations from five different passage numbers of NCI-H441 cells (i.e. passage no. 54, 62, 64, 67 and 77). All passages showed a distinct clear staining, although the protein band intensity varied. Figure 4 shows a representative Western blot of MRP1 using protein isolations from different passages of NCI-H441 cells.

No other band was detected, which confirmed the selectivity of the MRP1 antibody.
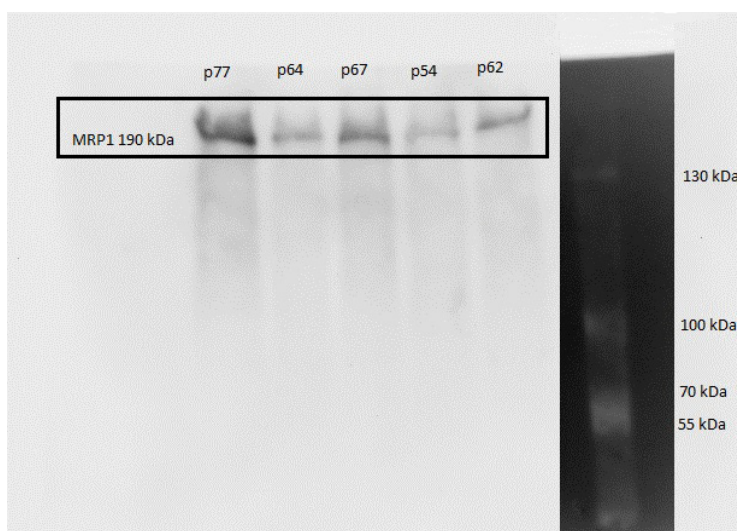
FIGURE 4

Western blot of cell lysates from NCI-H441 cells probed with MRP1 antibody (5 lanes represent protein isolations from 5 different passages). Samples were separated by a 7% polyacrylamide gel and transferred to an immunoblot polyvinylidene fluoride membrane. The molecular weight markers are shown on the left side.

3.1.2 CONFOCAL LASER SCANNING MICROSCOPY - EXPRESSION AND MEMBRANE LOCALISATION OF MRP1 IN NCI-H441 CELLS

Additionally, confocal laser scanning microscopy was carried out to investigate the expression and localisation of MRP1 in NCI-H441 cells.

Cell nuclei were counterstained with NucBlue (Life Technology) and TRITC phalloidin was added to stabilise and stain the actin filaments. A negative control was used to adjust the microscope´s settings so that no positive signal was observed in the channel corresponding to the fluorescence of MRP1.

Two different fixation methods, i.e. methanol and paraformaldehyde fixation, were tested using different dilutions of the MRP1 monoclonal antibody (1:50, 1:100, 1:200). Comparing both techniques, the fixation with paraformaldehyde worked better than the methanol fixation, since a clear staining even at higher antibody dilutions was observed. Only a minimal staining was discovered in the methanol fixation with an antibody dilution of 1:50 and no signal was observed in higher antibody dilutions. The best results were obtained with an antibody dilution of 1:50 using paraformaldahyde fixation technique.

Figure 5 shows confocal laser scanning micrographs of NCI-H441 cells labelled with the MRP1 antibody. The cells displayed a similar staining pattern which is

consistent with the localisation to the membrane. No staining was observed in the intracellular region above the nucleus. This indicates a localisation to the basolateral membrane. In Figure 5 (A) the methanol fixation was tested and the cells were incubated with an antibody dilution of 1:50. A signal for the MRP1 antibody was observed in the membrane region. The negative control is shown in the second column.

Figure 5 (B) represents cells fixed by paraformaldehyde. Three different dilutions of the MRP1 antibody (1:50, 1:100, 1:200) were used. Distinctive punctuate staining was discovered and mainly localised to the membrane region, whereas none was observed in the intracellular region above the cell nuclei. The negative control is shown in the second column.
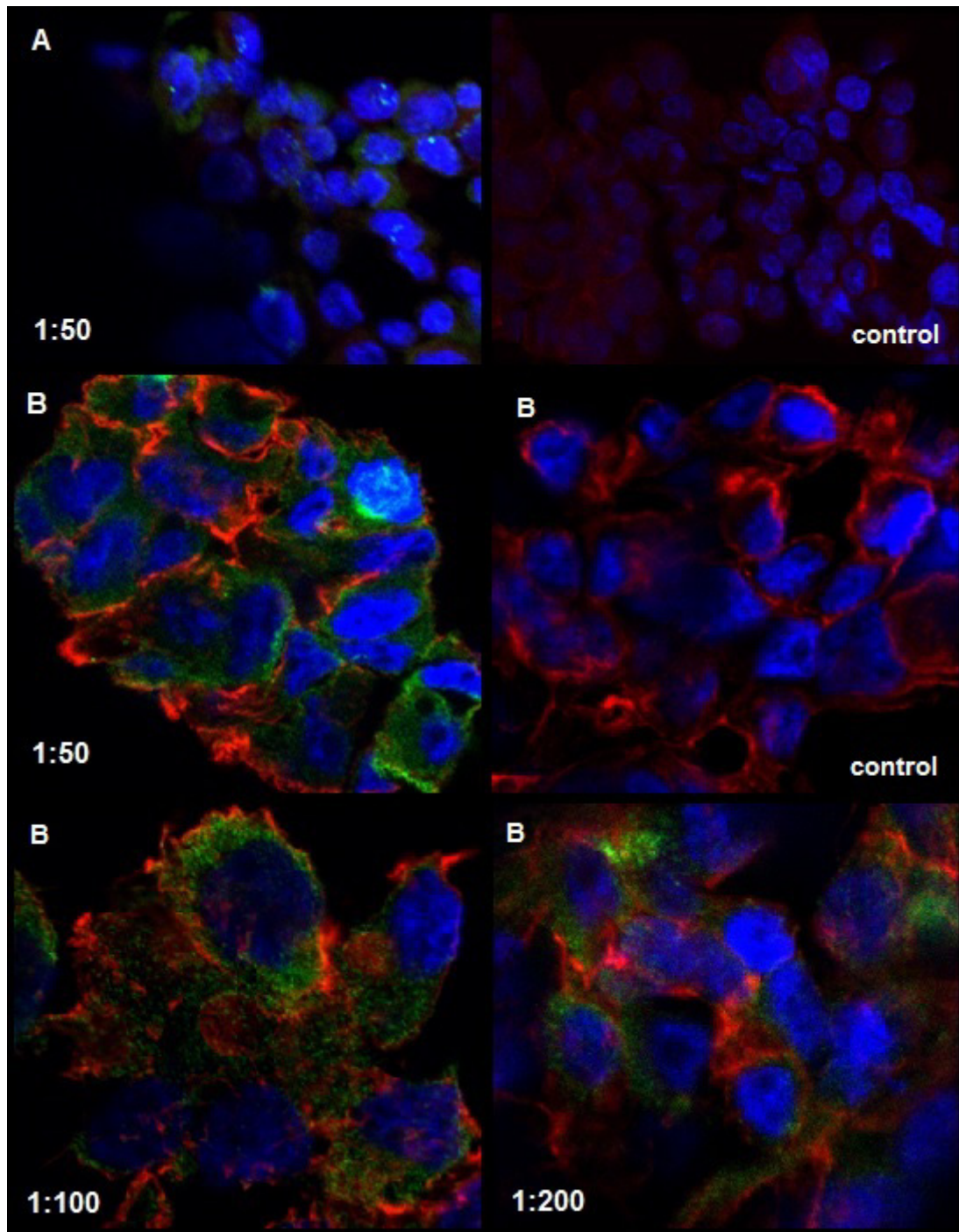
FIGURE 5

Confocal laser scanning microscopy for MRP1 in NCI-H441 cells. Cells were grown in chamber slides and were incubated with MRP1 antibody (green). Cell nuclei were counterstained by Nucblue (blue), the actin filament were stained by TRITC phalloidin (red); A: methanol fixation, 1:50; B: paraformaldehyde fixation 1;50,1:100, 1:200; the relevant negative controls are shown in the second column.

Furthermore, the membrane localisation of MRP1 was investigated by xyz-axes scans. Images are displayed in Figure 6 and 7.
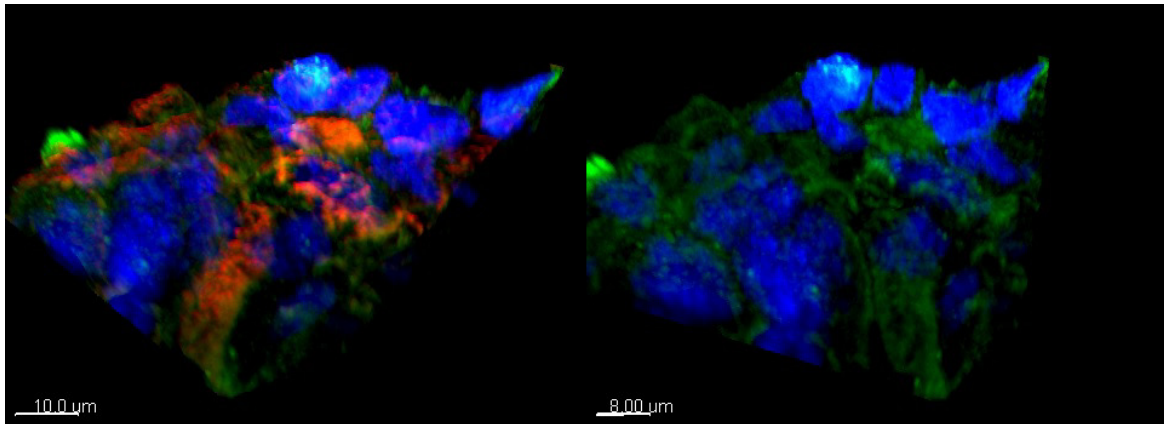
FIGURE 6

3D confocal laser scanning micrographs of z-scans showing MRP1 in NCI-H441 cells. Cells were fixed using paraformaldehyde and incubated with MRP1 antibody (1:50, green). Cell nuclei are counterstained by NucBlue (blue), actin filaments are stained by TRITC phalloidin (red), the image on the right side displays only 2 laser channels.

Figure 6 shows a distinct green staining of MRP1 in particular localised to the basolateral side of the membrane.

FIGURE 7

Different optical sections from the intracellular region towards the basolateral membrane obtained by a 2D sequential operation function us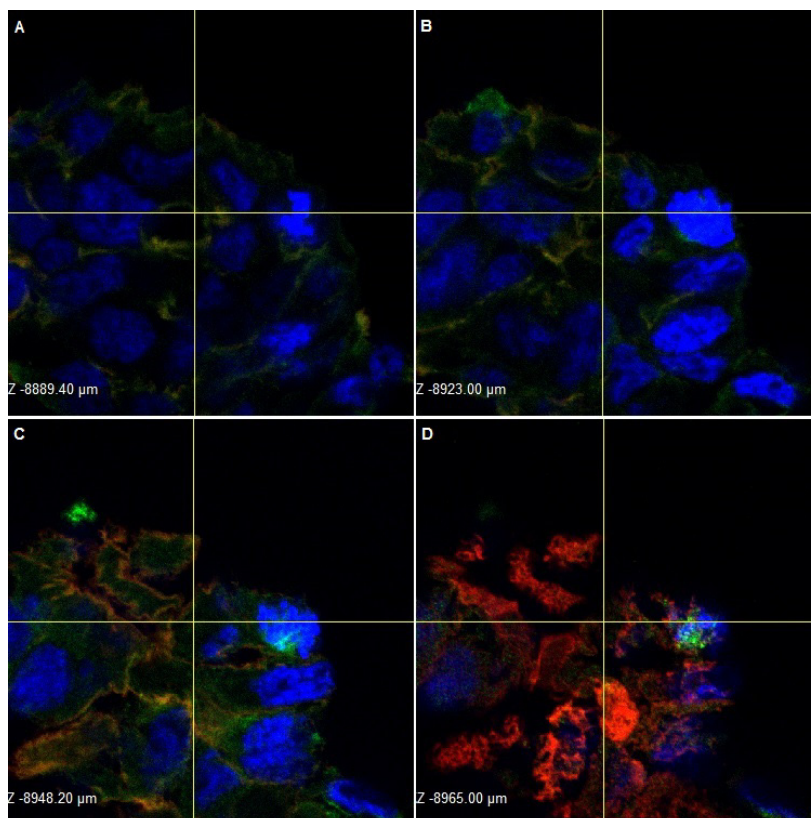ing confocal laser scanning microscopy. NCI-H441 cells were fixed using paraformaldehyde and incubated with MRP1 antibody (1:50). Cell nuclei are counterstained by NucBlue

27

Figure 7 displays different 2D optical sections obtained by z-scans in confocal laser scanning microscopy. First, in 7 (A) the intracellular region is shown. A weak activity of the MRP1 antibody (green) and a distinct staining of the cell nuclei (blue) were observed. Figures 7 (B,C) depict a distinct signal of MRP1 antibody and the cell nuclei as well as a faint staining of actin filaments (red). Figure 7 (D) shows a distinctive staining of the actin filaments implicating the proximity to the basolateral membrane but only a weak activity of MRP1 antibody and the cell nuclei.

In conclusion, Western Blot revealed the expression of MRP1 on protein level in NCI-H441 cells. Confocal laser scanning microscopy confirmed the expression and the localisation of MPR1 to the basolateral membrane of NCI-H441 cells.

3.2 FUNCTION OF MRP1 IN NCI-H441 CELLS

Generally, many transporters in cell lines are expressed, but their functional activity is unknown. Thus, uptake, release and transport studies were performed to determine the function of MRP1 in NCI-H441 cells. Additionally, transport studies were carried out to confirm the membrane localisation of MRP1.

3.2.1 UPTAKE STUDIES

Uptake studies were conducted in order to examine the intracellular uptake of 5(6)-carboxyfluorescein-diacetate. Cells were incubated for 60 min with CFDA solutions. After different time points, the CFDA solution was removed and cell monolayers were lysed in order to detect the intracellular fluorescence activity of CF. Additionally, the effect of the inhibitor MK-571 on the CFDA uptake was tested.

Figure 8 compares the CFDA uptake to the additional application of 20 µM MK-571 in NCI-H441 cell monolayers. Data are presented in Table 3.
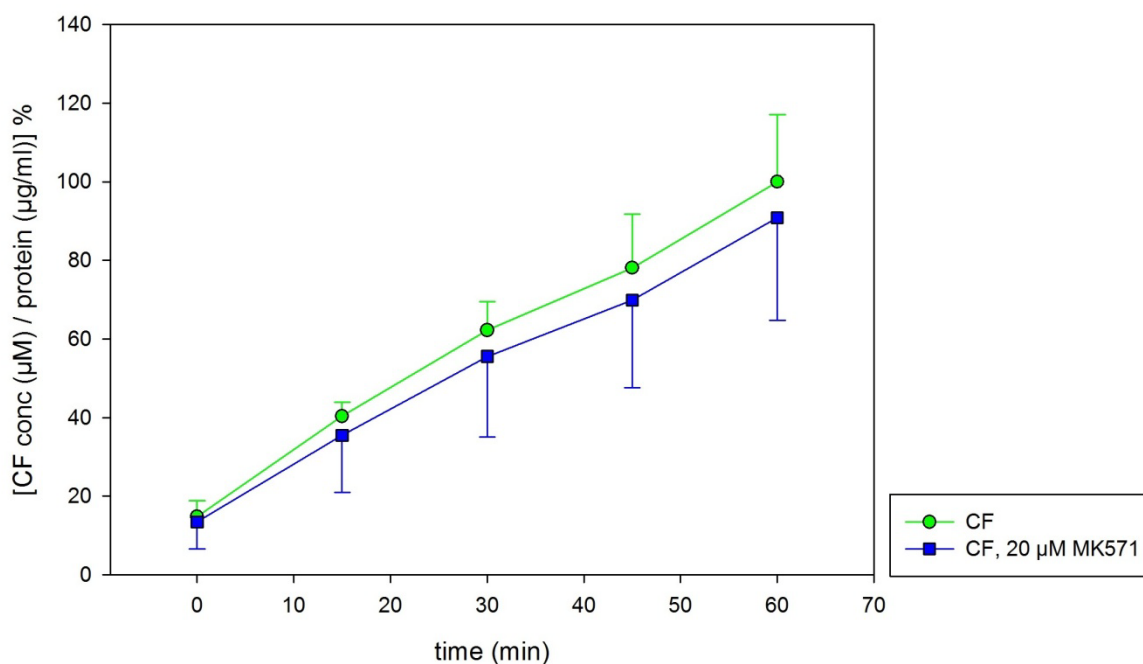
FIGURE 8

Linear and time dependent CFDA uptake in NCI-H441 cells grown on 24 well plates. The inhibitor MK-571 did not significantly alter the uptake. Results are expressed as means ± SD (CFDA n = 16, MK-571 n = 12), $P < 0.05$.

Time (min)	CFDA CF ± SD (%)	n	CFDA, 20 µM MK-571 CF ± SD (%)	n	P
0	14.82 ± 4.07	16	13.51 ± 6.84	12	0.5334
15	40.34 ± 3.63	16	35.48 ± 14.45	12	0.2058
30	62.20 ± 7.25	16	55.56 ± 20.54	12	0.2397
45	78.12 ± 13.64	16	69.87 ± 22.20	12	0.2353
60	100.00 ± 17.05	16	90.82 ± 26.08	12	0.2704

TABLE 3

Data of CFDA uptake studies plus 20 µM MK-571 in NCI-H441 cells.

Figure 8 displays a linear and time-dependent uptake of CFDA in NCI-H441 cells. Addition of the MRP inhibitor MK-571 did not result in a statistical significant decrease in CFDA uptake, which was unexpected, due to the fact that MRP1 function as an efflux transporter.

3.2.2 RELEASE STUDIES

In order to determine the MRP1-mediated efflux of 5(6)-carboxyfluorescein (CF), NCI-H441 cells were loaded for 60 min with CFDA. Afterwards, the CFDA solution was replaced by KRB or KRB plus MRP inhibitor MK-571 in different concentrations (10 µM, 20 µM, 50 µM). Lysed cell monolayers were used to detect

the intracellular fluorescence activity of CF and samples of the supernatant were analysed to determine the MRP1-mediated efflux of CF.

In Figure 9 the efflux of CF from NCI-H441 cells was examined. Cell monolayers showed time-dependent release of the fluorescent probe. However, a statistical significant retention was discovered while adding the MRP1 inhibitor MK-571 at different concentrations, consistent with the inhibition of the MRP1-mediated efflux of CF in the cells.

At the same time, in the supernatants' linear and time-dependent increases in CF concentrations were detected, which could be inhibited by all tested MK-571 concentrations. Statistical significant differences were found in every tested sample at all points in time.
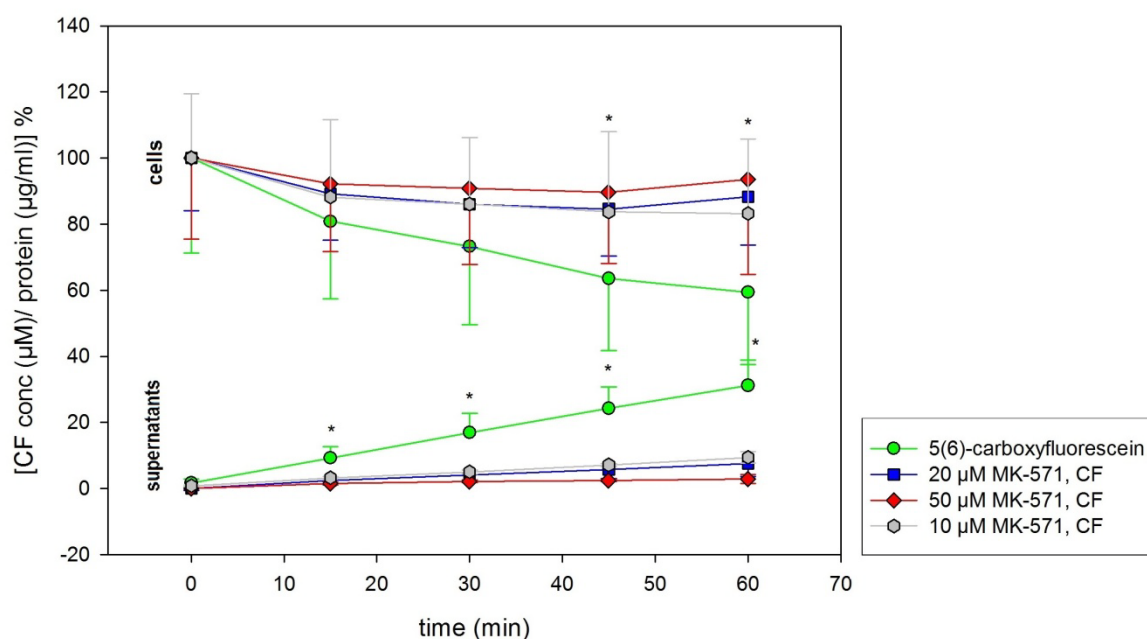
FIGURE 9

Time-dependent and linear CF release from NCI-H441 cells grown in 24-well plates. The supernatants and the lysed cell monolayers were analysed. MK-571 (10 µM, 20 µM and 50 µM) significantly inhibited the MRP1 mediated efflux of CF detected in the supernatant at all particular points in time. The efflux of CF tested in lysed cell monolayers was significantly diminished by all tested concentrations of MK-571 at 45 and 60 min. Results are expressed as means ± SD (CF n = 50-54, MK-571 n = 6). Statistical significance is expressed as *, $P < 0.05$.

T (min)	CFDA, CF ± SD (%)	N	10 µM MK-571, CF ± SD (%) n = 6	P	20 µM MK-571, CF ± SD (%) n = 6	P	50 µM MK-571, CF ± SD (%) n = 6	P
Cells								
0	100.00 ± 28.74	53	100.0 ± 19.49	1.000	100.00 ± 15.89	1.000	100.00 ± 24.51	1.000
15	80.82 ± 23.45	53	88.16 ± 23.45	0.4704	89.20 ± 14.05	0.3967	92.09 ± 20.34	0.2640
30	73.24 ± 23.64	54	86.03 ± 20.17	0.2084	86.05 ± 13.16	0.1993	90.82 ± 22.95	0.0885
45	63.55± 21.83	52	83.70 ± 24.25	*0.0386*	84.59 ± 14.29	*0.0255*	89.58 ± 21.51	*0.0076*
60	59.39 ± 21.88	54	83.20± 22.55	*0.0144*	88.21 ± 14.55	*0.0027*	93.55 ± 28.71	*0.0008*
Supernatants								
0	0.00 ± 1.11	52	0.00 ± 0.23	1.000	0.00 ± 0.62	1.000	0.00 ± 0.29	1.000
15	7.56 ± 3.33	52	2.40 ± 0.36	*0.0004*	2.48 ± 1.02	*0.0005*	1.61 ± 0.43	*< 0.0001*
30	15.23 ± 5.77	53	4.20 ± 0.65	*< 0.0001*	4.06 ± 2.25	*< 0.0001*	2.17 ± 0.38	*< 0.0001*
45	22.51 ± 6.61	50	6.29 ± 0.44	*< 0.0001*	5.74 ± 2.75	*< 0.0001*	2.51 ± 0.42	*< 0.0001*
60	29.48 ± 7.75	53	8.59 ± 1.74	*< 0.0001*	7.53 ± 3.91	*< 0.0001*	2.86 ± 1.33	*< 0.0001*

TABLE 4

Data of CF release studies plus MK-571 (10, 20 and 50 µM) in NCI-H441 cells.

Comparing the CF efflux in KRB without inhibitor to KRB plus 10 µM MK-571, 20 µM MK-571 or 50 µM MK-571, the administration of the MRP inhibitor MK-571 significantly influenced the retention from the cell monolayers (Table 4). Significant increases to the level of 83.70 ± 24.25% (10 µM MK-571), 84.59 ± 14.29% (20 µM MK-571) and 89.58 ± 21.51% (50 µM MK-571) CF were detected at 45 min. Further significant elevations in the percentage of the fluorophore were observed at 60 min (10 µM MK-571: 83.20± 22.55%, 20 µM MK-571: 88.21 ± 14.55%, 50 µM MK-571: 93.55 ± 28.71%).

In total, over 60 min a MRP1-mediated efflux of 40.61 ± 23.91% CF was observed, whereas the inhibition of MRP1 by MK-571 led to a reduction to the level of 6.45 ± 23.60% (50 µM MK571). Hence, an almost complete inhibition of MRP1 by 50 µM MK-571 was observed during 60 min.

Additionally, in the supernatants' significant differences were detected at all points in time (Table 4). Finally, after 60 min, the percentage of fluorophore in the KRB was 29.48 ± 7.75% in comparison to the addition of MK-571 to KRB, which attenuated the CF concentrations to 8.59 ± 1.74% (10 µM MK-571), 7.53 ± 3.91% (20 µM MK-571) or 2.86 ± 1.33% (50 µM MK-571).
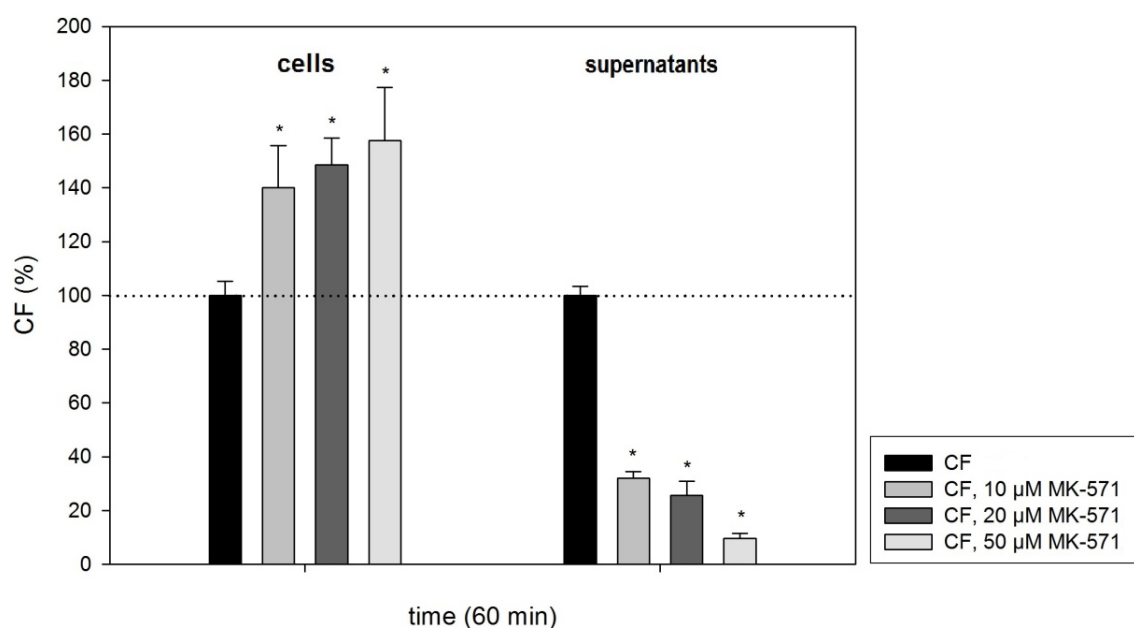
FIGURE 10

Comparison of the CF concentrations in lysed cell monolayers and supernatants at 60 min. Addition of the MRP1 inhibitor MK-571 significantly alters the CF concentrations in the cells and the supernatants. The dotted line symbolises the level of the control and represents the CF concentrations in cells and supernatants without inhibitor expressed as 100%. Results are expressed as means ± standard error (SE) (CF n = 54, 53, MK-571 n = 6). Statistical significance is noted as * ($P < 0.05$).

CFDA, CF ± SE (%)	CFDA, 10 µM MK-571, CF ± SE (%)	CFDA, 20 µM MK-571, CF ± SE (%)	CFDA, 50 µM MK-571, CF ± SE (%)
Cells			
100.00 ± 5.11	140.09 ± 15.50	148.52 ± 10.00	157.51 ± 19.73
Supernatants			
100.00 ± 3.41	31.98 ± 2.41	25.54 ± 5.41	9.71 ± 1.84

TABLE 5

Data of CFDA release studies plus 10, 20 or 50 µM MK-571. CF without inhibitor is expressed as 100%.

Figure 12 displays the concentrations of CF in the cells and supernatants in CFDA release studies expressed as 100% in comparison to the alterations observed by the addition of different concentrations of MK-571 at 60 min.

In cell monolayers the administration of MK-571 increased the accumulation by 40.09 ± 10.30% (10 µM MK-571), 48.52 ± 7.56% (20 µM MK-571) and 57.51 ± 12.42% (50 µM MK-571), respectively. At the same time, the addition of MK-571 decreased the levels of the fluorophore in the supernatants by 68.02 ± 2.91% (10 µM MK-571), 74.46 ± 4.41% (20 µM MK-571) and 90.29 ± 2.62% (50 µM MK-571), respectively. The changes in the detected CF concentrations in the cell

monolayers and the supernatants were significantly different from the effect observed in KRB without inhibitors.

In summary, the release studies revealed the function of the MRP1-mediated efflux in NCI-H441. The application of 50 µM MK-571 led to the highest (and significant) inhibition of MRP1-mediated efflux after 60 min, indicating an almost complete blocking of MRP1.

3.2.3 TRANSPORT STUDIES

In order to examine the MRP1-mediated bidirectional transport of CF in NCI-H441 cells, transport studies were performed using NCI-H441 cells grown in Transwell Clear inserts for 10 days. Additionally, these transport studies were employed to confirm the membrane localisation of MRP1.

The calculated apparent permeability coefficients (P_{app}) are shown in Figure 11 and in Table 6.
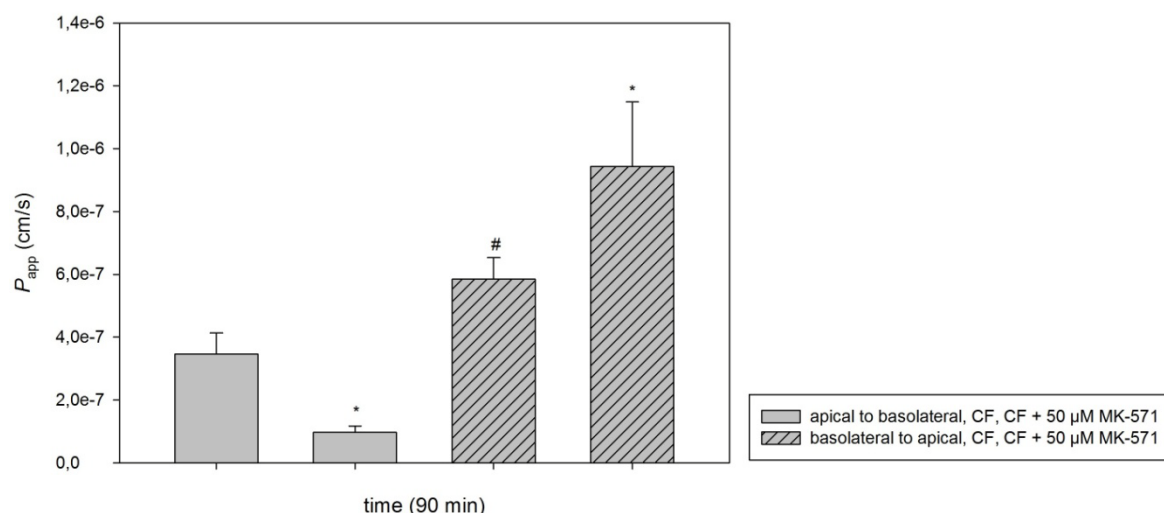
FIGURE 11

Bidirectional transport of CFDA in NCI-H441 cells grown in Transwell Clear inserts for 10 days. The calculated P_{app} of the CF transport without inhibitor is displayed on the left bar in both directions. MK-571 (50 µM) significantly altered the transport in both directions. Results are expressed as means ± SD. Comparing the CF transport to the CF transport plus MK-571, statistical significant differences are expressed as * ($P < 0.05$, $n = 3$). Concerning the CF transport, statistical differences between both transport directions are expressed as # ($P < 0.05$, $n = 3$).

CFDA, a-b $P_{app} \pm$ SD (cm/s)	CFDA, 50 µM MK-571 a-b $P_{app} \pm$ SD (cm/s)	P (*) a-b	CFDA, b-a $P_{app} \pm$ SD (cm/s)	CFDA, 50 µM MK-571 b-a $P_{app} \pm$ SD (cm/s)	P (*) b-a	P (#) CFDA
$3.47{*}10^{-7} \pm$ $6.73{*}10^{-8}$	$9.73{*}10^{-8} \pm 2.07{*}10^{-8}$	0.0036	$5.85{*}10^{-7} \pm$ $6.94{*}10^{-8}$	$9.43{*}10^{-7} \pm 2.06{*}10^{-7}$	0.0463	0.013

TABLE 6

Calculated apparent permeability coefficients of CFDA transport and CFDA plus MK-571 in NCI-H441 cells.

Across NCI-H441 monolayers, the P_{app} of CF in the apical-to-basolateral (a-b) direction was $3.47{*}10^{-7} \pm 6.73{*}10^{-8}$ cm/s (n = 3) in comparison to $5.85{*}10^{-7} \pm 6.94{*}10^{-8}$ cm/s (n = 3) in the basolateral-to-apical (b-a) direction. A statistical relevant difference was observed between the a-b and the b-a direction.

Moreover, the addition of the MRP inhibitor MK-571 (50 µM) significantly altered the transport in both directions. In the a-b direction a significant reduction in the transport was observed, as expected, due to the localisation of MRP1 to the basolateral membrane. In terms of the CF transport, the addition of 50 µM MK-571 attenuated the speed to $9.73{*}10^{-8} \pm 2.07{*}10^{-8}$ cm/s (n = 3). Interestingly, a significant increase in the transport from the b-a direction was detected. The administration of 50 µM MK-571 accelerated the transport to P_{app} $9.43{*}10^{-7} \pm 2.06{*}10^{-7}$ cm/s (n = 3). Additionally, a statistical significant difference was detected between both transport directions.

Regarding the b-a transport, an intracellular accumulation of CF was expected due to the fact that the relevant transporter was inhibited. However, an increase of CF in the apical compartment was observed. Therefore, it was considered that another apical transporter protein, which does not belong to the MRP transporter family, might be involved in the CF transport.

Moreover, the intracellular fluorescence activity of CF in the cell monolayers was detected after the end of the transport study. Hence, the cells were lysed and transferred to a 24-well plate. The results are shown in Figure 12.
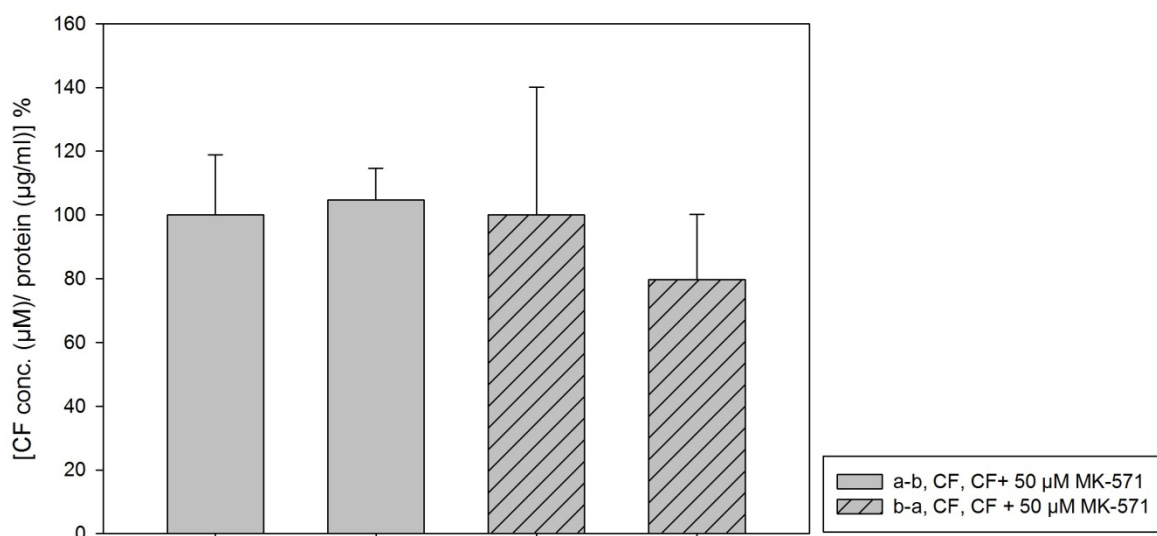
FIGURE 12

Intracellular concentration of CF detected in the lysed cells after the end of the transport study in a 24-well plate ($P < 0.05$, $n = 3$).

Although the addition of 50 µM MK-571 led to increased intracellular fluorescence in the a-b direction (104.64 ± 10.06%) and a loss in the fluorescence intensities in the b-a direction (79.78 ± 20.35%), no statistical significant differences were observed due to the high standard deviations.

3.3 APICAL TRANSPORTER IS INVOLVED IN THE TRANSPORT AND EFFLUX OF 5(6)-CARBOXYFLUORESCEIN

3.3.1 TRANSPORT STUDIES

In regard to the results mentioned in the previous paragraph, another apically localised transporter might be involved in the CF transport. Endter *et al*. stated a moderate expression of the organic anion transporter 4 (OAT4) in several human lung epithelial cell culture models (Endter et al., 2009). Additionally, OAT4 is expressed on the apical membrane in human kidneys (Hagos et al., 2007). Up to the present, the membrane localisation of OAT4 in the human lung is unknown. Therefore, the impact of 10 µM telmisartan, an inhibitor of OAT4, on the CF transport in NCI-H441 cells was tested (Burckhardt, 2012).

The calculated apparent permeability coefficients (P_{app}) are shown in Figure 13 and Table 11.

FIGURE 13

Influence of the OAT4 inhibitor telmisartan (10 µM) on the CF transport in NCI-H441 cells. Results are expressed as means ± SD ($n = 3$). Significant differences are expressed as * ($P < 0.05$).

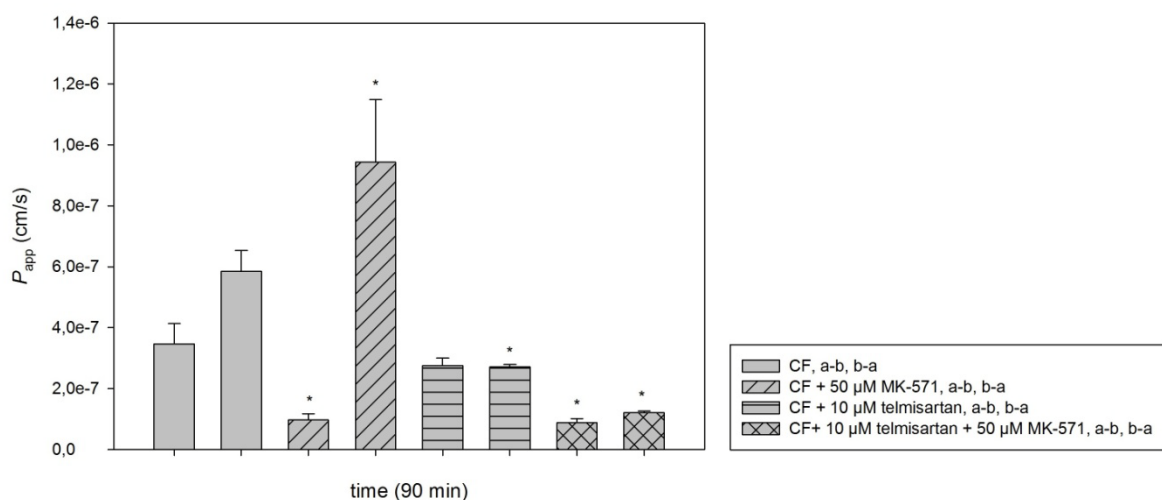| CFDA, 10 µM telmisartan a-b $P_{app} \pm SD$ (cm/s)	P	CFDA, 10 µM telmisartan b-a $P_{app} \pm SD$ (cm/s)	P	CFDA, 10 µM telmisartan, 50 µM MK-571 a-b $P_{app} \pm SD$ (cm/s)	P	CFDA, 10 µM telmisartan, 50 µM MK-571 b-a $P_{app} \pm SD$ (cm/s)	P
$2.76*10^{-7} \pm 2.47*10^{-8}$	0.1616	$8.78*10^{-8} \pm 1.42*10^{-8}$	0.0015	$8.78*10^{-8} \pm 1.42*10^{-8}$	0.0028	$1.21*10^{-7} \pm 5.21*10^{-9}$	0.0003

TABLE 7

Data of the CF transport plus telmisartan and telmisartan plus MK-571 in NCI-H441 cells.

Addition of 10 µM telmisartan significantly reduced the P_{app} in the b-a direction to $8.78*10^{-8} \pm 1.42*10^{-8}$ cm/s ($n = 3$) in comparison to $5.85*10^{-7} \pm 6.94*10^{-8}$ cm/s ($n = 3$), whereas the a-b direction was not altered in a statistically significant way (P_{app} telmisartan $2.76*10^{-7} \pm 2.47*10^{-8}$ cm/s ($n = 3$) vs. $3.47*10^{-7} \pm 6.73*10^{-8}$ cm/s ($n = 3$)). No statistical difference was observed between both transport directions.

Moreover, the effect of the addition of both inhibitors, 50 µM MK-571 and 10 µM telmisartan, was tested. In NCI-H441 monolayers a significant reduction of the transport in both directions was observed. The addition of both inhibitors reduced the P_{app} in the a-b direction to $8.78*10^{-8} \pm 1.42*10^{-8}$ cm/s ($n = 3$) compared to $1.21*10^{-7} \pm 5.21*10^{-9}$ cm/s ($n = 3$) in the b-a direction.

36

MK-571 predominantly reduced the a-b transport while telmisartan attenuated the b-a transport. This supports the assumption of an involvement of OAT4 in the b-a transport of CF as well as the apical expression of OAT4 in NCI-H441 cells.

In summary, the addition of both inhibitors, MK-571 and telmisartan, significantly diminished the CF transport in both directions.

3.3.2 EFFLUX STUDIES

The following release studies investigated the effect of telmisartan on the CF efflux from NCI-H441 cells and were carried out by Sergey Zaichik.
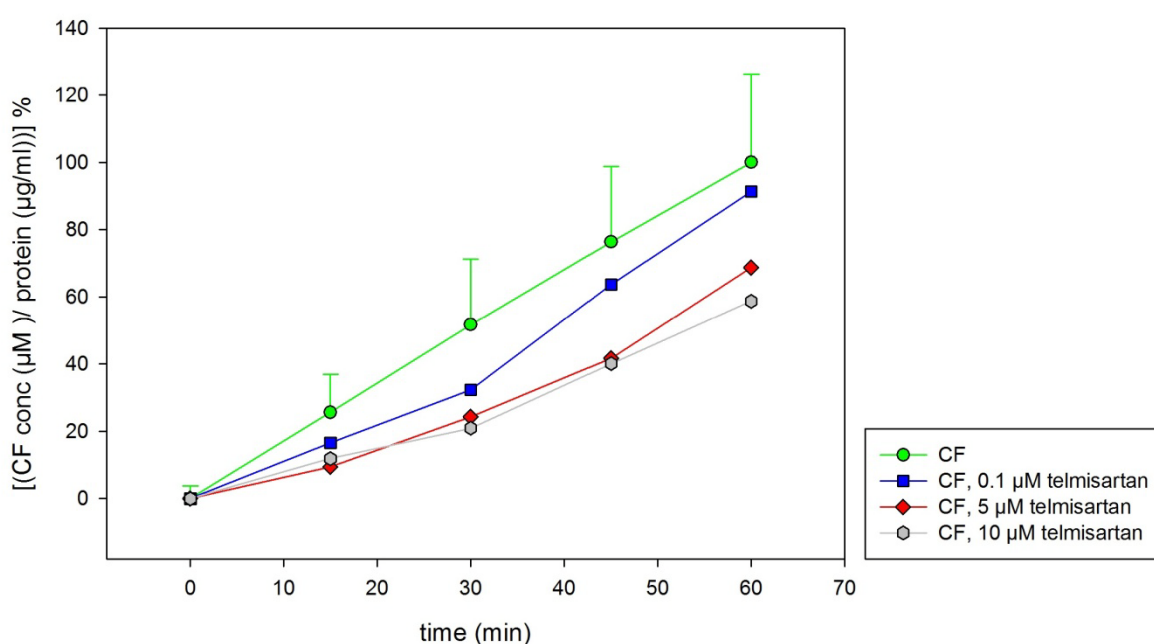
FIGURE 14

Influence of 0.1, 5 and 10 μM telmisartan on the CF efflux in NCI- H441 cells. Only supernatants were shown and CF in KRB without temisartan is expressed as 100%. Addition of 5 and 10 μM telmisartan significantly reduced the CF concentration in the supernatants. Results are expressed as means ± SD (CFDA) or as means (telmisartan) (CF n = 50-53, telmisartan n = 2).

Time (min)	CFDA CF ± SD (%)	N	CFDA, 0.1 μM telmisartan CF (%) n = 2	CFDA, 5 μM telmisartan CF (%) n = 2	CFDA, 10 μM telmisartan CF (%) n = 2
0	0.000 ± 3.751	52	0.00	0.00	0.00
15	25.65 ± 11.29	52	16.59	9.42	11.92
30	51.67 ± 19.58	53	32.31	24.33	20.92
45	76.38 ± 22.43	50	63.67	41.70	40.14
60	100.0 ± 26.29	53	91.32	68.82	58.72

TABLE 8

Figure 14 shows reductions in the CF concentration in the supernatants caused by the administration of 5 and 10 µM telmisartan, while the addition of 0.1 µM telmisartan did not influence the retention of the fluorophore. However, due to the small number of repetitions (n = 2), no statistical analysis could be performed.

Addition of 5 µM and 10 µM telmisartan diminished the CF efflux resulting in decreased amounts of the fluorescent probe in the supernatants. Data are shown in Table 8.

In total, reductions of the concentration of fluorophore by 41.28% were observed. In comparison to the effect observed by the addition of the MRP inhibitor MK-571, the reductions were less pronounced.

Unfortunately, this study was only performed twice so that the significance had to be assessed with caution.

3.4 EFFECT OF POTENTIAL MODULATORS OF THE MRP1 FUNCTION ON THE CF EFFLUX FROM NCI-H441 CELLS

A side project of this thesis was concerned with determining the effect caused by respective activators or inhibitors of MRP1 in NCI-H441 cells.

3.4.1 VERAPAMIL

Several reports in the literature stated a stimulating effect of verapamil on MRP1-mediated GSH transport in different human cell culture models, however, verapamil itself is not transported by MRP1 and has a weak inhibitory effect on MRP1 (Loe et al., 2000; Perrotton et al., 2007). Moreover, verapamil is a known inhibitor of P-glycoprotein and interacts with other transporters as well. Thus, verapamil can be seen as a broad-spectrum inhibitor. The objective was to investigate the impact of 50 µM verapamil on the MRP1-mediated CF transport in NCI-H441 cells. Results are shown in Figure 15 and in Table 9.
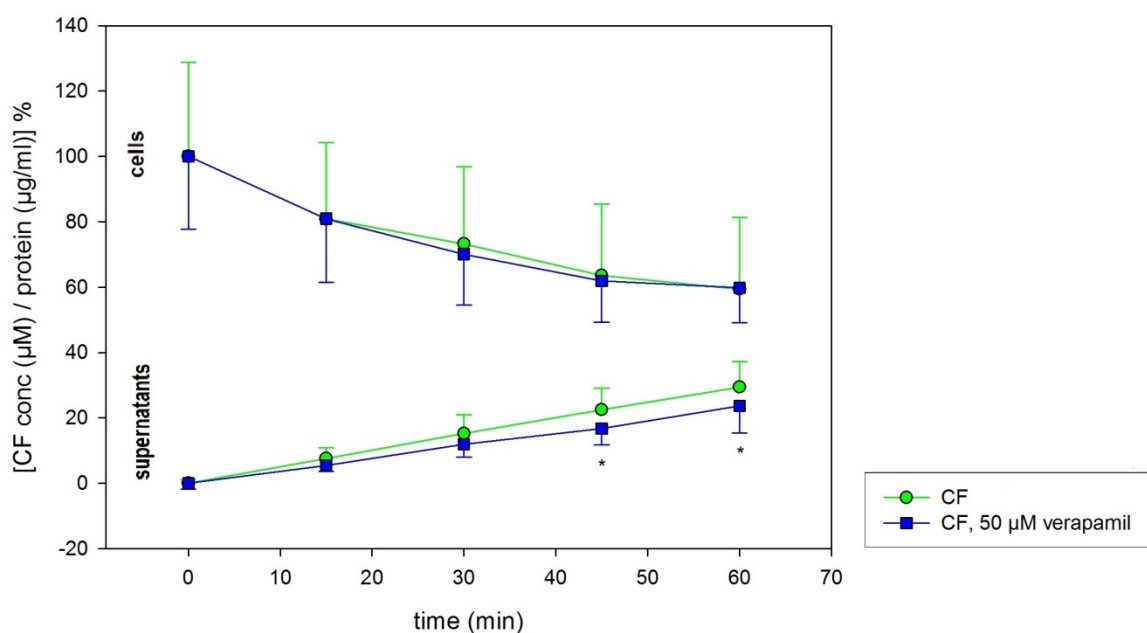
FIGURE 15

Impact of verapamil on the CF efflux. Significant differences were observed in the supernatants at 45 and 60 min. Results are expressed as means ± SD (CF n = 50-54, verapamil n = 9-10). Significant differences were expressed as * (P < 0.05).

Time (min)	CFDA CF ± SD (%)	N	CFDA, 50 µM verapamil CF ± SD (%)	N	P
			Cells		
0	100.0 ± 28.74	53	100.0 ± 22.87	9	1.000
15	80.82 ± 23.45	53	80.96 ± 19.98	9	0.9869
30	73.24 ± 23.64	54	70.12 ± 15.98	9	0.7052
45	63.55 ± 21.83	52	61.94 ± 13.12	9	0.8320
60	59.39 ± 21.88	54	59.92 ± 11.20	10	0.9412
			Supernatants		
0	0.00 ± 1.11	52	0.00 ± 1.79	9	1.000
15	7.56 ± 3.32	52	5.51 ± 1.98	9	0.0795
30	15.23 ± 5.77	53	11.97 ± 4.08	9	0.1100
45	22.51 ± 6.61	50	16.72 ± 5.14	9	0.0157
60	29.48 ± 7.75	53	23.67 ± 8.47	10	0.0362

TABLE 9

Data of CFDA release studies plus 50 µM verapamil.

The addition of 50 µM verapamil had no effect on the retention of CF from the cell monolayers. No statistical significant differences were observed. Interestingly, in the supernatants significant decreases in the concentration of the fluorophore were detected at 45 (16.72 ± 5.14%, n = 9) and 60 min (23.67 ± 8.47%, n = 10).

39

Despite the fact that verapamil has been reported to be an inducer of MRP1-mediated GSH transport, no stimulating effects on MRP1-mediated efflux of CF were detected in NCI-H441 cells. However, as expected, a slight but statistically significant inhibitory impact was discovered.

3.4.2 INDOMETHACIN

In the literature, indomethacin has been reported as an inhibitor of MRP1-mediated transport (de Groot et al., 2007). The impact of the administration of 10 µM indomethacin on the MRP1-mediated CF transport was examined in release studies. Results are shown in Figure 16 and Table 10.

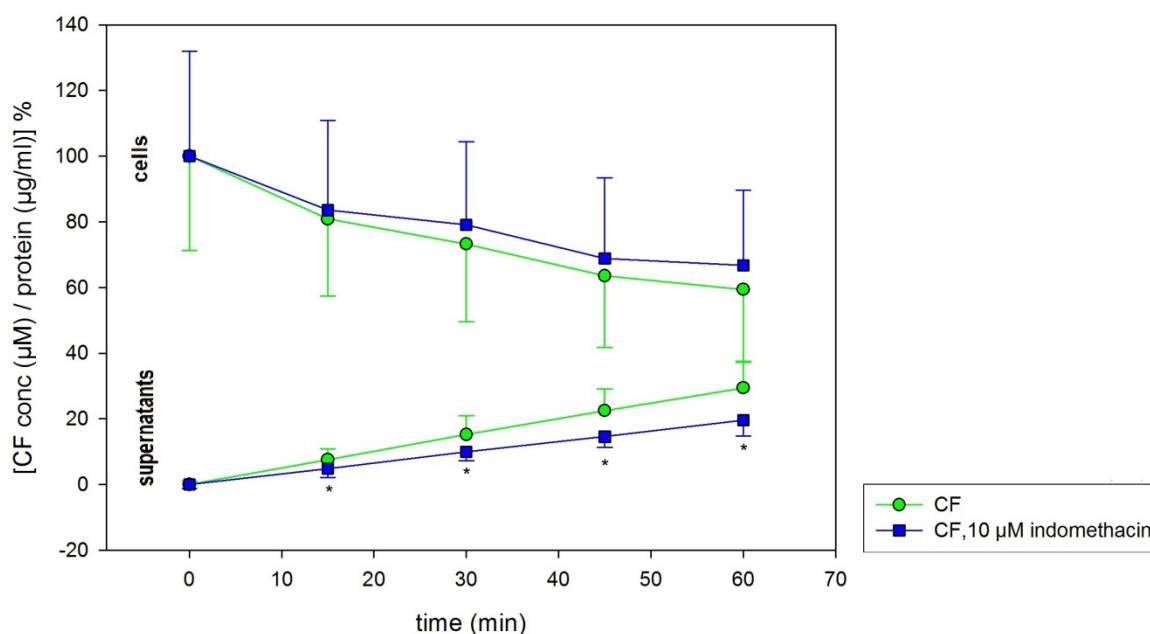**FIGURE 16**

Significant decreases of the CF concentration were observed in all tested supernatant samples. Results are expressed as means ± SD (CF n = 50-54, indomethacin n = 9-14). Statistically significance is expressed as * (P < 0.05).

Time (min)	CFDA CF ± SD (%)	N	CFDA, 10 µM indomethacin CF ± SD (%)	N	P
			Cells		
0	100.00 ± 28.74	53	100.00 ± 31.89	12	1.000
15	80.82 ± 23.45	53	83.51 ± 27.27	12	0.7288
30	73.24 ± 23.64	54	79.05 ± 25.29	12	0.4493
45	63.55 ± 21.83	52	68.79 ± 24.62	12	0.4670
60	59.39 ± 21.88	54	66.67 ± 23.00	14	0.2766
			Supernatants		
0	0.00 ± 1.11	52	0.00 ± 1.25	9	1.000
15	7.56 ± 3.33	52	4.91 ± 2.73	9	0.0276
30	15.23 ± 5.77	53	9.95 ± 2.76	9	0.0095
45	22.51 ± 6.61	50	14.58 ± 3.21	9	0.0009
60	29.48 ± 7.75	53	19.64 ± 4.90	10	0.0003

TABLE 10

Data of CFDA release studies plus 10 µM indomethacin.

The addition of 10 µM indomethacin did not alter CF accumulation in the cell monolayers in a statistical significant way. Nevertheless, in the supernatants statistical significant attenuations were detected at all tested points in time (Table 10). In comparison to KRB, the addition of indomethacin to KRB decreased the amount of fluorophore to 19.64 ± 4.90% CF (n = 10) at end of the study.

In summary, data show an inhibitory effect of indomethacin on the transport of CF in NCI-H441 cells.

3.4.3 QUINIDINE

Furthermore, literature stated an inhibitory influence of quinidine on MRP1-mediated transport in human lung epithelial cell cultures (Hamilton et al., 2001). In addition, quinidine was also reported to be an inhibitor of P-gp and the OCT/N family. In order to investigate the impact of 100 µM quinidine on the MRP1-mediated transport in NCI-H441 cells, CFDA release studies were conducted. Results are demonstrated in Figure 17 and in Table 11.
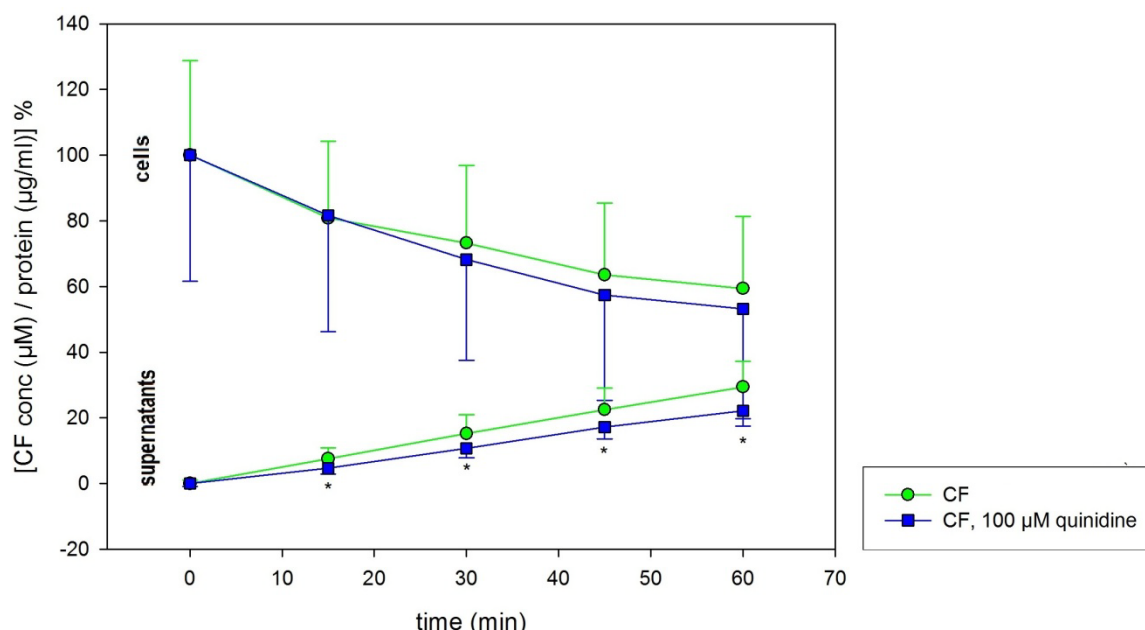
FIGURE 17

Quinidine significantly reduced the CF concentration in the supernatants at all tested samples. Results are expressed as means ± SD (CF *n* = 50-54, quinidine *n* = 9-11) Statistical significance is noted as * (*P* < 0.05).

Time (min)	CFDA CF ± SD (%)	*N*	CFDA, 100 µM quinidine CF ± SD (%)	*N*	*P*
			Cells		
0	100.00 ± 28.74	53	100.00 ± 38.33	9	1.000
15	80.82 ± 23.45	53	81.59 ± 35.26	9	0.9331
30	73.24 ± 23.64	54	68.16 ± 30.67	9	0.5698
45	63.55 ± 21.83	52	57.44 ± 32.05	9	0.4743
60	59.39 ± 21.88	54	53.16 ± 35.69	11	0.4466
			Supernatants		
0	0.00 ± 1.11	52	0.00 ± 0.94	9	1.000
15	7.56 ± 3.33	52	4.63 ± 1.81	9	*0.0127*
30	15.23 ± 5.77	53	10.68 ± 2.88	9	*0.0246*
45	22.51 ± 6.61	50	17.15 ± 3.52	9	*0.0215*
60	29.48 ± 7.75	53	22.18 ± 2.42	11	*0.0031*

TABLE 11

Data of CFDA release studies plus 100 µM quinidine.

No statistical significant alterations were detected in the lysed cell monolayers due to high standard deviations.

However, at the same time significant differences were observed in all supernatant samples at all points in time (Table 11). At the end of the study, addition of 100 µM quinidine to KRB resulted in reductions of the CF concentration to the level of 22.18 ± 2.42% (*n* = 11) compared to 29.48 ± 7.75% in KRB (*n* = 53).

In summary, an inhibitory effect of quinidine on the CF release from NCI-H441 cells was detected.

3.4.4 COMPARISON OF THE EFFECTS EXHIBITED BY THE ALLEGED INHIBITORS OR ACTIVATORS OF MRP1 FUNCTION

Figure 18 provides an overview on the impact of different substances on the CF efflux. Data are shown in Table 12.
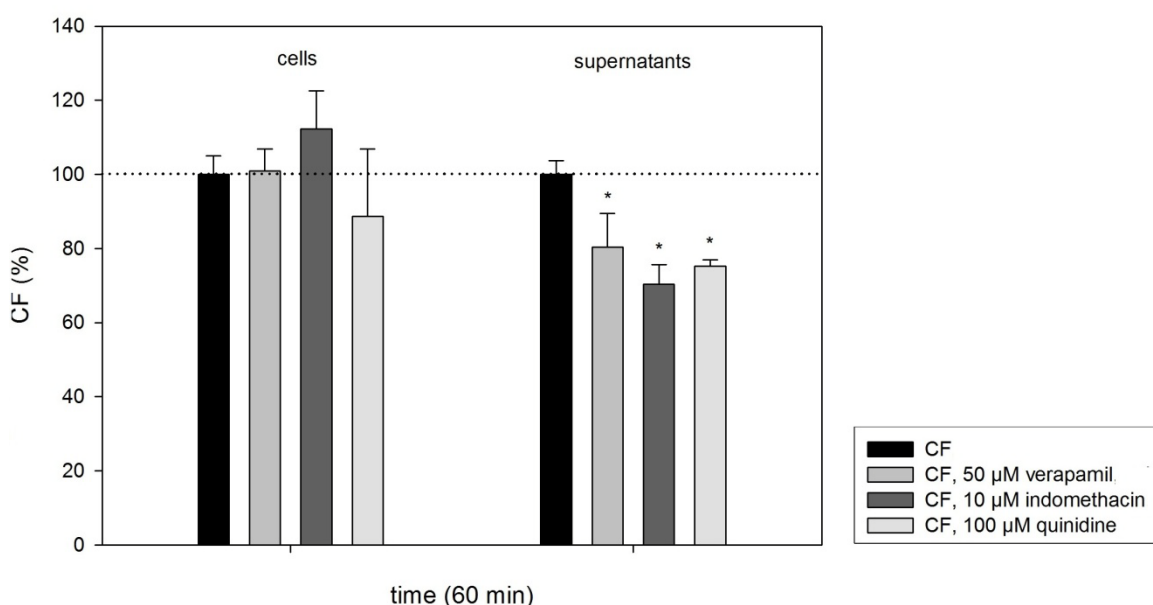
FIGURE 18

Comparison of inhibitory effects on MRP1-mediated CF efflux. The dotted line symbolises the CF release in cells and supernatants without inhaled glucocorticoids, which is expressed as 100%. Results are presented as means ± SE (CF n = 54, 53, verapamil n = 10, indomethacin n = 14,10, quinidine n = 11). Statistical significance is expressed as * ($P < 0.05$).

CFDA CF ± SE (%)	CFDA, 50 µM verapamil CF ± SE (%)	CFDA, 10 µM indomethacin CF ± SE (%)	CFDA, 100 µM quinidine CF ± SE (%)
Cells			
100.00 ± 5.01	100.89 ± 5.96	112.25 ± 10.35	88.72 ± 18.12
Supernatants			
100.00 ± 3.61	80.31 ± 9.09	70.32 ± 5.26	75.25 ± 1.74

TABLE 12

Data of release studies. CF without inhibitors is expressed as 100%.

Figure 18 compares the responses in the CF transport to the application of 50 µM verapamil, 10 µM indomethacin and 100 µM quinidine. The concentrations of the fluorophore in the cell monolayers and in the supernatants in CFDA release

studies were expressed as 100%. In the cell monolayers, no significant alterations were detected. Addition of 50 µM verapamil resulted in a minimal increase in the level of CF by $0.89 \pm 8.86\%$ (SE) (n = 10) as well as the administration of indomethacin by $12.25 \pm 11.89\%$ (SE) (n = 14). In regard to quinidine an unexpected reduction of the amount of fluorophore by $11.28 \pm 17.46\%$ (SE) (n = 11) was observed, which could be explained by rather high standard deviations.

In contrast, significant decreases were observed in the supernatant samples. Addition of verapamil attenuated the levels of the fluorescent probe by $19.69 \pm 4.60\%$ (SE) (n = 10), indomethacin by $29.68 \pm 3.19\%$ (SE) (n = 10) and quinidine by $24.75 \pm 2.37\%$ (SE) (n = 11). All three effects were significantly different from the CF efflux without inhibitors in NCI-H441 cells.

In summary, all three compounds showed significant inhibitory effects on the CF efflux. Therefore, they might act as weak inhibitors or substrates of MRP1 or in another indirect way in NCI-H441 cells.

3.5 DRUGS USED IN THE THERAPY OF PULMONARY DISEASES AND THEIR INFLUENCE ON THE CF EFFLUX

Van der Deen *et al.* examined the impact of therapeutics used in the therapy COPD (i.e. bronchodilators, inhaled glucocorticoids and N-acetylcysteine) on the MRP1-mediated transport in the human bronchial epithelial cell line 16HBE14o- by CFDA efflux studies (van der Deen et al., 2008). Significant differences were observed, but up to the present, no other human lung epithelial cell line, was tested in regard of the influence of COPD treatments on MRP1-mediated transport. The aim was to investigate the effect of bronchodilators, inhaled glucocorticoids and cromolyn sodium on the MRP1-mediated efflux in the human bronchiolar epithelial cell line NCI-H441.

3.5.1 BRONCHODILATORS

Van der Deen *et al.* reported an impact of formoterol on MRP1-mediated transport and detected an increase in the MRP1-mediated CF transport in 16HBE14o- cells (van der Deen et al., 2008). Up to the present, no other study analysed the influence of β-agonists on MPR1 in human lung epithelial cell lines so far.

Beta-agonists are commonly prescribed drugs in the therapy of bronchial asthma and COPD. The aim was to test the supplement of β-agonists, terbutaline hemisulphate salt, salbutamol, formoterol fumarate and GW597901 regarding its influence on MRP1-mediated CF transport in NCI-H441 by efflux studies.

3.5.1.1 TERBUTALINE HEMISULPHATE SALT

In order to investigate, if the addition of terbutaline hemisulphate salt altered the CF efflux from NCI-H441 cells, two different concentrations (i.e. 100 µM and 200 µM) were tested in release studies. Results are shown in Figure 19 and Table 13.
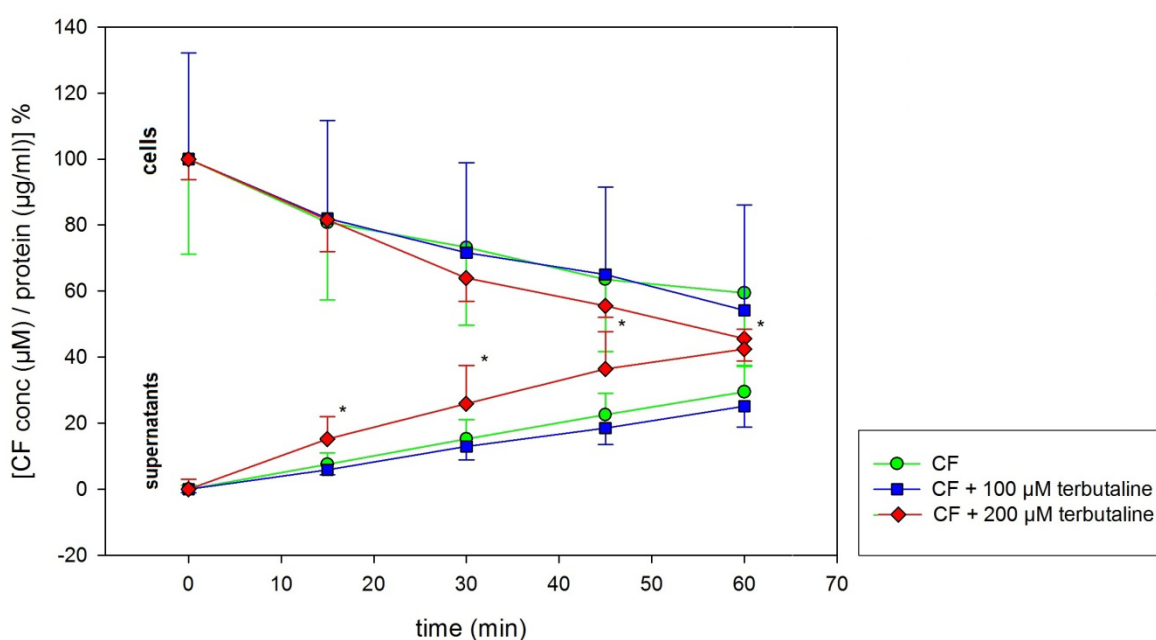
FIGURE 19

Effect of 100 µM and 200 µM terbutaline hemisulphate salt on the CF efflux from NCI-H441 cells. Supernatants and lysed cell monolayers were analysed. Addition of 200 µM terbutaline hemisulphate salt significantly increased the CF concentration in supernatant samples. Results are expressed as means ± SD (CF n = 52-54, 100 µM terbutaline hemisulphate salt n = 12-14, 200 µM terbutaline hemisulphate salt n = 6-7). Statistical significance is marked as * (P < 0.05).

T (min)	CFDA CF ± SD (%)	n	CDFA, 100 μM terbutaline hemisulphate salt CF ± SD (%)	N	P	CFDA, 200 μM terbutaline hemisulphate salt CF ± SD (%)	N	P
Cells								
0	100.00 ± 28.74	53	100.00 ± 32.17	12	1.000	100.00 ± 6.22	6	1.000
15	80.82 ± 23.45	53	82.10 ± 29.63	12	0.8715	81.65 ± 9.66	6	0.9327
30	73.24 ± 23.64	54	71.61 ± 27.29	12	0.8342	64.02 ± 7.11	6	0.3492
45	63.55 ± 21.83	52	64.95 ± 26.64	12	0.8483	55.47 ± 3.33	6	0.3728
60	59.39 ± 21.88	54	54.20 ± 31.83	14	0.4762	45.64 ± 6.84	8	0.1336
Supernatants								
0	0.00 ± 1.11	52	0.00 ± 1.16	12	1.000	0.00 ± 2.98	6	1.000
15	7.56 ± 3.33	52	5.91 ± 1.54	12	0.1007	15.13 ± 6.91	6	*< 0.0001*
30	15.23 ± 5.77	53	12.90 ± 4.09	12	0.1904	25.92 ± 11.60	6	*0.0003*
45	22.51 ± 6.61	50	18.47 ± 4.92	12	0.0514	36.47 ± 11.29	6	*< 0.0001*
60	29.48 ± 7.75	53	25.11 ± 6.33	14	0.0565	42.38 ± 6.16	8	*< 0.0001*

TABLE 13

Data of CFDA release studies plus terbutaline hemisulphate salt (100, 200 μM).

Addition of 100 μM terbutaline hemisulphate salt did not change the CF release from NCI-H441 cells in a statistical significant way. Differences were observed in the lysed cell monolayers and in the supernatant samples, however, they were not statistical significant.

The effect, however, was concentration-dependent, since addition of 200 μM terbutaline hemisulphate salt increased the CF concentrations in the supernatant samples at all tested points in time in a statistical significant way (Table 13). Finally, at 60 min, the levels of the fluorophore ascended to 42.38 ± 6.16% (*n* = 8) in comparison to 29.48 ± 7.75% (*n* = 53) in the control.

No statistically significant alterations regarding the CF accumulation in the analysed cell monolayer samples were observed.

3.5.1.2 SALBUTAMOL

Moreover, the influences of 100 μM and 200 μM salbutamol on the MRP1-mediated CF efflux were tested. Results are shown in Figure 20 and Table 14.
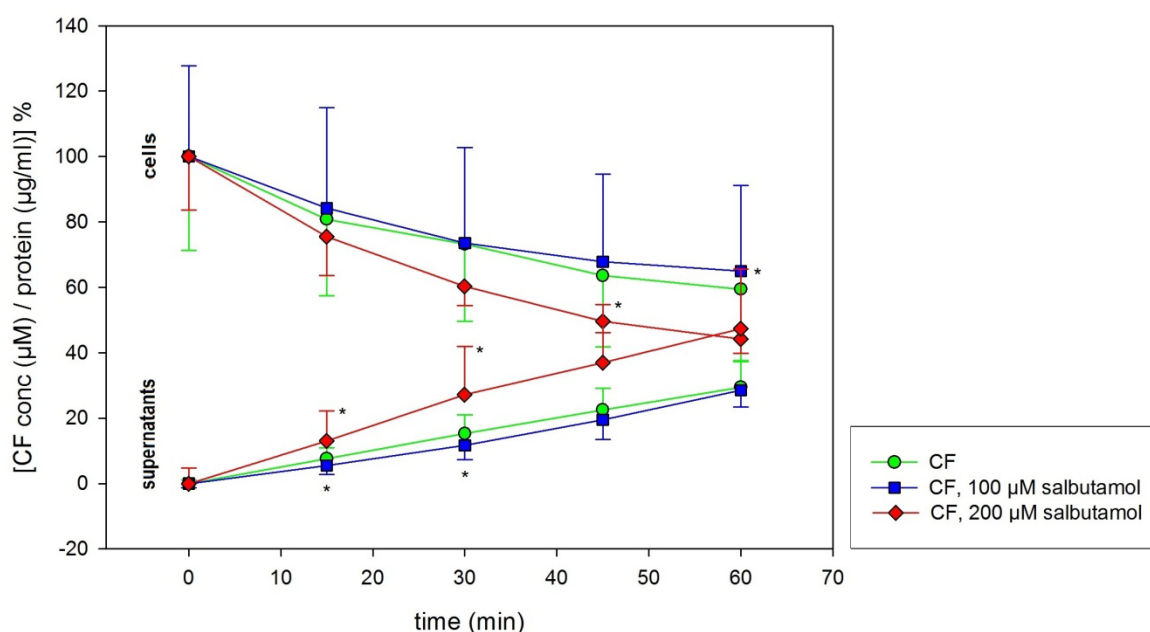
FIGURE 20

In the supernatants 100 µM salbutamol reduced CF concentrations at 15 min and 30 minutes in significant way, whereas 200 µM salbutamol significantly altered CF concentrations at all tested points in time. No significant differences were detected in the lysed cell monolayers. Results are expressed as means ± SD (CFDA n = 50-53, 100 µM salbutamol n = 12-13, 200 µM salbutamol n = 6-7). Statistical significance is marked as * ($P < 0.05$).

T (min)	CFDA CF ± SD (%)	n	CFDA, 100 µM salbutamol CF ± SD (%)	N	P	CFDA, 200 µM salbutamol CF ± SD (%)	n	P
Cells								
0	100.00 ± 28.74	53	100.00 ± 27.74	12	1.000	100 ± 16.36	6	1.000
15	80.82 ± 23.45	53	84.16 ± 30.75	12	0.6758	75.56 ± 11.94	6	0.5919
30	73.24 ± 23.64	54	73.55 ± 29.19	12	0.9683	60.28 ± 5.94	6	0.1890
45	63.55 ± 21.83	52	67.79 ± 26.76	12	0.5630	49.56 ± 3.41	6	0.1255
60	59.39 ± 21.88	54	64.96 ± 26.16	13	0.4307	44.19 ± 4.42	7	0.0737
Supernatants								
0	0.00 ± 1.11	52	0.00 ± 1.21	12	1.000	0.00 ± 4.70	6	1.000
15	7.56 ± 3.33	52	5.44 ± 2.68	12	*0.0436*	12.93 ± 9.32	6	*0.0047*
30	15.23 ± 5.77	53	11.65 ± 4.35	12	*0.0478*	27.11 ± 14.77	6	*0.0002*
45	22.51 ± 6.61	50	19.51 ± 5.96	12	0.1551	36.90 ± 17.86	6	*0.0002*
60	29.48 ± 7.75	53	28.51 ± 5.14	13	0.6726	47.37 ± 18.21	7	*< 0.0001*

TABLE 14

Data of CFDA release studies plus different concentrations of salbutamol (100 µM, 200 µM)

Addition of 100 µM and 200 µM salbutamol did not alter the accumulation of CF in cell monolayers in a statistical significant way due to rather high standard deviations whilst at the same time, in the supernatant samples statistical significant differences in the amount of fluorophore were observed (Table 10).

47

Addition of 100 µM salbutamol reduced the CF concentrations in a significant way at 15 min and 30 min (5.44 ± 2.68% (*n* = 12), 11.65 ± 4.35% (*n* = 12)). However, no statistical relevant difference was observed at the end of the studies after 60 min. Interestingly, supplement of 200 µM revealed a different effect on MRP1. Addition of 200 µM salbutamol significantly increased the amount of CF in the supernatant samples at all time points (Table 14). Finally at 60 min, the addition of 200 µM salbutamol elevated the levels of the fluorescent probe to 47.37 ± 18.21% (*n* = 7) in comparison to 29.48 ± 7.75% (*n* = 53) in the control.

It can be summarised that the supplement of salbutamol increased the CF efflux from NCI-H441 cells, however, this observed effect is concentration-dependent.

3.5.1.3 FORMOTEROL FUMARATE

In order to determine the effect of formoterol fumarate on the CF transport in NCI-H441 cells, efflux studies were conducted. The results are shown in Figure 21 and Table 15.
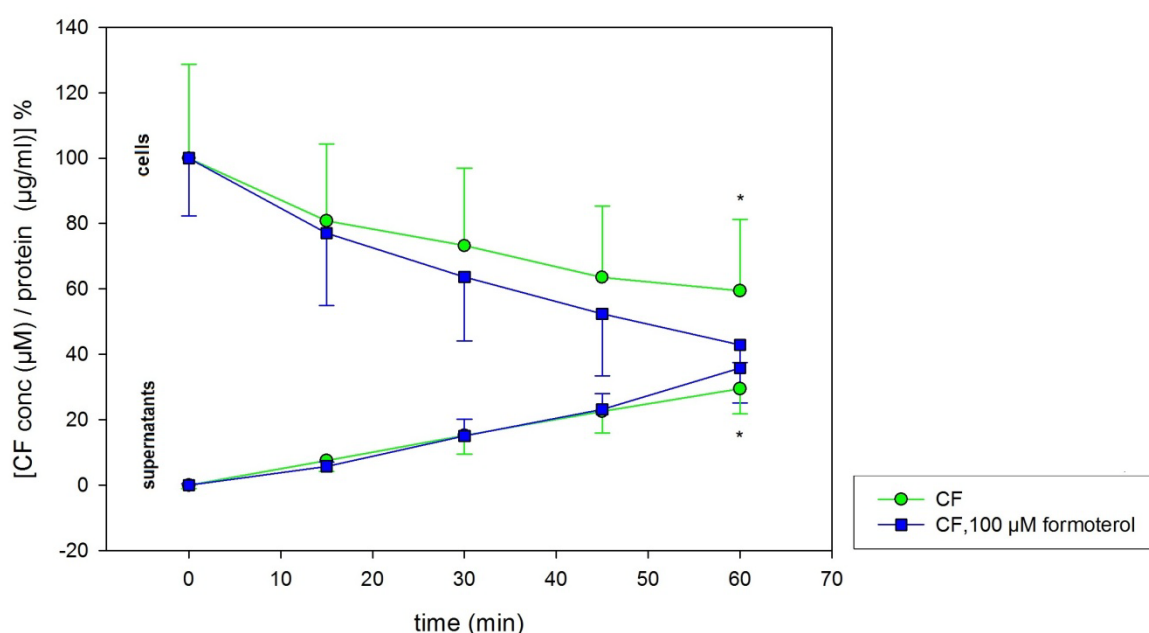

FIGURE 21

Formoterol fumarate significantly altered CF concentrations in the cells and in the supernatants after 60 min. Results are expressed as means ± SD (CF *n* = 50-54, formoterol fumarate *n* = 9). Statistical significance is noted as * (*P* < 0.05)

Time (min)	CFDA CF ± SD (%)	N	CFDA, 100 µM formoterol fumarate CF ± SD (%) $n = 9$	P
Cells				
0	100.0 ± 28.74	53	100.00 ± 17.75	1.000
15	80.82 ± 23.45	53	77.01 ± 22.04	0.6514
30	73.24 ± 23.64	54	63.68 ± 19.55	0.2555
45	63.55 ± 21.83	52	52.39 ± 18.95	0.1554
60	59.39 ± 21.88	54	42.91 ± 17.71	*0.0363*
Supernatants				
0	0.00 ± 1.11	52	0.00 ± 0.38	1.000
15	7.56 ± 3.33	52	5.77 ± 1.25	0.1187
30	15.23 ± 5.77	53	15.01 ± 5.10	0.9131
45	22.51 ± 6.61	50	23.92 ± 4.88	0.5472
60	29.48 ± 7.75	53	35.81 ± 1.66	*0.0182*

TABLE 15

Data of CFDA release studies plus 100 µM formoterol fumarate.

Significant differences were observed in the lysed cell monolayers and in the supernatant samples after 60 min. Addition of formoterol fumarate resulted in an increased CF efflux from cells. Hence, concentrations of the fluorescent probe in the cell layers decreased to 42.91% ($n = 9$) whereas it increased to 35.81% ($n = 9$) in the supernatant samples at the same time.

3.5.1.4 GW597901

Additionally, an investigational long-acting β-agonist, GW597901 (100 µM), was tested in efflux studies regarding its impact on the CF transport in NCI-H441 cells. Results are shown in Figure 22 and in Table 16.

No significant differences were observed in the supernatants or in the lysed cell monolayers. Therefore, the β-agonist, GW597901, did not influence the MRP1-mediated efflux in the tested concentration of 100 µM GW597901.
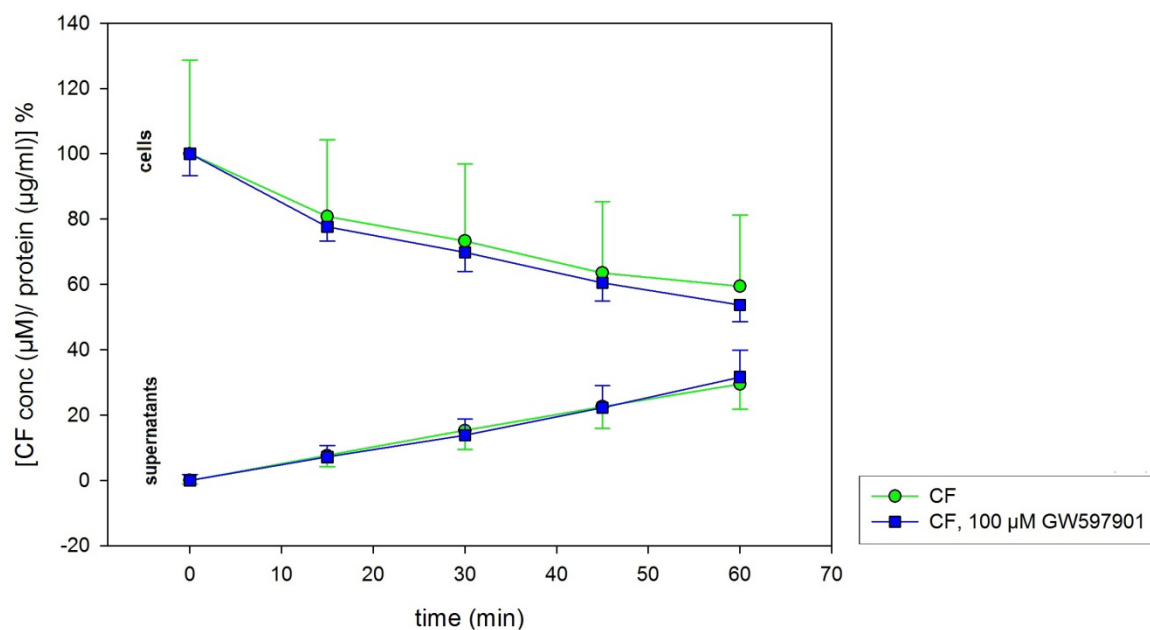
FIGURE 22

The addition of 100 µM GW597901 did not influence significantly the CF efflux from NCI-H441 cells. Results are expressed as means ± SD (CF *n* = 50-54, GW597901 *n* = 7-9), *P* < 0.05.

Time (min)	CFDA CF ± SD (%)	*N*	CFDA, 100 µM GW597901 CF ± SD (%)	*N*
		Cells		
0	100.00 ± 28.74	53	100.0 ± 6.69	9
15	80.82 ± 23.45	53	77.68 ± 4.41	9
30	73.24 ± 23.64	54	69.86 ± 5.93	9
45	63.55 ± 21.83	52	60.48 ± 5.61	9
60	59.39 ± 21.88	54	51.99 ± 4.34	8
		Supernatants		
0	0.00 ± 1.11	52	0.00 ± 1.82	7
15	7.56 ± 3.33	52	7.11 ± 3.58	9
30	15.23 ± 5.77	53	13.87 ± 4.95	9
45	22.51 ± 6.61	50	22.23 ± 6.84	9
60	29.48 ± 7.75	53	34.51 ± 6.20	8

TABLE 16

Data of CFDA release studies plus 100 µM GW597901.

3.5.1.5 COMPARISON OF DIFFERENT BRONCHODILATORS REGARDING THEIR IMPACTS ON THE MRP1-MEDIATED CF TRANSPORT

Figure 23 gives an overview on the effect of different β-agonists on CF efflux in NCI-H441 cells. Data are shown in Table 17.

FIGURE 23

Comparison of CF accumulation in cell monolayers and supernatants after 60 min. Addition different β-agonists significantly alters the CF concentration in the cells and the supernatants. The dotte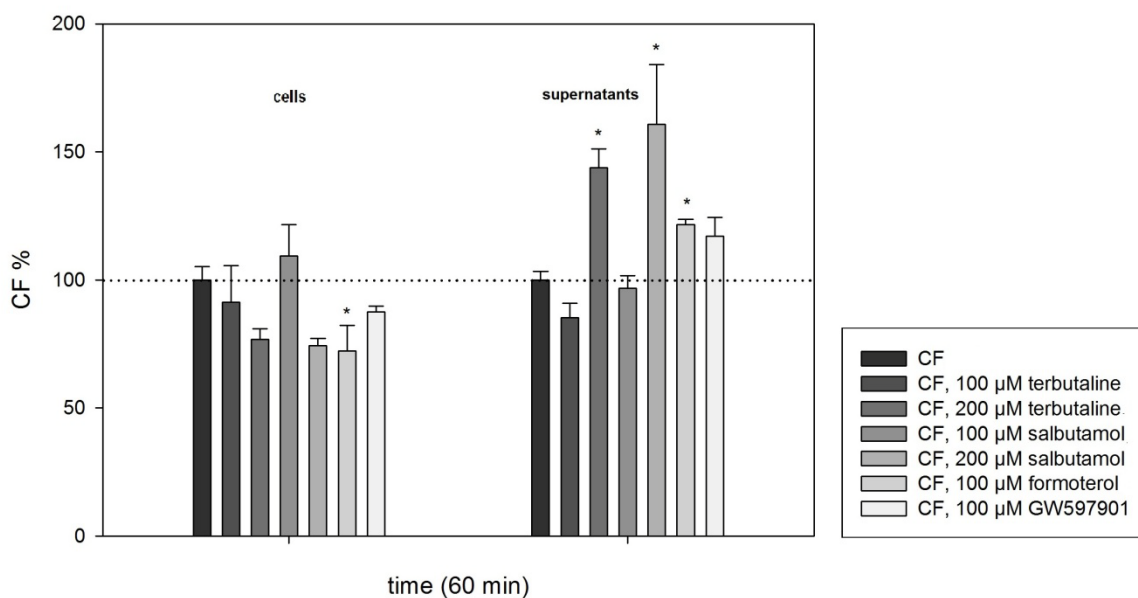d line symbolises the level of the control and represents the CF release in cells and supernatants without β-agonists, expressed as 100%. Results are expressed as means ± standard error (SE) (CF n = 54, 53, 100 µM terbutaline hemisulphate n = 14, 200 µM terbutaline hemisulphate n = 8, 100 µM salbutamol n = 13, 200 µM salbutamol n = 7, formoterol fumarate n = 9, GW597901 n = 8). Statistical significance is expressed as * ($P < 0.05$).

CFDA CF ± SE (%)	CFDA, 100 µM terbutaline hemisulphate salt CF ± SE (%)	CFDA, 200 µM terbutaline hemisulphate salt CF ± SE (%)	CFDA, 100 µM salbutamol CF ± SE (%)	CFDA, 200 µM salbutamol CF ± SE (%)	CFDA, 100 µM formoterol fumarate CF ± SE (%)	CFDA, 100 µM GW597901 CF ± SE (%)
Cells						
100.00 ± 5.01	91.26 ± 14.32	76.84 ± 4.07	109.37 ± 12.22	74.40 ± 2.81	72.26 ± 9.94	87.53 ± 2.32
Supernatants						
100.00 ± 3.61	85.18 ± 5.74	143.77 ± 7.39	96.73 ± 4.84	160.70 ± 23.35	121.50 ± 2.12	117.07 ± 7.43

TABLE 17

Data describes the influence of different bronchodilators on CF efflux.

Figure 23 displays the concentrations of CF in the cells and in supernatants in CFDA release studies expressed as 100% in comparison to the alterations observed by the addition of different bronchodilators at 60 min.

Addition of 100 µM terbutaline hemisulphate salt resulted in an increased translocation of the CF from cell monolayers by 8.74 ± 13.28% (SE) (n = 14) as well as in an unexpected decrease at the same time in the supernatant samples by 14.82 ± 3.27% (SE) (n = 14). However, both observed alterations were not statistical significant. An increase in the added terbutaline hemisulphate salt concentration (200 µM) attenuated the amount of fluorophore by 23.16 ± 3.95% (SE) (n = 8) in the lysed cell monolayers while it significantly increased its concentration by 43.77 ± 9.34% (SE) (n = 8) in the supernatant samples. Moreover, the administration of 100 µM salbutamol elevated CF by 9.38 ± 13.13% (SE) (n = 13) in the cells while it reduced fluorescence levels by 3.27 ± 3.64% (SE) (n = 13) in the supernatants. Both effects were not statistical significant. Addition of 200 µM salbutamol reduced the CF accumulation in the cells by 25.60 ± 5.35% (SE) (n = 7) and increased it significantly in the supernatant samples by 60.70 ± 16.63% (SE) (n = 7). Furthermore, addition of 100 µM formoterol fumarate resulted in diminished levels of the fluorophore in the cells by 27.74 ± 10.78% (SE) (n = 9) but increased its amount in the supernatants by 21.50 ± 3.00% (SE) (n = 9). Both alterations were considered as statistically significant. Additionally, the administration of 100 µM GW597901 increased the release of CF from cells by 12.47 ± 3.16% (SE) (n = 8) and elevated its levels in the supernatant samples by 17.07 ± 5.61% (SE) (n = 8). None of these changes were statistical significant.

In summary, among all tested β-agonists concentration dependent increases in the CF transport in NCI-H441 cells were observed resulting in decreases in the CF accumulation in the cell monolayers and increases in the CF concentrations in the analysed supernatant samples at the same time.

It can be assumed that β-agonists might enhance CF transport in NCI-H441 cells as stimulating substances of MRP1, substrates of MRP1 or due to the stimulation of β$_2$-adrenic receptors in an indirect way.

3.5.2 INHALED GLUCOCORTICOIDS

Up to the present, two studies examined the effect of the inhaled glucocorticoid, budesonide on the MRP1 expression and MRP1-mediated transport in human bronchial epithelial cell lines, Calu-1 and 16HBE14o- (Bandi and Kompella, 2002; van der Deen et al., 2008). The studies stated significant decreases in the MRP1 expression as well as in the MRP1-mediated transport caused by budesonide. The impact of beclomethasone on MRP1 was not mentioned in the literature so far. Both inhaled glucocorticoids are commonly prescribed in the therapy of bronchial asthma and COPD.

Another aim of this thesis was to study the effect of inhaled glucocorticoids, budesonide and beclomethasone, regarding their impact on MRP1-mediated CF transport in NCI-H441 cells by release studies.

3.5.2.1 BUDESONIDE

In order to investigate, if the addition of budesonide altered the CF efflux from NCI-H441 cells, two different concentrations, 20 µM and 50 µM budesonide, were tested. Due to solubility problems no higher concentrations were used.
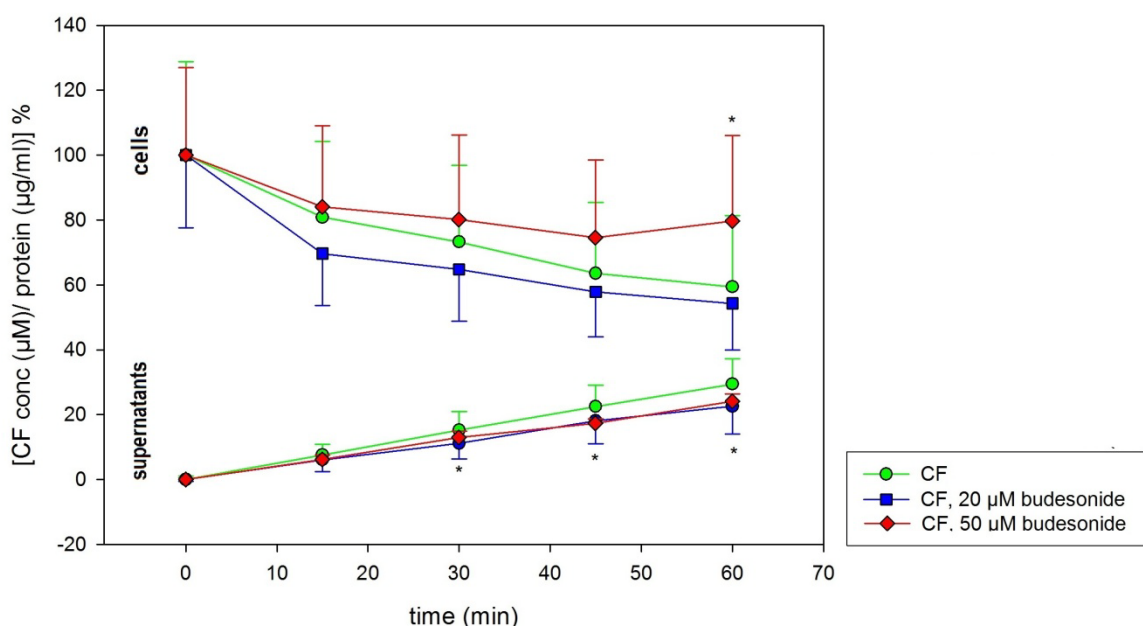
Results are shown in Figure 24 and Table 18.

FIGURE 24

Budesonide reduced the CF efflux from NCI-H441 cells. Significant differences were observed in the supernatants at 30, 45 and 60 min at both budesonide concentrations and in the lysed cell monolayers at 60 min (50 µM budesonide). Results are expressed as means ± SD (CF n = 50-54, 20 µM budesonide n = 12-13, 50 µM budesonide n = 9-14). Statistical significance is expressed as * (P < 0.05).

Time (min)	CFDA CF ± SD (%)	N	CFDA, 20 µM budesonide CF ± SD (%)	N	P	CFDA, 50 µM budesonide CF ± SD (%)	N	P
			Cells					
0	100.00 ± 28.74	53	100.00 ± 22.41	12	1.000	100.00 ± 26.97	12	1.000
15	80.82 ± 23.45	53	69.68 ± 16.05	12	0.1239	84.00 ± 25.07	12	0.6767
30	73.24 ± 23.64	54	64.77 ± 15.89	12	0.2423	80.08 ± 26.09	12	0.3770
45	63.55 ± 21.83	52	57.88 ± 13.92	12	0.3948	74.61 ± 23.95	12	0.1251
60	59.39 ± 21.88	54	54.29 ± 14.34	13	0.4279	79.69 ± 26.33	14	*0.0042*
			Supernatants					
0	0.00 ± 1.11	52	0.00 ± 0.53	12	1.000	0.00 ± 0.49	9	1.000
15	7.56 ± 3.33	52	6.12 ± 3.62	12	0.1872	6.16 ± 1.45	9	0.2196
30	15.23 ± 5.77	53	11.20 ± 4.79	12	*0.0282*	13.01 ± 1.94	9	0.2601
45	22.51 ± 6.61	50	18.16 ± 7.13	12	*0.0479*	17.26 ± 1.43	9	*0.0219*
60	29.48 ± 7.75	53	22.62 ± 8.63	13	*0.0068*	24.08 ± 2.28	11	*0.0263*

TABLE 18

Data of CFDA release studies plus budesonide (20 µM, 50 µM).

The addition of 20 µM budesonide did not change the intracellular CF accumulation in a statistically significant way. However, 50 µM budesonide elevated the amount of the fluorescent probe at 60 min in the cells to 79.69 ± 26.33% (n = 14). This observed effect was considered as statistically significant.

Moreover, both budesonide concentrations, 20 µM and 50 µM, significantly attenuated the levels of the fluorophore in the supernatants at 45 and 60 min. Interestingly, the addition on 20 µM budesonide also resulted in significant decreases in the CF concentration at 30 min (Table 18). At the end of the study, the addition of 20 µM budesonide diminished the levels of the fluorescent probe to 22.62 ± 8.63% (n = 13) whereas the administration of 50 µM budesonide resulted in a decrease to 24.08 ± 2.28% (n = 11) in comparison to 29.48 ± 7.75% (n = 53) in KRB without budesonide.

In conclusion, 20 µM and 50 µM budesonide diminished the CF efflux in NCI-H441 cells.

3.5.2.2 BECLOMETHASONE

Furthermore, the influence of the addition of 50 µM beclomethasone to KRB regarding the CF transport in NCI-H441 cells was tested. Results are displayed in Figure 25 and Table 19.
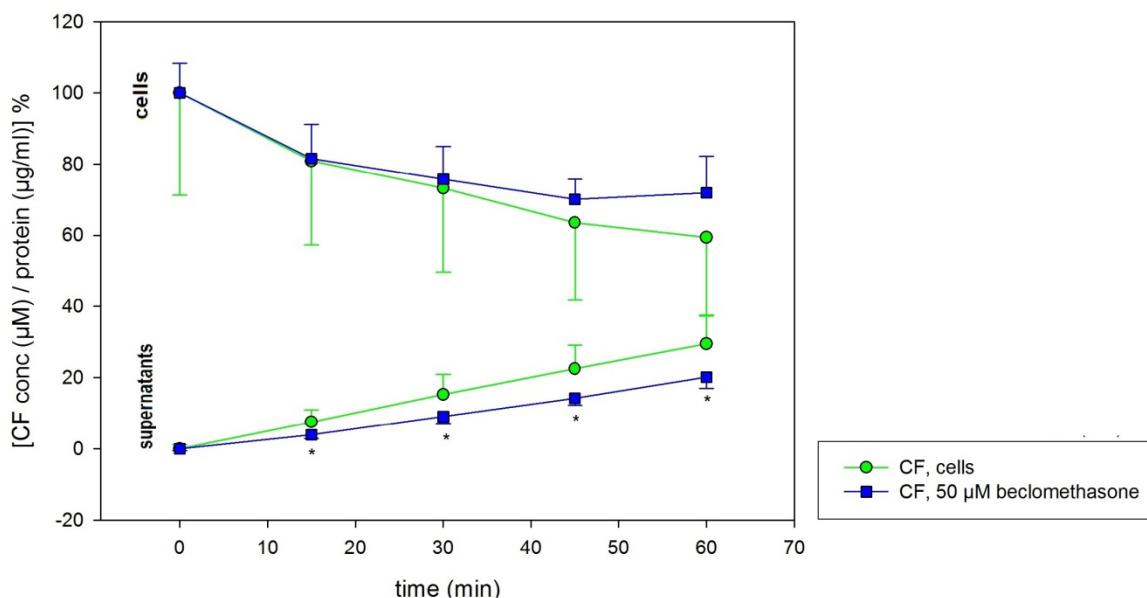
FIGURE 25

Effect of 50 µM beclomethasone on the CF efflux. In the supernatant samples significant differences were observed at all points in time. Results are displayed as means ± SD (CF n = 50-54, beclomethasone n = 9-14) Significance is expressed as * (P < 0.05).

Time (min)	CFDA CF ± SD (%)	n	CFDA, 50 µM beclomethasone CF ± SD (%)	N	P
Cells					
0	100.00 ± 28.74	53	100.00 ± 8.25	9	1.000
15	80.82 ± 23.45	53	81.56 ± 9.57	9	0.9262
30	73.24 ± 23.64	54	75.78 ± 9.25	9	0.7529
45	63.55 ± 21.83	52	70.08 ± 5.68	9	0.3790
60	59.39 ± 21.88	54	71.90 ± 10.34	11	0.0697
Supernatants					
0	0.00 ± 1.11	52	0.00 ± 0.53	12	1.000
15	7.56 ± 3.33	52	3.97 ± 1.12	12	*0.0005*
30	15.23 ± 5.77	53	9.02 ± 1.95	12	*0.0005*
45	22.51 ± 6.61	50	14.19 ± 1.91	12	*< 0.0001*
60	29.48 ± 7.75	53	20.12 ± 3.10	14	*< 0.0001*

TABLE 19

Data of CFDA release studies plus 50 µM beclomethasone in NCI-H441 cells.

55

Whilst the decreases in the CF concentrations in the supernatant samples were significant, the efflux from the cells was reduced. However, the observed differences in the lysed cell monolayers were not statistical significant.

On the other hand, in the supernatant samples the addition of 50 µM beclomethasone reduced the amount of the fluorophore significantly at all points in time (Table 19). At the end of the study, the supplement of beclomethasone resulted in a decrease to 20.12 ± 3.10% CF (n = 14) in comparison to 29.48 ± 7.75% (n = 53) in the control.

It can be summarised that beclomethasone reduced the CF release from NCI-H441 cells.

3.5.2.3 COMPARISON OF DIFFERENT INHALED GLUCOCORTICOIDS REGARDING THEIR INFLUENCES ON THE MRP1-MEDIATED CF TRANSPORT

Figure 26 shows the effect of different inhaled glucocorticoids on the CF efflux. Data are presented in Table 20.
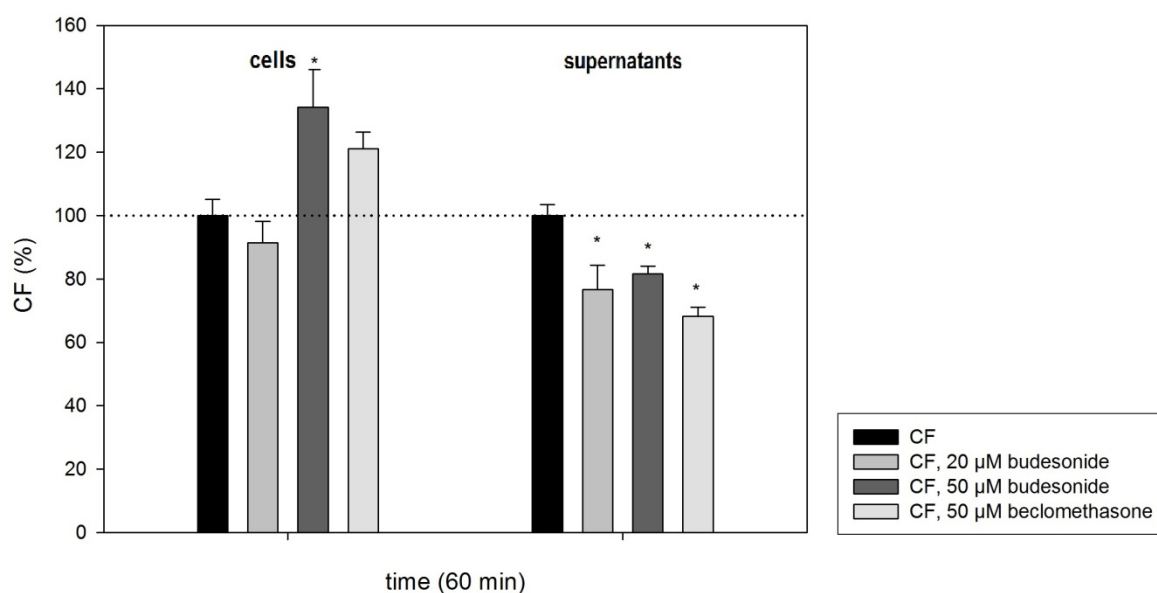
FIGURE 26

Addition of different inhaled glucocorticoids significantly altered the CF concentration in the cells and the supernatants. The dotted line symbolises the level of the control and represents the CF release in cells and supernatants without inhaled glucocorticoids expressed as 100%. Results are presented as means ± SE (CF n =54, 53, 20 µM budesonide n = 13, 50 µM budesonide n = 14, 11, beclomethasone n = 11, 14). Statistical significance is expressed as * (P < 0.05).

CFDA CF ± SE (%)	CFDA, 20 µM budesonide CF ± SE (%)	CFDA, 50 µM budesonide CF ± SE (%)	CFDA, 50 µM beclomethasone CF ± SE (%)
Cells			
100.00 ± 5.01	91.41 ± 6.70	134.18 ± 11.85	121.05 ± 5.25
Supernatants			
100.00 ± 3.61	76.72 ± 8.12	81.69 ± 2.33	68.25 ± 2.81

TABLE 20

Data of CFDA release studies. CF without inhaled glucocorticoids is expressed as 100%.

Figure 26 displays the concentrations of CF the cells and supernatants in CFDA release studies expressed as 100% in comparison to the alterations observed by the addition of different inhaled glucocortioids at 60 min.

Addition of 20 µM budesonide resulted in an unexpected decrease of the CF accumulation by 8.59 ± 7.72% (n = 13) in the cell monolayers, although the observed effect was not statistically significant. At the same time, in the supernatants, a significant reduction by 23.28 ± 4.65% (n = 13) was observed. An increase in the budesonide concentration (50 µM) led to significant retention of CF in the cell monolayers while its concentration in the supernatants was reduced. In the cells the administration of 50 µM budesonide resulted in an increase by 34.18 ± 13.04% CF (n =14) while in supernatants a reduction by 18.31 ± 1.55% CF (n = 14) was detected.

Furthermore, the impact of 50 µM beclomethasone on the MRP1-mediated CF efflux was analysed. The addition of beclomethasone increased the accumulation of the fluorescent probe in the lysed cell monolayers by 21.05 ± 4.37% (n = 11). However, this increase was not considered as statistically significant. At the same time, beclomethasone reduced its amount in the supernatant samples by 31.75 ± 1.56% (n = 14) in a statistical significant way.

In summary, the addition of inhaled glucocorticoids resulted in increases in the amount of CF in the lysed cell monolayers while the percentage of the CF in the supernatant samples decreased.

The results show that inhaled glucocorticoids reduced the CF efflux from NCI-H441 cells. Therefore, it can be speculated that inhaled glucocorticoids might interfere with MRP1 function as inhibitors, substrates or in another indirect way.

3.5.3 MAST CELL STABILISER CROMOLYN SODIUM

The mast cell stabiliser, cromolyn sodium was tested in regard of its impact on the MRP1-mediated CF transport in NCI-H441 cells. Currently, no study reported an effect of cromolyn sodium on MRP1-mediated transport. The lysed cell monolayers and the supernatants were analysed. The results are shown in Figure 28 and in Table 21.

Addition of cromolyn sodium (100 µM) did not significantly alter the CF efflux, neither in the analysed cell monolayers nor in the supernatants at no points in time.

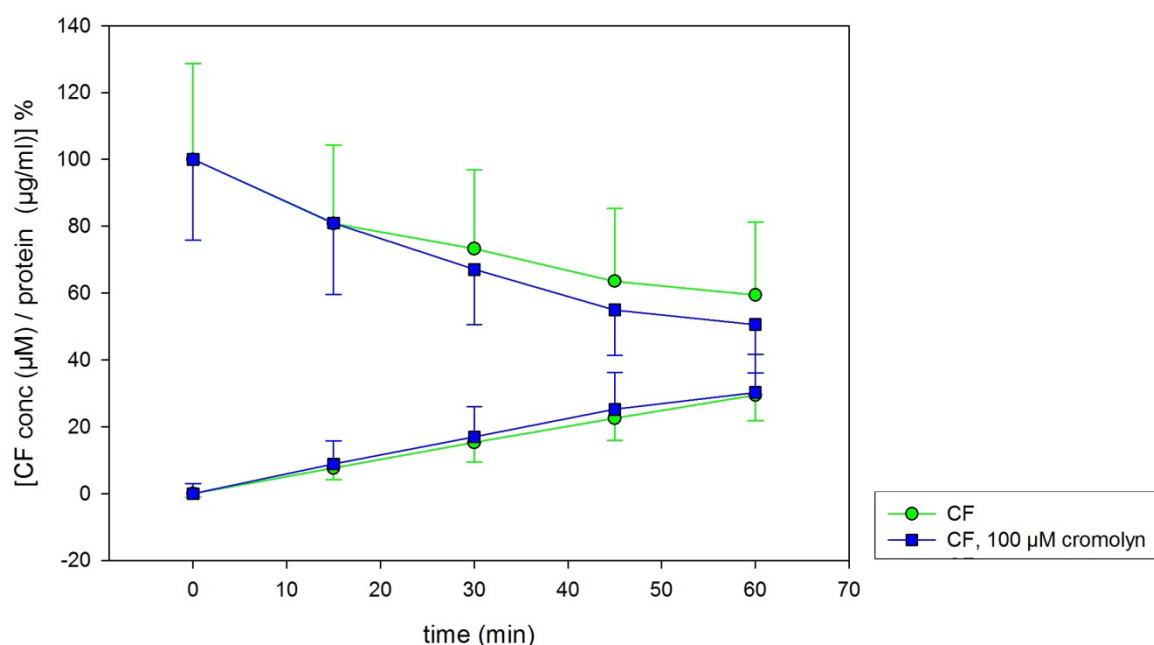In conclusion, cromolyn sodium did not interact with MRP1.

FIGURE 27

Cromolyn sodium did not influence the CF release in a statistical significant way ($P < 0.05$). Results are expressed as means ± SD (CF n = 50-54, cromolyn sodium n = 12-13).

Time (min)	CFDA CF ± SD (%)	N	CFDA, 100 µM cromolyn sodium CF ± SD (%)	n
Cells				
0	100.00 ± 28.74	53	100.00 ± 24.13	12
15	80.82 ± 23.45	53	81.00 ± 21.39	12
30	73.24 ± 23.64	54	67.07 ± 16.46	12
45	63.55 ± 21.83	52	54.97 ± 13.62	12
60	59.39 ± 21.88	54	50.63 ± 14.54	13
Supernatants				
0	0.00 ± 1.11	52	0.00 ± 2.91	12
15	7.56 ± 3.33	52	8.82 ± 6.95	12
30	15.23 ± 5.77	53	17.02 ± 8.95	12
45	22.51 ± 6.61	50	25.18 ± 11.05	12
60	29.48 ± 7.75	53	30.30 ± 11.37	13

TABLE 21

Data of CFDA release studies plus 100 µM cromolyn sodium.

3.6 FUNCTION OF P-GLYCOPROTEIN IN NCI-H441 CELLS

A side project of this thesis was aiming to determine the function of P-gp in NCI-H441 cells. Therefore, rhodamine123 (Rh123) release studies were carried out and the inhibitory effect of the specific P-gp inhibitor, LY335979 and the broad-spectrum inhibitor verapamil was determined (Figure 28). Rh123 release from NCI-H441 monolayers was time dependent and showed low, albeit significant attenuation by addition of both inhibitors over 60 min. Over the time, the amount of fluorophore in the cells decreases, whilst at the same time the concentration in the supernatant increases. Interestingly, the effects of verapamil and LY335979 were similar, suggesting that Rh123 efflux is predominantly mediated by P-gp.
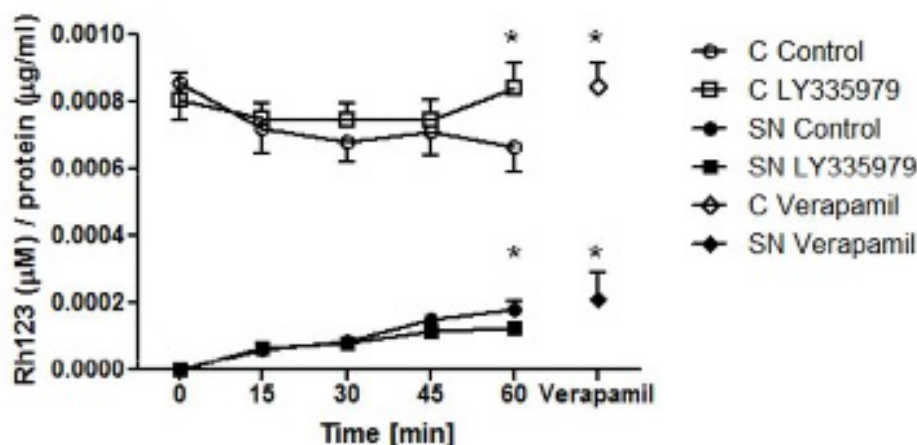
FIGURE 28

Iinhibitory effects on Rh123 release from NCI-H441 cell monolayers grown in 24well plates. Rh123 decrease in cells (C) and increase in supernatant (SN) was measured in the presence of LY335979 (10 µM) or verapamil (50 µM) at pH 7.4, 37°C for 60 min. Values are represented as means ± SD ($n = 7 – 16$, $*P < 0.05$).

3.7 FLUORESCEIN SODIUM SALT AND FLUORESCEINISOTHIOCYANATE (FITC)-DEXTRAN TRANSPORT STUDIES

The paracellular diffusion is a characteristic for the tightness of the cell monolayers and the functional expression of the tight junctions. In order to investigate the transport of paracellular marker compounds across NCI-H441 cell monolayers in the a-b direction, transport studies were carried out using fluorescein sodium and FITC-labelled dextrans of the molecular weights ranging from 4,000 - 70,000 (Figure 29). The highest transported amount was observed in the case of fluorescein sodium, whereas the compound with the highest molecular weight, FITC-dextran 70,000, showed lowest transport. The apparent permeability coefficients (P_{app}) were calculated and shown in Table 22.

Fluorescein sodium (FNa), a-b, $P_{app} \pm SD$ (cm/s)	FITC-dexran 4,000 (FD4k), a-b $P_{app} \pm SD$ (cm/s)	FITC-dextran 10,000 (FD10k, a-b, $P_{app} \pm SD$ (cm/s)	FITC-dextran 20,000 (FD20k), a-b, $P_{app} \pm SD$ (cm/s)	FITC-dextran 70,000 (FD70k), a-b, $P_{app} \pm SD$ (cm/s)
$4.85 * 10^{-7} \pm 0.33 * 10^{-7}$	$1.51 * 10^{-7} \pm 0.17 * 10^{-7}$	$1.58 * 10^{-7} \pm 0.63 * 10^{-7}$	$1.17 * 10^{-7} \pm 0.27 * 10^{-7}$	$2.52 * 10^{-8} \pm 0.98 * 10^{-8}$

TABLE 22

Permeability coefficients of the transport of paracellular marker compounds across NCI-H441 cell monolayers.
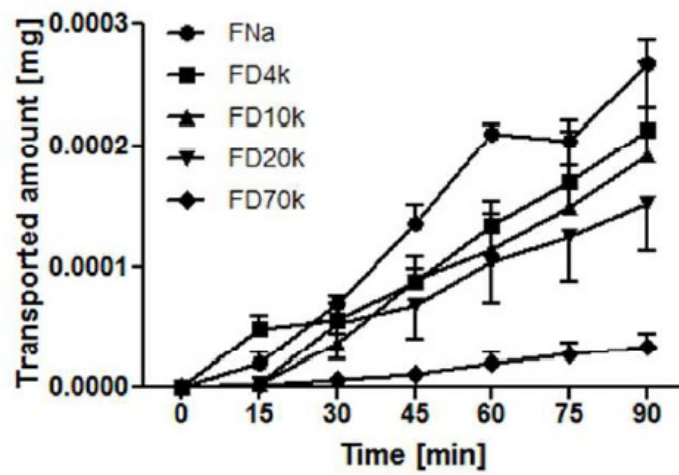
FIGURE 29

Time course of paracellular marker transport in apical-to-basolateral direction across NCI-H441 cell monolayers. Cells were seeded on Transwell Clear membrane inserts and grown for 12 days before transport experiments with fluorescein sodium (FNa) and FITC-labelled dextrans of molecular weight 4000 (FD4k), 10,000 (FD10k), 20,000 (FD20k) and 70,000 (FD70k) were carried out. Each data point represents the means ± SD for n = 3 - 4.

4 DISCUSSION

The objective of this thesis was to investigate the expression, cellular localisation and function of multidrug resistant-related protein 1 in the distal lung epithelial cell line NCI-H441. Furthermore, several potential modulators of MRP1 were tested regarding their effect on MRP1-mediated CF efflux from NCI-H441 cells. Additionally, drugs commonly used in the inhalation therapy of chronic obstructive pulmonary disease and asthma, were investigated regarding their influence on MRP1-mediated transport. Finally, a side project of this thesis aimed to determine the function of P-gp in NCI-H441 cells by release studies and the transport characteristics of paracellular markers across NCI-H441 cell monolayers were studied.

In the first step, Western blot analysis and confocal laser scanning microscopy were carried out aiming to demonstrate MRP1 expression as well as its localisation in NCI-H441 cells.

Western blot probed with MRP1 antibodies revealed one prominent band corresponding to the size of the protein, confirming the expression of MRP1 in NCI-H441 cells on protein level. These findings were consistent with the expression of MRP1 at high levels in the distal region of the human lung (Sakamoto et al., 2013). Moreover, the results were according to the previous detection of MRP1 in several human lung epithelial cell lines as well as in primary cells using Western Blot analysis (Bandi and Kompella, 2002; Lehmann et al., 2001).

Confocal laser scanning micrographs showed a distinct signal, confirming MRP1 expression in the cell line. In addition, z-scans discovered the highest signal intensity in the membrane region localised to the basolateral membrane. This is consistent with the observations by Scheffer *et al.*, who detected MRP1 on the basolateral aspect of frozen sections of the bronchiolar and alveolar region of the normal human lung by immunohistochemisty (Scheffer et al., 2002). MRP1 localisation to the basolateral membrane in human alveolar and bronchial epithelial cell lines was previously also reported by Torky *et al.* (A549 cells, PLC and NHBEC) as well as van der Deen *et al.* (16HBE14o−) (Torky et al., 2005; van der Deen et al., 2007). Torky *et al.* examined the expression pattern of MPR1

using confocal laser scanning microscopy. When comparing the spatial expression and the intensity of the signal in this thesis to these previous observations, results are in accordance with their findings. However, up to the present, no research group reported evidence of the MRP1 expression in NCI-H441 cells.

To support the expression data of MRP1 in NCI-H441 cells, uptake, efflux and transport studies were carried out using the fluorescent substrate, CF.

Uptake studies showed a linear and time-dependent uptake of CFDA into NCI-H441 cell monolayers. Since MRP1 is working as an efflux transporter, which mediates the transport of substances from the cytosol to the extracellular space, the uptake was not affected by the addition of the specific MRP inhibitor MK-571. These results confirmed the functional expression of MRP1 as an efflux transporter.

In efflux studies, the concentration of CF in the lysed cell monolayers decreased in a linear way, while at the same time the concentration in the supernatant samples increased linearly and time-dependently. As expected, the addition of MK-571 inhibited the MRP1-mediated efflux from the cell monolayers, leading to significant increases in the CF signal intensity, whereas in the supernatant samples the percentage of the fluorophore was reduced. In the presence of 50 µM, MK-571 led to the most pronounced inhibition of MRP1. Lehmann *et al.* reported that the addition of MK-571 decreased the in 5,6-carboxy-2',7'-dichlorofluorescein translocation from normal human bronchial epithelial cells (NHBEC) due to the inhibition of MRP1. Thus, the results in this thesis are similar to previous observations, although, a stronger impact of MK-571 was observed in this thesis. However, the more pronounced effect can only be compared with cautions due to use of a different fluorophore, higher concentrations of the inhibitor (37 µM vs. 50 µM MK-571) and different experimental techniques (Lehmann et al., 2001). Also, van der Deen *et al.* investigated the impact of CSE and MK-571 on the CFDA efflux from the bronchial epithelial cell line 16HBE14o- and detected significant alterations (van der Deen et al., 2007).

Up to the present, MK-571 has been only described as an MRP inhibitor, however, it is not MRP1-specific and inhibits other transporters of the MRP family as well. Therefore, it is possible, that other MRP transporters also contributed to the

observed effects. Consequently, it can be assumed that members of the MRP family are involved in the CF efflux, however, further studies with a specific MRP1 inhibitor were required to determine if MRP1 is the relevant transporter.

CF is a frequently used substrate of MRP1. Up to now, it was not described as a substrate of other MRP transporters, however, it is possible that other members of the MRP family might be involved in its transport. In addition, CFDA is also transported by members of the OAT family, including OAT4, which is also expressed in the human lung and in different human lung epithelial cell lines (Endter et al., 2009; Hagos et al., 2007; Sakamoto et al., 2013).

It can hence, be summarised that release studies confirmed the functional expression of a member of the MRP family as efflux transporters in NCI-H441 cells, which is likely to be MRP1.

The bidirectional transport of CFDA by MRP1 across NCI-H441 cells was also investigated. The MRP inhibitor MK-571 and the OAT4 inhibitor telmisartan were added to study their effect on transport. Figure 31 summarises the hypothetical involvement of several pathways in CF translocation across NCI-H441 cells. MRP1 is localised to the basolateral membrane of NCI-H441 cells. As expected, the addition of MK-571 resulted in a reduction of the P_{app} in the a-b direction. Interestingly, in the b-a direction an unexpected increase in the CF flux was observed, which could be only explained by the involvement of other transporter proteins localised to the apical membrane of NCI-H441 cells. Hence, it was assumed that OAT4 might be involved in the transport. OAT4 is located on the apical side of kidney epithelial cells and was reported to transport CFDA (Hagos et al., 2007). Endter *et al.* have previously shown that OAT4 is expressed in different human lung epithelial cell lines (Endter et al., 2009). Moreover, Sakamoto *et al.* detected OAT4 in human lung samples (Sakamoto et al., 2013). Generally, OAT are not ATP-powered and mainly transport their substrates in a concentration gradient dependent way. In contrast, MRP1 belongs to the ATP-driven efflux transporters. The inhibition of MRP1 by MK-571 accelerated the transport of CF in the b-a direction due to the involvement of OAT4, which transport capacity is triggered by a concentration gradient. Based on this theory, the blocking of OAT4 using telmisartan reduced the P_{app} in the b-a direction whereas the transport in the opposite direction was not influenced. Taken all results together, MK-571

predominately reduced a-b transport, while telmisartan attenuated the b-a-transport. Complete inhibition of the transport was observed after the simultaneous administration of both inhibitors.
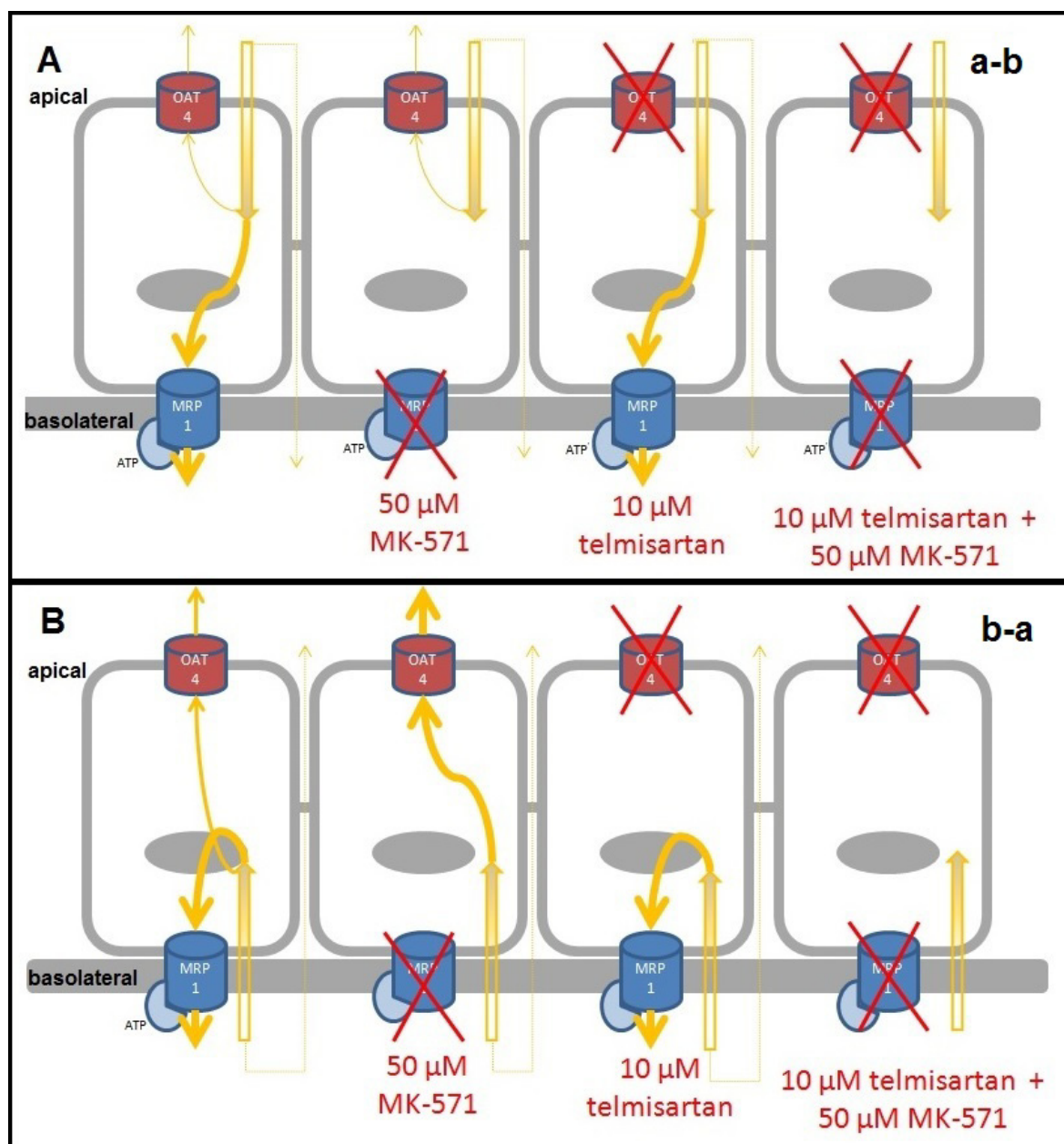
FIGURE 30

Hypothetic model of MRP1 and OAT4 involvement in CFDA transport. A: CFDA transport apical to basolateral (a-b), B: CFDA transport from the basolateral to the apical compartment (b-a), the orange arrows display the CFDA transport. CFDA permeates the cell membrane. Intracellular esterase cleaves of the acetate group and the compound becomes fluorescent. A: CF is transported mainly by the ATP-powered MRP1 and probably to a lesser extent by OAT4. Inhibition of MRP1 resulted in increased intracellular levels and reduced amounts of CF in the basolateral compartment. Inhibition of OAT4 did not influence the CF transport. Blocking of both transporters greatly inhibited the transport. B: Both transporters are involved in the CF transport. OAT4 transport is mediated by a concentration gradient. Addition of MK-571 increased the amount of the fluorescent probe in the apical compartment and reduced the intracellular levels, whereas the supplement of telmisartan reduced its transport. Addition of both inhibitors reduced the transport as well.

Based on these results, it can be concluded that MRP1 is functionally expressed in NCI-H441 cells. In addition, the functional expression of OAT4 in NCI-H441 cells as well as its involvement in the transport of CF was discovered. Up to now, no functional data reporting the expression of OAT4 in a lung cell line was available.

Nevertheless, it should be noted, that further studies are required to reassure that the relevant transporters are OAT4 and MRP1. Therefore, it is necessary to down-regulate the relevant transporter expression level in NCI-H441 cells by RNAi. Transport studies should be repeated across OAT4 or MRP1 down-regulated NCI-H441 cell monolayers and compared to the results of this thesis.

Furthermore, the influence of different broad-spectrum modulators, i.e. verapamil, indomethacin and quinidine on MRP1 activity in NCI-H441 cells was tested and compared to the inhibitory effect of MK-571.

Verapamil is a well characterised substrate and inhibitor of P-gp. Its effect on the OCT/N transporters and P-gp in NCI-H441 cells has already been demonstrated (Salomon et al., 2014). Moreover, verapamil was described as an inducer of MRP1-mediated GSH transport and weak inhibitor of MRP1 function (Loe et al., 2000). However, verapamil is not a substrate of MRP1. In this thesis it was shown that verapamil did not induce MRP1, but significantly inhibits MRP1-mediated efflux. Thus, as no stimulating effects were detected, it can be assumed that CF is transported independently from GSH. Perrotton *et al.* described a weak inhibitory effect on MRP1 which can be compared to the attenuation observed in this thesis (Perrotton et al., 2007).

Indomethacin has frequently been used as an MRP1 inhibitor in the literature. De Groot *et al.* reported the inhibition of MRP1-mediated CF transport by the addition of indomethacin in small-cell lung cancer cells (de Groot et al., 2007). In addition, indomethacin inhibited other MRP transporters (i.e MRP2 and MRP4) (El-Sheikh et al., 2007) as well as different members of the OAT family including OAT4 (Khamdang et al., 2002). In this thesis the results showed significant inhibitory effects on CF efflux from NCI-H441 cell monolayers. Therefore, data support the findings of de Groot *et al.* and suggest an inhibitory effect on MRP1. Nevertheless, an additional inhibition of OAT4 by indomethacin could also contribute to the observed attenuations.

Quinidine is known to inhibit P-gp as well as transporters of the OCT/N family (i.e. OCT1, OCT2 and OCT3). So, quinidine's inhibition of ASP$^+$ uptake in NCI-H441 cell monolayers was indicative of OCT/N transporters being expressed in the cell line. Moreover, quinidine was reported to inhibit the transport of etoposide, a substrate of P-gp and MRP1 in the human bronchial epithelial cell line, Calu-3 (Hamilton et al., 2001). In this thesis, quinidine significantly reduced MRP1-mediated efflux from NCI-H441 cell monolayers. However, this effect could not be compared to the findings of Hamilton *et al.* as P-gp is not involved in the CF transport.

It can be summarised that all three modulators revealed significant inhibitory effects on MRP1 activity. Albeit the effects were less pronounced than the specifically inhibition of MRP1 by MK-571. In addition, the involvement of other transporters cannot be excluded.

The influence of inhaled drugs used in the therapy of pulmonary diseases on the functional activity of MRP1 was also analysed. Since MRP1 has a protective function in the lung epithelium and decreased levels of MRP1 in the lung are associated with COPD, the impact of inhaled drugs on MRP1 function might have an effect on the progression of COPD and asthma, particularly, as it is linked to long-term treatment. For example, it is a well known fact that the long-term therapy using inhaled glucocorticoids did not improve COPD, whereas the administration of β-agonists does. In this thesis it was shown that all tested β-agonists, induced the MRP1-mediated CF efflux from NCI-H441 cell monolayers. However, in case of 100 µM terbutaline hemisulphate salt, 100 µM salbutamol and GW597901 the observed effects were not statistical significant. Interestingly, formoterol fumarate, a long acting β-agonist, had a stronger effect on MRP1 than the short acting β-agonists. Nevertheless, GW597901, an investigational long-acting β-agonist, did not influence MRP1 function. Based on these results it can be hypothesised that β-agonists directly interact with MRP1. Another possible explanation could be a stimulation of the β$_2$-receptors and resulting increased intracellular levels of second messengers, which in turn activate MRP1. Van der Deen *et al.* reported a slight stimulating effect of formoterol on CF efflux in the human bronchial epithelial cell line 16HBE14o-, however, this effect was not statistical significant (van der Deen et al., 2008). The more pronounced effect of formoterol on MRP1-mediated

efflux in this thesis can be explained due to the fact that van der Deen *et al.* used a bronchial epithelial cell line, however, MRP1 was reported to be expressed in the highest abundance in the distal region of the lung (Sakamoto et al., 2013). Therefore, it is possible that the human distal lung epithelial NCI-H441 cell line shows another expression pattern of MRP1 than bronchial epithelial cells. It should be noted that van der Deen's group used different analytical methods (i.e. flow cytometry vs. fluorescence plate reader) as well as different CFDA concentrations. Up to now, no other group investigated the impact β-agonists on MRP1-mediated transport so far.

Moreover, in this thesis the impact of glucocorticoids on MRP1 was investigated. Budesonide and beclomethasone attenuated CF translocation from the cell monolayers, while at the same time, significant reductions in the fluorescence were discovered in the supernatant samples. In the case of budesonide, the effect was concentration dependent. Van der Deen *et al.* also investigated the influence of budesonide on MRP1-mediated CF efflux and discovered statistical significant alterations (van der Deen et al., 2008). However, different concentrations of budesonide were used in their experiments so that the observed effects could only be compared with caution. In van der Deen's experiments the addition of 10 µM budesonide resulted in significant increases of CF in the cells by 26%, while increases by 97% CF were observed using 100 µM budesonide. In this thesis two different concentrations of budesonide (20 µM and 50 µM) were tested. In the experiments using 20 µM budesonide, significant reductions in the CF concentration by 23.28 ± 4.65% in the supernatants were discovered, although no statistical significant differences were detected in the cell monolayers. The addition of 50 µM budesonide resulted in significant increases in the CF accumulation in the cell monolayers by 34.18 ± 13.04%. In contrast to van der Deen's results, a slightly less pronounced effect of budesonide on MRP1-mediated efflux was discovered in this work. The observed differences can be explained by differences in the used concentrations, the analytical methods or the different cell line. Van der Deen discovered a reduction of the inhibitory effect of budesonide by the addition of formoterol. Furthermore, it was shown that budesonide was able to affect the transcriptional expression of MRP1 in the bronchial cell line Calu-1 after long-time incubation with budesonide (Bandi and Kompella, 2002). It is tempting to assume,

that long time therapy could also affect the expression levels of MRP1 due to transcription-down regulation.

In this thesis, beclomethasone showed a similar effect on MRP1-mediated efflux resulting in increased intracellular concentrations of CF and reduced levels in the supernatants. Therefore, it can be assumed that both glucocorticoids interact with the MRP1 function, possibly as inhibitors or substrates or in another indirect way. Glucocorticoids inhibit phospholipase A_2, which is essential for the biosynthesis of archidonic acid and subsequently for the biosynthesis of leucotrienes and prostaglandin A_2. Both are endogenous substrates of MRP1 (Evers et al., 1997; Leier et al., 1994). Possibly, the lack of endogenous substrates could cause a decreased transport activity of MRP1.

Furthermore, in case of cromolyn sodium no significant influences on MRP1-mediated efflux were discovered. Up to now, no publication reported its involvement in MRP1-mediated transport processes. Therefore, it can be assumed that cromolyn sodium did not interfere with MRP1 function.

The side project of this thesis was aiming to determine the function of P-gp in NCI-H441 cells. Rh123 release from cell monolayers was time dependent. Addition of the selective P-gp inhibitor LY335979 and verapamil resulted in attenuated Rh123 translocation over 60 min. Although the decrease was significant after 60 min, the observed effect was less pronounced than for example the inhibition of MRP1 in release studies by MK-571. However, P-gp expression levels in the lung epithelium are lower than MRP1 expression levels and are paralleled by a lower transporter activity in respiratory cells *in vitro (Madlova et al., 2009; Sakamoto et al., 2013)*.

In addition, the paracellular transport of different markers was investigated. Differences in the P_{app} were detected, which were according to the molecular size of the transported compound with the slowest transport observed in case of the FITC-dextran 70,000. These studies revealed the tightness of the NCI-H441 cell monolayers and confirmed the functionality of the tight junctions. The presence of tight and polarised cell layers in NCI-H441 cells can be considered as an improvement to currently available cell lines of the distal lung epithelial barrier (i.e. the alveolar epithelial cell line A549).

Finally, it can be concluded that MRP1 is expressed on the basolateral membrane of NCI-H441 cells. Moreover, the function of MRP1 in NCI-H441 cells was confirmed by uptake, efflux and transport studies. Transport studies also suggested the functional expression of OAT4 in NCI-H441 cells. Hence, further studies are required to determine the impact of OAT4 in CFDA efflux studies. Moreover, this thesis shows that drugs that are frequently used in the therapy of COPD and asthma are very likely to interfere with MRP1 function and MRP1-mediated transport. Therefore, further studies are required to determine, if for example smokers or COPD patients would benefit from the positive effect of new MRP1 stimulating substances. A side project of this thesis revealed the functional expression of P-gp in NCI-H441 cells. Transport of different paracellular marker compounds confirmed the tightness of the NCI-H441 monolayers.

Consequently, taken these data together, the NCI-H441 cell line can be considered as an improvement to currently available cell lines of the human distal lung epithelial as both investigated drug transporters, MRP1 and P-gp are functionally expressed and the cell line is able to form tight monolayers. Particularly, in the case of biopharmaceutical research, the knowledge of the expression of key drug transporters (i.e. MRP1 and P-gp) can be of advantage. The understanding of the involvement of MRP1 in the transport of inhaled drugs is essential in case of a long-term therapy as well as prognosis of drug-drug interactions.

5 SUMMARY

MRP1 is an ATP powered efflux transporter, which is widely expressed throughout the human body. It shows the highest abundance of all ABC transporter proteins in human lung, particularly in the distal region of the lung. MRP1 plays an important role in the transport of endogenous and exogenous substances. Its presence in the human lung has been linked to a protective role against oxidative stress, which is for example caused by tobacco smoke. Moreover, diminished levels of MRP1 in the lung have been related to the development and severity of COPD and previous studies have discovered significant effects of different inhaled therapeutics of COPD and asthma on MRP1 function.

The aim of this thesis was to investigate MRP1 expression, cellular localisation and function in the human distal lung epithelial cell line NCI-H441 in the context of characterising it for biopharmaceutical research applications. A number of drugs, e.g. indomethacin, verapamil and quinidine, have been suggested to be MRP1 modulators. In this project their influence on MRP1 function was assessed. In addition, the impact of inhaled drugs used in the therapy of COPD and bronchial asthma on MRP1 was tested. The side project of this thesis was concerned with determining the functional expression of P-gp in NCI-H441 cells.

In this thesis Western blots with a monoclonal MRP1 antibody showed the expression of MRP1 on protein level in NCI-H441 cells. Additionally, confocal laser scanning microscopy showed clear signals of the MRP1 antibody in the membrane region. Z-scans demonstrated its expression on the basolateral side of the membrane.

In order to investigate the function of MRP1 in NCI-H441 cells, uptake studies, release studies and transport studies were carried out using the fluorescent MRP1 substrate CFDA. The CFDA uptake was linear and time-dependent and was not altered by the addition of the MRP1 inhibitor, MK-571. In contrast, the efflux of CF was also linear and time-dependent but was significantly inhibited by the addition of MK-571 indicating the functional expression of MRP1 as an efflux transporter. Transport studies detected an asymmetric transport of CFDA in NCI-H441 cells. The supplement of MK-571 reduced the transport in the a-b direction which also

73

confirmed its expression on the basolateral membrane. However, the transport in the b-a direction was accelerated. This was rather unexpected but can be explained due to the involvement of an apically localised transporter. Further experiments showed that the inhibition of OAT4 using telmisartan significantly reduced the transport in the b-a direction. Supplement of both inhibitors almost completely inhibited the CFDA transport in both directions.

Release studies were carried out to determine the impact of different broad spectrum modulators on MRP1 function. Verapamil, indomethacin and quinidine significantly inhibited the CF release from NCI-H441 monolayers. Albeit their impact was less pronounced than the effect of MK-571. All used modulators also influence other transporter proteins, therefore, the observed effect could be unspecific.

Inhaled drugs used in the therapy of COPD and asthma showed significant effects on MRP1 function in release studies. Beta-agonists (i.e. salbutamol, terbutaline hemisulphate salt and formoterol fumarate) induced the CF efflux from NCI-H441 cell monolayers. Therefore, β-agonists might be substrates of MRP1, induce MRP1 function or interact with MRP1 in another indirect way. In contrast, glucocorticoids (i.e. budesonide and beclomethasone) reduced CF efflux from NCI-H441 cell monolayers, possibly due to the inhibition of MRP1 function, as substrates or in another indirect way. Cromolyn sodium did not interact with MRP1 function.

In the side project release studies using the fluorescent probe Rh123 demonstrated the functional expression of P-gp in NCI-H441 cells. The Rh123 efflux was time-dependent and could be significantly attenuated by the supplement of the specific P-gp inhibitor LY335979 and verapamil over 60 min, however, the observed effect was less pronounced than in case of MRP1 release studies.

Moreover, transport studies using paracellular marker compounds revealed the tightness of the NCI-H441 cell monolayers.

Collectively, this thesis revealed that NCI-H441 cells are an improvement to other available cell lines due to the functional expression of key transporters (i.e. MRP1 and P-gp) and the tightness of the cell monolayers, which are important for *in-vitro*

studies in biopharmaceutical research. Additionally, it was shown that several frequently prescribed inhaled drugs interfere with MRP1 function.

6 ZUSAMMENFASSUNG

MRP1 ist ein ATP abhängiger Effluxtransporter, der der ABC Transporterfamilie angehört und in verschiedenen Bereichen des menschlichen Körpers nachgewiesen wurde. In den distalen Arealen der menschlichen Lunge wurde das MRP1 Protein in großen Mengen detektiert. MRP1 spielt eine wichtige Rolle beim Transport von endogenen und exogenen Substanzen im Körper. In der Lunge übt MRP1 eine wichtige Schutzfunktion gegenüber oxidativem Stress aus, der zum Beispiel auch durch Tabakrauch generiert wird. COPD Patienten weisen verringerte MRP1-Spiegel auf. Des Weiteren zeigten Studien, dass Inhalanda, die zur Therapie von COPD und von Asthma bronchiale eingesetzt werden, die MRP1-Funktion signifikant beeinflussen.

Das Ziel der vorliegenden Diplomarbeit war es die Expression, die zelluläre Lokalisation und die Funktion von MRP1 in der humanen Bronchiolarepithelialzelllinie NCI-H441 für die biopharmazeutischen Forschung zu untersuchen. Aus der Literatur sind Indomethacin, Verapamil und Chinidin als MRP1-Modulatoren bekannt und wurden in dieser Arbeit bezüglich ihres Einflusses auf den MRP1-vermittelten Transport untersucht. Zusätzlich wurden die Auswirkungen von Inhalanda auf MRP1 ermittelt, die in der Therapie von COPD und Asthma eingesetzt werden. Darüber hinaus wurde die funktionelle Expression von P-gp in der NCI-H441 Zelllinie charakterisiert.

Durch Western Blots und Detektion mit einem MRP1-spezifischen monokonalen Antikörper wurde die Expression von MRP1 in NCI-H441 Zellen auf Proteinlevel nachgewiesen. Anhand von Konfokaler Laser Scanning Mikroskopie in Gegenwart eines MRP1-spezifischen monoklonalen Antikörpers konnte MRP1 in der basolateralen Membran von NCI-H441 Zellen lokalisiert werden.

Durch Aufnahme-, Efflux- und Transportstudien mit dem fluoreszierenden MRP1-Substrat 5(6)-Carboxyfluorescein-diacetat (CFDA) wurde die Funktion von MRP1 in der NCI-H441 Zelllinie untersucht. Die CFDA-Aufnahme verlief linear und zeitabhängig und konnte durch den spezifischen MRP-Inhibitor MK-571 nicht gehemmt werden. Der Efflux von 5(6)-Carboxyfluorescein-diacetat (CF) erfolgte ebenfalls linear und zeitabhängig, wurde jedoch durch den Zusatz von MK-571

signifikant inhibiert. Daraus lässt sich die funktionale Expression des MRP1-Transporters in NCI-H441 ableiten.

Die Transportstudien ergaben einen asymmetrischen Transport von CFDA in NCI-H441 Zellen. Der Zusatz von MK-571 reduzierte den Transport in der a-b Richtung, wodurch die Expression von MRP1 auf der basolateralen Membran erneut bestätigt wurde. Jedoch wurde durch den Zusatz des Inhibitors der Transport in der b-a Richtung beschleunigt. Dieses vollkommen unerwartete Ergebnis kann durch die Beteiligung eines zusätzlichen apikalen Transporters erklärt werden. Weitere Experimente zeigten, dass die Hemmung von OAT4 mittels Telmisartan den b-a Transport deutlich verringerte. Der Zusatz beider Inhibitoren blockierte den CF-Transport fast vollständig.

Effluxstudien wurden durchgeführt, um den Einfluss verschiedener Modulatoren auf die MRP1-Funktion zu erkennen. Verapamil, Indomethacin und Chinidin hemmten den CF Efflux aus NCI-H441 Zellmonolayern signifikant. Trotzdem war der erzielte Effekt deutlich schwächer als die Inhibition durch MK-571. Da alle untersuchten Modulatoren auch Substrate und Inhibitoren von anderen Transportern sind, kann ein unspezifischer Effekt nicht ausgeschlossen werden.

Inhalanda, die in der Therapie von COPD und Asthma häufig eingesetzt werden, zeigten in Effluxstudien signifikante Einflüsse auf die MRP1-Funktion. Beta-Agonisten wie Salbutamol, Terbutalin-hemisulphat und Formoterol-fumarat beschleunigten den CF Efflux aus NCI-H441 Zellmonolayern. Aus diesem Grund ist es möglich, dass β-Agonisten den MRP1-Transport induzieren, als Substrate transportiert werden oder aber mit MRP1 auf indirektem Weg interagieren.

Im Gegensatz dazu reduzierten die Glukokortikoide Budesonid und Beclomethason den CF Efflux aus NCI-H441 Zellmonolayern. Der beobachtete Effekt könnte durch die Inhibition von MRP1 durch Glukokortikoide, aber auch durch Substrattransport oder eine Interaktion über andere indirekte Wege erklärt werden. Der Mastzellstabilisator Cromoglicinsäure beeinflusst die MRP1-Funktion nicht.

Zusätzlich wurde in dieser Diplomarbeit die funktionelle Expression von P-Glykoprotein (P-gp) in NCI-H441 Zellen an Hand von Effluxstudien mit dem fluoreszierenden Substrat Rhodamin123 (Rh123) untersucht. Der Rh123 Efflux

verlief zeitabhängig und konnte mit Hilfe des spezifischen P-gp Inhibitors LY335979 sowie mit Verapamil über einen Zeitraum von 60 Minuten statistisch signifikant verringert werden. Jedoch war der Effekt geringer ausgeprägt als in den MRP1-Effluxstudien.

Transportstudien mit parazellulären Markern zeigten die Dichtheit von NCI-H441 Zellmonolayern.

Die vorliegende Diplomarbeit verdeutlicht, dass NCI-H441 Zellen einen Fortschritt gegenüber anderen etablierten Zelllinien des distalen Bereichs der Lunge darstellen, da sie wichtige Transporter, wie MRP1 und P-gp, funktionell exprimieren und in der Lage sind, dichte Zellmonolayer zu bilden, welche für *in vitro* Studien in der biopharmazeutischen Forschung benötigt werden. Zusätzlich beeinflussen viele gängige Inhalanda die Funktion des Transporters MRP1.

7 REFERENCES

Bakos, E., R. Evers, G. Calenda, G. E. Tusnády, G. Szakács, A. Váradi, and B. Sarkadi, 2000, Characterization of the amino-terminal regions in the human multidrug resistance protein (MRP1): J Cell Sci, v. 113 Pt 24, p. 4451-61.

Bakos, E., and L. Homolya, 2007, Portrait of multifaceted transporter, the multidrug resistance-associated protein 1 (MRP1/ABCC1): Pflugers Arch, v. 453, p. 621-41.

Bandi, N., and U. B. Kompella, 2002, Budesonide reduces multidrug resistance-associated protein 1 expression in an airway epithelial cell line (Calu-1): Eur J Pharmacol, v. 437, p. 9-17.

Baptist, A. P., and R. C. Reddy, 2009, Inhaled corticosteroids for asthma: are they all the same?: J Clin Pharm Ther, v. 34, p. 1-12.

Beck, K., K. Hayashi, K. Dang, M. Hayashi, and C. D. Boyd, 2005, Analysis of ABCC6 (MRP6) in normal human tissues: Histochem Cell Biol, v. 123, p. 517-28.

Bleasby, K., J. C. Castle, C. J. Roberts, C. Cheng, W. J. Bailey, J. F. Sina, A. V. Kulkarni, M. J. Hafey, R. Evers, J. M. Johnson, R. G. Ulrich, and J. G. Slatter, 2006, Expression profiles of 50 xenobiotic transporter genes in humans and pre-clinical species: a resource for investigations into drug disposition: Xenobiotica, v. 36, p. 963-88.

Bosquillon, C., 2010, Drug transporters in the lung--do they play a role in the biopharmaceutics of inhaled drugs?: J Pharm Sci, v. 99, p. 2240-55.

Boumendjel, A., J. Boutonnat, and J. Robert, 2009, ABC Transporters and Multidrug Resistance: Wiley Series in Drug Discovery and Development: Hoboken, New Jersey, John Wiley & Sohns, Inc.

Bréchot, J. M., I. Hurbain, A. Fajac, N. Daty, and J. F. Bernaudin, 1998, Different pattern of MRP localization in ciliated and basal cells from human bronchial epithelium: J Histochem Cytochem, v. 46, p. 513-7.

Budulac, S. E., D. S. Postma, P. S. Hiemstra, L. I. Kunz, M. Siedlinski, H. A. Smit, J. M. Vonk, B. Rutgers, W. Timens, H. M. Boezen, and G. L. U. C. i. O. L. D. G. s. group, 2010, Multidrug resistance-associated protein-1 (MRP1) genetic variants, MRP1 protein levels and severity of COPD: Respir Res, v. 11, p. 60.

Budulac, S. E., D. S. Postma, P. S. Hiemstra, T. S. Lapperre, L. I. Kunz, J. M. Vonk, H. Marike Boezen, W. Timens, and G. S. Group, 2012, Multidrug resistance-associated protein 1 and lung function decline with or without long-term corticosteroids treatment in COPD: Eur J Pharmacol, v. 696, p. 136-42.

Burckhardt, G., 2012, Drug transport by Organic Anion Transporters (OATs): Pharmacol Ther, v. 136, p. 106-30.

Cole, S. P., 2013, Targeting Multidrug Resistance Protein 1 (MRP1, ABCC1): Past, Present, and Future: Annu Rev Pharmacol Toxicol.

Cole, S. P., G. Bhardwaj, J. H. Gerlach, J. E. Mackie, C. E. Grant, K. C. Almquist, A. J. Stewart, E. U. Kurz, A. M. Duncan, and R. G. Deeley, 1992, Overexpression of a transporter gene in a multidrug-resistant human lung cancer cell line: Science, v. 258, p. 1650-4.

de Groot, D. J., M. van der Deen, T. K. Le, A. Regeling, S. de Jong, and E. G. de Vries, 2007, Indomethacin induces apoptosis via a MRP1-dependent mechanism in doxorubicin-resistant small-cell lung cancer cells overexpressing MRP1: Br J Cancer, v. 97, p. 1077-83.

Döring, G., P. Flume, H. Heijerman, J. S. Elborn, and C. S. Group, 2012, Treatment of lung infection in patients with cystic fibrosis: current and future strategies: J Cyst Fibros, v. 11, p. 461-79.

Ehrhardt, C., C. Kneuer, C. Bies, C. M. Lehr, K. J. Kim, and U. Bakowsky, 2005, Salbutamol is actively absorbed across human bronchial epithelial cell layers: Pulm Pharmacol Ther, v. 18, p. 165-70.

Ehrhardt, C., C. Kneuer, M. Laue, U. F. Schaefer, K. J. Kim, and C. M. Lehr, 2003, 16HBE14o- human bronchial epithelial cell layers express P-glycoprotein, lung resistance-related protein, and caveolin-1: Pharm Res, v. 20, p. 545-51.

Ejiofor, S., and A. M. Turner, 2013, Pharmacotherapies for COPD: Clin Med Insights Circ Respir Pulm Med, v. 7, p. 17-34.

El-Sheikh, A. A., J. J. van den Heuvel, J. B. Koenderink, and F. G. Russel, 2007, Interaction of nonsteroidal anti-inflammatory drugs with multidrug resistance protein (MRP) 2/ABCC2- and MRP4/ABCC4-mediated methotrexate transport: J Pharmacol Exp Ther, v. 320, p. 229-35.

Endter, S., U. Becker, N. Daum, H. Huwer, C. M. Lehr, M. Gumbleton, and C. Ehrhardt, 2007, P-glycoprotein (MDR1) functional activity in human alveolar epithelial cell monolayers: Cell Tissue Res, v. 328, p. 77-84.

Endter, S., D. Francombe, C. Ehrhardt, and M. Gumbleton, 2009, RT-PCR analysis of ABC, SLC and SLCO drug transporters in human lung epithelial cell models: J Pharm Pharmacol, v. 61, p. 583-91.

Evers, R., N. H. Cnubben, J. Wijnholds, L. van Deemter, P. J. van Bladeren, and P. Borst, 1997, Transport of glutathione prostaglandin A conjugates by the multidrug resistance protein 1: FEBS Lett, v. 419, p. 112-6.

Flens, M. J., G. J. Zaman, P. van der Valk, M. A. Izquierdo, A. B. Schroeijers, G. L. Scheffer, P. van der Groep, M. de Haas, C. J. Meijer, and R. J. Scheper, 1996, Tissue distribution of the multidrug resistance protein: Am J Pathol, v. 148, p. 1237-47.

Forbes, B., and C. Ehrhardt, 2005, Human respiratory epithelial cell culture for drug delivery applications: Eur J Pharm Biopharm, v. 60, p. 193-205.

Grant, C. E., G. Valdimarsson, D. R. Hipfner, K. C. Almquist, S. P. Cole, and R. G. Deeley, 1994, Overexpression of multidrug resistance-associated protein (MRP) increases resistance to natural product drugs: Cancer Res, v. 54, p. 357-61.

Gumbleton, M., G. Al-Jayyoussi, A. Crandon-Lewis, D. Francombe, K. Kreitmeyr, C. J. Morris, and M. W. Smith, 2011, Spatial expression and functionality of drug transporters in the intact lung: objectives for further research: Adv Drug Deliv Rev, v. 63, p. 110-8.

Hagos, Y., D. Stein, B. Ugele, G. Burckhardt, and A. Bahn, 2007, Human renal organic anion transporter 4 operates as an asymmetric urate transporter: J Am Soc Nephrol, v. 18, p. 430-9.

Hamilton, K. O., E. Topp, I. Makagiansar, T. Siahaan, M. Yazdanian, and K. L. Audus, 2001, Multidrug resistance-associated protein-1 functional activity in Calu-3 cells: J Pharmacol Exp Ther, v. 298, p. 1199-205.

He, L., K. Vasiliou, and D. W. Nebert, 2009, Analysis and update of the human solute carrier (SLC) gene superfamily: Hum Genomics, v. 3, p. 195-206.

Hooijberg, J. H., H. J. Broxterman, M. Kool, Y. G. Assaraf, G. J. Peters, P. Noordhuis, R. J. Scheper, P. Borst, H. M. Pinedo, and G. Jansen, 1999, Antifolate resistance mediated by the multidrug resistance proteins MRP1 and MRP2: Cancer Res, v. 59, p. 2532-5.

Horvath, G., N. Schmid, M. A. Fragoso, A. Schmid, G. E. Conner, M. Salathe, and A. Wanner, 2007, Epithelial organic cation transporters ensure pH-dependent drug absorption in the airway: Am J Respir Cell Mol Biol, v. 36, p. 53-60.

Jedlitschky, G., I. Leier, U. Buchholz, K. Barnouin, G. Kurz, and D. Keppler, 1996, Transport of glutathione, glucuronate, and sulfate conjugates by the MRP gene-encoded conjugate export pump: Cancer Res, v. 56, p. 988-94.

Keppler, D., 2011, Multidrug Resistance Proteins (MRPs, ABCCs): Importance for pathophysiology and drug therapy, in M. F. Fromm, and R. B. Kim, eds., Drug Transporters, v. Handbook of Experimental Pharmacology 201 2011, Springer.

Khamdang, S., M. Takeda, R. Noshiro, S. Narikawa, A. Enomoto, N. Anzai, P. Piyachaturawat, and H. Endou, 2002, Interactions of human organic anion transporters and human organic

cation transporters with nonsteroidal anti-inflammatory drugs: J Pharmacol Exp Ther, v. 303, p. 534-9.

Koepsell, H., 2013, The SLC22 family with transporters of organic cations, anions and zwitterions: Mol Aspects Med, v. 34, p. 413-35.

König, J., F. Müller, and M. F. Fromm, 2013, Transporters and drug-drug interactions: important determinants of drug disposition and effects: Pharmacol Rev, v. 65, p. 944-66.

Lehmann, T., C. Köhler, E. Weidauer, C. Taege, and H. Foth, 2001, Expression of MRP1 and related transporters in human lung cells in culture: Toxicology, v. 167, p. 59-72.

Leier, I., G. Jedlitschky, U. Buchholz, S. P. Cole, R. G. Deeley, and D. Keppler, 1994, The MRP gene encodes an ATP-dependent export pump for leukotriene C4 and structurally related conjugates: J Biol Chem, v. 269, p. 27807-10.

Leslie, E. M., K. Ito, P. Upadhyaya, S. S. Hecht, R. G. Deeley, and S. P. Cole, 2001, Transport of the beta -O-glucuronide conjugate of the tobacco-specific carcinogen 4-(methylnitrosamino)-1-(3-pyridyl)-1-butanol (NNAL) by the multidrug resistance protein 1 (MRP1). Requirement for glutathione or a non-sulfur-containing analog: J Biol Chem, v. 276, p. 27846-54.

Lima, J. J., S. Zhang, A. Grant, L. Shao, K. G. Tantisira, H. Allayee, J. Wang, J. Sylvester, J. Holbrook, R. Wise, S. T. Weiss, and K. Barnes, 2006, Influence of leukotriene pathway polymorphisms on response to montelukast in asthma: Am J Respir Crit Care Med, v. 173, p. 379-85.

Loe, D. W., R. G. Deeley, and S. P. Cole, 1998, Characterization of vincristine transport by the M(r) 190,000 multidrug resistance protein (MRP): evidence for cotransport with reduced glutathione: Cancer Res, v. 58, p. 5130-6.

Loe, D. W., R. G. Deeley, and S. P. Cole, 2000, Verapamil stimulates glutathione transport by the 190-kDa multidrug resistance protein 1 (MRP1): J Pharmacol Exp Ther, v. 293, p. 530-8.

Madlova, M., C. Bosquillon, D. Asker, P. Dolezal, and B. Forbes, 2009, In-vitro respiratory drug absorption models possess nominal functional P-glycoprotein activity: J Pharm Pharmacol, v. 61, p. 293-301.

Nakamura, T., T. Nakanishi, T. Haruta, Y. Shirasaka, J. P. Keogh, and I. Tamai, 2010, Transport of ipratropium, an anti-chronic obstructive pulmonary disease drug, is mediated by organic cation/carnitine transporters in human bronchial epithelial cells: implications for carrier-mediated pulmonary absorption: Mol Pharm, v. 7, p. 187-95.

Neuhaus, W., F. Samwer, S. Kunzmann, R. M. Muellenbach, M. Wirth, C. P. Speer, N. Roewer, and C. Y. Förster, 2012, Lung endothelial cells strengthen, but brain endothelial cells weaken barrier properties of a human alveolar epithelium cell culture model: Differentiation, v. 84, p. 294-304.

Newton, D. A., K. M. Rao, R. A. Dluhy, and J. E. Baatz, 2006, Hemoglobin is expressed by alveolar epithelial cells: J Biol Chem, v. 281, p. 5668-76.

O'Connell, E. J., 2003, Review of the unique properties of budesonide: Clin Ther, v. 25 Suppl C, p. C42-60.

Olson, D. P., D. T. Scadden, R. T. D'Aquila, and M. P. De Pasquale, 2002, The protease inhibitor ritonavir inhibits the functional activity of the multidrug resistance related-protein 1 (MRP-1): AIDS, v. 16, p. 1743-7.

Patton, J. S., J. D. Brain, L. A. Davies, J. Fiegel, M. Gumbleton, K. J. Kim, M. Sakagami, R. Vanbever, and C. Ehrhardt, 2010, The particle has landed--characterizing the fate of inhaled pharmaceuticals: J Aerosol Med Pulm Drug Deliv, v. 23 Suppl 2, p. S71-87.

Patton, J. S., and P. R. Byron, 2007, Inhaling medicines: delivering drugs to the body through the lungs: Nat Rev Drug Discov, v. 6, p. 67-74.

Perrotton, T., D. Trompier, X. B. Chang, A. Di Pietro, and H. Baubichon-Cortay, 2007, (R)- and (S)-verapamil differentially modulate the multidrug-resistant protein MRP1: J Biol Chem, v. 282, p. 31542-8.

Qian, Y. M., W. C. Song, H. Cui, S. P. Cole, and R. G. Deeley, 2001, Glutathione stimulates sulfated estrogen transport by multidrug resistance protein 1: J Biol Chem, v. 276, p. 6404-11.

Rehan, V. K., J. S. Torday, S. Peleg, L. Gennaro, P. Vouros, J. Padbury, D. S. Rao, and G. S. Reddy, 2002, 1Alpha,25-dihydroxy-3-epi-vitamin D3, a natural metabolite of 1alpha,25-dihydroxy vitamin D3: production and biological activity studies in pulmonary alveolar type II cells: Mol Genet Metab, v. 76, p. 46-56.

Renes, J., E. G. de Vries, E. F. Nienhuis, P. L. Jansen, and M. Müller, 1999, ATP- and glutathione-dependent transport of chemotherapeutic drugs by the multidrug resistance protein MRP1: Br J Pharmacol, v. 126, p. 681-8.

Sakamoto, A., T. Matsumaru, N. Yamamura, Y. Uchida, M. Tachikawa, S. Ohtsuki, and T. Terasaki, 2013, Quantitative expression of human drug transporter proteins in lung tissues: analysis of regional, gender, and interindividual differences by liquid chromatography-tandem mass spectrometry: J Pharm Sci, v. 102, p. 3395-406.

Salomon, J. J., V. E. Muchitsch, J. C. Gausterer, E. Schwagerus, H. Huwer, N. Daum, C. M. Lehr, and C. Ehrhardt, 2014, The cell line NCI-H441 is a useful in vitro model for transport studies of human distal lung epithelial barrier: Mol Pharm.

Sandusky, G. E., K. S. Mintze, S. E. Pratt, and A. H. Dantzig, 2002, Expression of multidrug resistance-associated protein 2 (MRP2) in normal human tissues and carcinomas using tissue microarrays: Histopathology, v. 41, p. 65-74.

Scheffer, G. L., A. C. Pijnenborg, E. F. Smit, M. Müller, D. S. Postma, W. Timens, P. van der Valk, E. G. de Vries, and R. J. Scheper, 2002, Multidrug resistance related molecules in human and murine lung: J Clin Pathol, v. 55, p. 332-9.

Sharom, F. J., 2008, ABC multidrug transporters: structure, function and role in chemoresistance: Pharmacogenomics, v. 9, p. 105-27.

Torky, A. R., E. Stehfest, K. Viehweger, C. Taege, and H. Foth, 2005, Immuno-histochemical detection of MRPs in human lung cells in culture: Toxicology, v. 207, p. 437-50.

van der Deen, M., E. G. de Vries, H. Visserman, W. Zandbergen, D. S. Postma, W. Timens, and H. Timmer-Bosscha, 2007, Cigarette smoke extract affects functional activity of MRP1 in bronchial epithelial cells: J Biochem Mol Toxicol, v. 21, p. 243-51.

van der Deen, M., S. Homan, H. Timmer-Bosscha, R. J. Scheper, W. Timens, D. S. Postma, and E. G. de Vries, 2008, Effect of COPD treatments on MRP1-mediated transport in bronchial epithelial cells: Int J Chron Obstruct Pulmon Dis, v. 3, p. 469-75.

van der Deen, M., H. Marks, B. W. Willemse, D. S. Postma, M. Müller, E. F. Smit, G. L. Scheffer, R. J. Scheper, E. G. de Vries, and W. Timens, 2006, Diminished expression of multidrug resistance-associated protein 1 (MRP1) in bronchial epithelium of COPD patients: Virchows Arch, v. 449, p. 682-8.

Wang, Q., and W. T. Beck, 1998, Transcriptional suppression of multidrug resistance-associated protein (MRP) gene expression by wild-type p53: Cancer Res, v. 58, p. 5762-9.

8 CURRICULUM VITAE

NAME: Viktoria Elisabeth Muchitsch

ADRESSE: Lerchenfelderstraße 124/2/9, 1080 Wien

EMAIL: viktoria.muchitsch@chello.at

GEBURTSDATUM: 08.10.1988

GEBURTSORT: Wien, Österreich

AUSBILDUNG

1995 - 1999	Volksschule Mater Salvatoris, Kenyongasse 4-12, 1070 Wien
1999 - 2007	Gymnasium Mater Salvatoris
SEIT 2007	Diplomstudium Pharmazie, Universität Wien

BERUFSERFAHRUNG

Juli 2008	Wiener Gebietskrankenkasse, Wienerbergstraße 15-19, 1103 Wien, Ferialpraktikum
Juli 2009, 2010, 2011, 2012	Linden-Apotheke, Hernalser Hauptstraße 155, 1170 Wien, Ferialpraktika
August 2010	Baxter, Industriestraße 131, 1210 Wien, Ferialpraktikum
Oktober 2010 - Januar 2011, März 2011 - Juni 2011	Universität Wien, Department für pharmazeutische Chemie Althanstraße 14, 1090 Wien Tutor (PR Quantitative pharmazeutische Analytik)
Seit Dezember 2008	Linden-Apotheke, geringfügig beschäftigt
Seit März 2014	Universität Wien, Department für Pharmazeutische Technologie und Biopharmazie Tutor (PR Grundpraktikum aus Pharmazeutischer Technologie)

PUBLIKATIONEN

Salomon, J. J., V. E. Muchitsch, J. C. Gausterer, E. Schwagerus, H. Huwer, N. Daum, C. M. Lehr, and C. Ehrhardt, 2014, The cell line NCI-H441 is a useful *in vitro* model for transport studies of human distal lung epithelial barrier: Mol Pharm.